THE UNIVERSITY OF NEW SOUTH WALES

SCHOOL OF MECHANICAL AND INDUSTRIAL ENGINEERING

SOLAR PHOTOVOLTAIC WATER PUMPING SYSTEM DESIGN AND PERFORMANCE

G.W.HOBBS

MASTER OF ENGINEERING SCIENCE

1987

SR P T02
Form 2
RETENTION

THE UNIVERSITY OF NEW SOUTH WALES

DECLARATION RELATING TO DISPOSITION OF PROJECT REPORT/THESIS

This is to certify that I Glen Hobbs being a candidate for the degree of M Eng Sc am fully aware of the policy of the University relating to the retention and use of higher degree project reports and theses, namely that the University retains the copies submitted for examination and is free to allow them to be consulted or borrowed. Subject to the provisions of the Copyright Act, 1968, the University may issue a project report or thesis in whole or in part, in photostat or microfilm or other copying medium.

In the light of these provisions I declare that I wish to retain my full privileges of copyright and request that neither the whole nor any portion of my project report/thesis be published by the University Librarian and that the Librarian may not authorize the publication of the whole or any part of it, and I further declare that this preservation of my copyright privileges shall lapse from the 26th day of AUGUST 1992 unless it shall previously have been extended or revoked in writing over my hand.

I also authorize the publication by University Microfilms of a 350 word abstract in *Dissertation Abstracts International* (applicable to doctorates only).

Signature Glen Hobbs

Witness [illegible]

Date 26-8-87

DECLARATION

"I hereby declare that this submission is my own work and that, to the best of my knowledge and belief, it contains no material previously published or written by another person nor material which to a substantial extent has been accepted for the award of any other degree or diploma of a university or other institute of higher learning, except where due acknowledgement is made in the text."

ACKNOWLEDGEMENT

I would sincerely like to thank Associate Professor G.Morrison for his willing guidance and advice throughout the preparation of this thesis, and my wife Julia for her patience and moral support and typing of the manuscript.

I would also like to thank the Department of Water Resources for allowing me to use the data collected from the solar pump installation and granting me some time to prepare this thesis; the Energy Authority, especially David Field, for down loading the data loggers; and Alex Litvak of the UNSW for the difficult task of transferring the data to the University's computer.

ABSTRACT

In recent years solar photovoltaic powered water pumps have become a practical and economic alternative to conventional forms of pumping in certain applications. However despite the large volume of information regarding the design and operation of pumps and electric motors and the present intensive research programs into photovoltaic cells, there is little information regarding the design, operation and selection of appropriately matched photovoltaic cells, electric motors and pumps.

This thesis considers the operation and matching of solar pump components and looks at the sensitivity of the solar pump performance to varying design parameters.This involves computer modelling and detailed performance monitoring, over a 15 month period, of a solar pump installed in an irrigation area of N.S.W. by the Department of Water Resources. The solar pump for this project is comprised of a stationary, non-concentrating PV array, a permanent magnet D.C. motor, a Maximum Power Point Tracker (MPPT) and a belt driven centrifugal pump.

The solar pump with MPPT performs well below that guaranteed by the manufacturer, with performance being closely related to the cell temperature of the array. With the MPPT removed performance is more than doubled but still well below specification. A non-linear relationship is found to exists between flowrate and radiation

The over-all efficiency of the solar pump is 1.8%, which is comparable with the most efficient pump tested in a study for the World Bank. The peak efficiency for the combined motor and pump is 47% and for the PV array ,over 9%.

The computer model requires an input of inclined radiation and cell temperature, plus static head, pipeline friction constant and cable losses. The model is shown to successfully simulate the performance of the photovoltaic array, D.C. motor, pump, MPPT and pipeline.

With the MPPT fitted the model predicts flow within 17%, and with it removed, 7%. Using the model the effect on over-all performance of varying design and installation parameters can be seen. The model shows performance could be readily improved by increasing the pulley ratio.

It is concluded that the use of average radiation data to predict pump performance can lead to significant errors; also the project pump is performing well below that expected by the manufacturer which supports the view that manufacturers are unsure about the design and selection of solar powered water pumps. However a computer program has been successfully developed which will assist in the design of solar pumps and the prediction of long-term performance.

NOMENCLATURE

Em	Back E.M.F. in motor (volts)
GI	Inclined Radiation (W/M^2)
GIst	Radiation in plane of array at test conditions (W/m^2)
H	Total head (Metres of water)
HS	Static head (Metres of water)
Ia	Motor armature current (amps)
Isc	Short circuit current at array test conditions (amps)
Ipm	Array current at maximum power point (amps)
Isc	Short circuit current of array (amps)
Io	Diode saturation current (amps)
I_L	Light generated current in array (amps)
I	Array current (amps)
Im	Motor current (amps)
I2	Current at array held by MPPT (amps)
J	Inertia of rotating components
Ke	Motor constant
K	" "
k	Pipeline friction constant
K	Boltzman constant
L	Constant used in array equation
MPPT	Maximum power point tracker
N	Number of PV cells in series
n	Speed (RPM)
OAE	Over-all array efficieny

ODE	Over-all daily efficiency for solar pump
OME	Over-all monthly efficiency for solar pump
Pm	Array power at maximum power point (watts)
Psm	Array power at maximum power point, test conditions(W)
P2	Power out of arrav, with MPPT fitted (W)
P_{out}	Power out of MPPT (W)
P_{hyd}	Pump hydraulic power (W)
PE	Peak efficiency for solar pump
q	Electronic charge in PV cell
Q	Flowrate (litres/sec)
R	Series resistance of array (ohms)
Ra	Motor armature resistance (ohms)
RP	Pulley ratio
t	time
T	Torque (Nm)
Tc	Cell temperature (°C)
Tcst	Cell temperature at test conditions (°C)
Tm	Motor torque (Nm)
Tp	Pump torque (Nm)
Voc	Open circuit voltage for array (volts)
Vsoc	Open circuit voltage for array at test conditions
V	Array voltage (volts)
V2	Voltage at array held by MPPT (volts)
Vm	Motor voltage (volts)
O	Magnetic flux
	Rate of change of short circuit current with cell temp.
	" " " " open " voltage " " "
	" " " " " " " with Incl. Rad.

CONTENTS

CHAPTER 1

INTRODUCTION

The solar powered water pump is a product of the space race of the 1950's and 1960's.

In the 1950's, experiments were being conducted into the electrical generating capacity of photovoltaic cells. By the end of the 1960's photovoltaics were widely used on space programmes. However it wasn't until the 1970's that the cost of photovoltaic cells had dropped significantly and their use in remote terrestrial applications became economically viable. The powering of water pumps became one area where photovoltaics was both a technical and commercial reality.

The solar powered water pump basically consists of a photovoltaic array, electric motor and pump, but there is a large scope for variation with each of these components.

The photovoltaic array may be fitted with concentrating lenses and a tracker to follow the sun. The motor may be either D.C.(shunt,series,combination or permanent magnet) or A.C., with an inverter between the PV array and motor. The pump may be either centrifugal or positive displacement: there is a wide variety of positive displacement pumps available, with helical rotor and piston pumps being commonly used in solar applications.

Other components may also be introduced to improve the

performance of the solar pump.For instance a device commonly called a Maximum Power Point racker(MPPT) may be fitted between motor and PV array to optimise the power transfer. For A.C. motors this power optimising can be achieved by varying the frequency output of the inverter and hence the speed of the motor. Also batteries may be fitted, ensuring storage of energy to be used during periods of low solar radiation. It is common however in water supply applications to use tanks and store water rather than electrical energy.

This thesis considers only the combination of stationary, non-concentrating PV array with a permanent magnet D.C. motor fitted with a MPPT, and a centrifugal pump.

1.1 The Developing Market For Solar Pumps

Solar powered water pumps presently represent a considerable capital outlay. For example, a solar pump sized to deliver 60,000 litres/day against 4 metres head would cost $10,000- $12,000. A similar sized diesel or kerosene powered pump would cost $3,000 and mains electric pump, assuming power is already at site, would be $1,500.

Obviously solar pumps are not an economic proposition where electric power is available at site or where diesel or kerosene is cheap, readily available and regular maintenance a possibility. Therefore solar pumps are limited to 'remote' applications.

In Australia the solar pump market is restricted to stock watering and village water supplies, (1) . However a recent study (2) suggests that solar pumps could be used in the desalination and transportation of some of Australia's

vast ground water supplies to areas deficient in water.

In developing countries solar pumps have applications not only for stock watering and village supplies but also for irrigation where crops and vegetables are grown intensively,(3 & 4).

An economic analysis for developing countries (3), shows that solar pumps are economical compared to high cost diesel installations but are not compared to wind pumps for village and stock water supplies. At present for irrigation, solar pumps are competitive with diesel power for heads up to 2m and should be competitive up to 7m in the next few years, while solar pumps cannot compete with wind pumps in areas with average monthly windspeeds greater than 2.5 m/sec. The study has concluded that as the cost of the solar array continues to fall, the range of applications for solar pumps will increase, eventually becoming the cheapest mechanised option for heads up to 30m in regions of low windspeeds.

A similar study has not been conducted for Australia but it is anticipated that as the cost of the PV array continues to fall the solar pump market will grow; especially in remote areas where the provision of fuel and the regular maintenance required of other power sources is difficult to achieve.

Although the economics and technology look good for the growth of the solar pump market, there are problems associated with the design and selection of solar pumps.

1.2 The Need for a Computer Model

The selection of a solar pump for a particular application is complicated and involves the matching of pump, motor and array to the specific hydraulic requirements as well as to the local solar radiation and temperature conditions. Various solar pump manufacturers and suppliers, contacted during the preparation of this thesis, have stated that they are unsure how to size a solar pump, being mainly guided by 'rule of thumb' and previous experience. Yet correct sizing of a solar pump is critical both from the manufacturer's point of view:-the unit must be competitively sized and priced to meet the duty; and from the user's viewpoint;- he can be confident that the solar pump will at least deliver the minimum required flow throughout the year,(5 & 6).

My own experience prior to this thesis project convinced me of the need for further information on the design , performance and selection of solar pumps. I was responsible for the purchase of the solar pump at Wakool (7) (used in this project) and involved in the purchase of another pump for a property near Bourke (8). In both situation different suppliers offered a variety of solar pumps, widely varying in PV array size and cost and yet all offering the same flow rate and head. No guarantees were offered on performance and clearly some pumps would not deliver the required flows. It was necessary to decide which solar pump was correctly sized and would perform as required.

Besides the difficulties of design and selection there are problems associated with testing a pump on site because it is not possible to quickly and easily assess long-term performance from instantaneous (or short term) radiation and pump measurements. This means a purchaser is unable to determine if the pump will perform as required.

The development of a computer model of a solar pump will assist in overcoming the difficulties mentioned above. The computer model will

a) Optimise a solar pump design for a particular climatic regime and range of applications.

b)Allow the performance of different solar pumps to be compared under identical operating conditions

c)Assist in the development of criteria for assessing a solar pump's performance on site.

CHAPTER 2

COMPUTER MODELLING OF SOLAR POWERED WATER PUMPS

2.1 DISCUSSION OF EXISTING MODELS

The computer model of a basic solar pump consists of the mathematical models of the PV array, motor, pump and pipeline. These are combined in a computer program with solar radiation and other relevant meteorological data as input.

Sir W. Halcrow & Partners (9), in a multimillion dollar study for the World Bank, have investigated the performance of nine solar photovoltaic water pumps, and developed computer models of these solar pumps. The study was aimed at the application of solar pumps in developing countries. Detailed monitoring of the pumps at site occurred only once per month, while solar radiation and basic pump data was totalised over each month.

From the test data, plus the computer models, the various solar pumps were compared on the basis of operating cost and efficiency. The effect of varying a solar pump design or component specification was predicted using the computer model.

One of the main conclusions of the investigation was that for a well designed system, a peak efficiency (total solar power falling on array divided by hydraulic power delivered by pump) of at least 3.7% is possible. To achieve

this, the combined motor/pump peak efficiency should be in excess of 45%, and the PV array in excess of 11%.(Cell Temp = 25°C.)

Baunstein & Kornfield (10) developed a simulation model of a solar pump using the mathematical model of a pump developed from first principles rather than directly from manufacturers' data. This approach allows the pump design to be optimised to best match the characteristics of the motor and array. When adapted for a specific application it requires a detailed knowledge of the subject pump with subsequent error due to the discrepency between pump theory and actual pump performance, although for the pump they tested this discrepency was only 5%. Unfortunately this test was limited to only the model for pump and D.C. Motor, no test was made of the complete unit under solar radiation.

For the purpose of this thesis project it was considered unnecessary to develop a model from the first principles of pump theory.

Hsaio & Bevins (11) sought to investigate the performance of a centrifugal pump coupled via a belt drive to a D.C. permanent-magnet motor directly powered by a PV array.

Rather than working from first principles of pump design, they based their pump model directly on manufacturers' data from an existing pump. Using a given operating point for the pump, they used the Laws of Similarity to generate other operating points. Hourly radiation data generated for a typical meteorological year by SOLMET was then input to the computer model and average monthly flows determined for a given head. By varying the

pulley ratio for the belt drive between motor and pump, the effect of the ratio on monthly flow was determined and an optimum ratio selected. This ratio is obviously specific to the type of pump, motor and array being modelled and the radiation for the region.

Unfortunately the paper contains no mention of any actual performance testing of the solar pump and so it is not possible to check the model's accuracy. Also the pump model is based on only one pump operating point supplied from manufacturers' data. All other operating points are generated from this one, leading to the possibility of fairly large errors when predicting pump performance.

2.2 MATHEMATICAL MODELLING OF SOLAR PUMPS

2.2.1. Characteristics of the PV Array

The solar cell is a semi-conductor device that converts the solar radiation to electrical energy with efficiencies for commercially available cells of around 12-15%. The cells are wired in series to form one panel, and the panels are wired in series or parallel to form the array. The panels are faced with an impact-resistant glass and backed with silicon to form a weather-resistant casing. The life of a panel is estimated by manufacturers to be around 20 years.

The panels are mounted in an aluminium or galvanised steel frame to form an array and wired in either series or parallel. The array, usually mounted on a concrete slab, must be designed to withstand high wind loads.

The output of the PV array is described by its current-voltage (I-V) curve, which varies as a function of cell temperature Tc and radiation intensity GI , such that

$$I=fn(V,GI,Tc) \qquad -1.$$

Manufacturers readily provide data for their PV panels, such as typical I-V curves for various radiation levels and cell temperatures. But before this data can be used in computer simulations and calculations it must be converted to some other form of presentation.

Singer et al (17) have developed a series of equations which describe the above relationship using three easily measurable parameters: open circuit voltage-Voc; short circuit current-Isc; and maximum power-Pm: plus an additional three parameters- the rate of change of open circuit voltage with cell temperature, $\partial Voc/\partial T_c$; the rate of change of open circuit voltage with radiation, $\partial Voc/\partial GI$; the rate of change of short circuit current with cell temperature, $\partial Isc/\partial T_c$.

The equations are based on the classical equation for the I-V relationship for one cell

$$I = I_L - I_o \left\{ exp\left[\frac{q}{A K_b T_c}(V+IR)-1\right\}\right. \qquad -2.$$

Using the simplification that I_L=Isc gives

$$I = I_{sc}\left[1-\left(\frac{I_o}{I_{sc}}\right)exp\,\lambda(V+IR)\right] \qquad -3.$$

for

$$\lambda = q/A K_b T_c$$

and under open circuit when I=O, V=Voc

$$\lambda = \frac{1}{V_{oc}} \ln\left(\frac{I_{sc}}{I_o}\right) \qquad -4.$$

Typical values for Isc/Io have been found to be in the range 10^{-8} to 10^{-10}, an average of 10^{-9} is assumed.(Checks conducted during the course of this thesis project have established that 10^{-9} is a reasonable ratio for PV panels used in this project.)

Also Singer et al have shown that at the maximum power point of the I-V curve

$$\frac{P_m}{I_{pm}^2} = \frac{V_{oc}}{20.7}\left(\frac{1}{I_{sc} - I_{pm}}\right) + R \qquad -5.$$

and

$$I_{pm}\left[1 + \frac{1}{20.7}\left(\frac{I_{pm}}{I_{sc} - I_{pm}} + \ln\left(\frac{I_{sc} - I_{pm}}{I_{sc}}\right)\right] - \frac{2P_m}{V_{oc}} = 0 \qquad -6.$$

Equation 6 is solved for Ipm numerically. R is then calculated using Eqn 5 which is substituted into Eqn 3 to give the I-V curve for a solar cell at a particular short circuit current and open circuit voltage.

Although these equations describe the performance of a single PV cell they can equally be used for a PV array with numerous cells in series and parallel, as the shape of the I-V curve for an array is similar to that for a single cell. Instead of the values of Isc, Voc etc being for a single cell, they are for the PV array and Pm & R are likewise determined for the total array with the effect of blocking diodes, wiring resistances etc being automatically accounted

for in the analysis. However for cases where the shape of the array I-V curve differs from the cell I-V curve, such as under partial illumination of the arrav, then the equations developed for the single cell are unsatisfactory.

The values of short circuit current and open circuit voltage vary with cell temperature and radiation. Therefore further relationships are required to account for the variation of these values from the values for standard test conditions mentioned in the manufacturer's data sheets.

Accordingly, three further relationships were developed by Singer et al.

Firstly, as Isc varies lineally with light intensity and is not a strong function of Tc

$$I_{sc}(Q, T_c) \cong I_{STc}\, GI\,(1+\alpha \Delta T) \qquad -7.$$

secondlv, as Voc is a logarithmic function of Q, decreasing with Tc,

$$V_{oc} = V_{soc}\left[1 - \frac{\gamma \Delta T}{V_{soc}} N\right] \ln(2.7183 + \beta \Delta GI) \qquad -8.$$

(The above equation is incorrectly presented in their paper)

Lastly,

$$P_m(GI, T_c) \cong P_{sm} \frac{I_{sc}(GI, T_c)\, V_{oc}(GI, T_c)}{I_{stc}\, V_{soc}} \qquad -9.$$

where

$$\Delta GI = (GI - GI_{ST}) \times 1\,SUN \qquad -10.$$

1 SUN=1000W/m^2

and

$$\Delta T = T_c - T_{cst} \qquad -11.$$

and Istc, Vsoc, Psm, are values for short circuit current, open curcuit voltage and maximum power, provided from manufacturer's data for standard conditions of radiation, GIst, and cell temperature Tcst.

Likewise, α is $\frac{\partial I_{sc}}{\partial T_c}$ a typical value suggested by Singer et al is α = 0.0025 1/C°, γ is $\frac{\partial V_{oc}}{\partial T_c}$ with a suggested value of γ =0.00288V/C° , and β is $\frac{\partial V_{oc}}{\partial GI}$ with β =0.5 1/1SUN.

Singer et al checked the PV model against various panels and arrays. The difference between approximated and real values was found to be less than 3%. When GI and Tc were varied the maximum difference was only 6%.

The above equations 3 to 11, are used to define the I-V characteristics of the solar array used in this project.

2.2.2 Characteristics of a Permanent Magnet D.C. Motor

Roger (13) has shown that the permanent magnet motor is most suited to PV applications, when compared with series or shunt D.C. motors. The permanent magnet provides a constant magnetic flux even at low light conditions resulting in a higher starting torque under these conditions than provided by the series motor which is generally considered a high torque motor under constant current supply.

The motor used in this project is a permanent magnet D.C. motor.

The fundamental relations for a D.C. motor are:

$$Em=Ke\phi n \qquad -12.$$

$$Vm=Em+IaRa \qquad -13.$$

$$T=K\phi Ia \qquad -14.$$

For a permanent magnet motor the magnetic flux is virtually constant and so the armature current Ia, equals the current supplied to the motor terminals Im,

$$Ia=Im \qquad -15.$$

therefore combining Eqns 12,13 &15 gives

$$n=\frac{V_m - I_m R_a}{k_e \phi} \qquad -16.$$

and combining 14 & 15 gives

$$T=K\phi Im \qquad -17.$$

From manufacturers' data for a particular motor, the slope of the current/torque curve gives the constant $K\phi$. However for the particular motor used in the project the current/torque curve did not pass through the origin, rather at T=O, current is a constant, B. It is likely that this is due to electrical and frictional losses within the motor which must be overcome before any torque is generated. Thus Equation 17 was modified for the particular motor to

$$T=K\phi(Im-B) \qquad -18.$$

Likewise from manufacturer's data, for zero speed (n=0), the terminal voltage in equation 16 equals the armature resistance multiplied by the given current. The armature resistance can then be calculated and the constants

$K_e\phi$ found from the slope of the curve.

2.2.3 Performance of a DC Motor Directly Connected to a PV Array

As shown, the PV array is not a constant current or voltage generator but rather the output varies as a function of the radiation and cell temperature, with the output voltage and current lying anywhere on the I-V curve. Accordingly when a D.C. motor is directly connected to this type of generator its performance varies markedly from performance under a constant voltage or current generator.

The operating voltage and current of the solar pump is determined by the intersection of the current/voltage curve for the motor/pump combination and the I-V curve for the array.Varying either the system conditions(Static Head or pipeline friction constant) or the input conditions(Radiation or cell temperature) will change the operating point of the system.

Performance therefore varies throughout the day as radiation and cell temperature varies, directly affecting the quantity of water pumped.

Initially, early in the morning, there is insufficient light falling on the PV array to generate enough current to overcome the starting torque of the motor and pump combination. Therefore for n=0 from equation 16

$$V_m = I_m R_a \qquad -19.$$

The values of Vm & Im are determined at the point where this relationship intersects the I-V curve for the array at the given radiation level.As shown in Figure 2.1, as the radiation level increases, the available current increases,

until the motor starts to turn at Im=Ip, the torque developed at this point is the starting torque of the motor/pump combination.

Roger (13) has found from tests conducted on a 1/2 kw submersible pump installation that immediately the motor starts to turn, back EMF,Em, is generated and the voltage rises rapidly (to Pt. B). Further increases in radiation increase the available current and hence torque. The motor/pump combination then increases in speed in accordance with equations 16 to 18, the operating point following line B,C,D.

For starting ,the curve O-A-B-C-D represents the relationship between I & V for the motor/pump combination. When stopping, the curve followed is D-C-B-E-F-O. It can be seen that the starting torque is higher than the stopping torque; the result of initial stiffness in bearings and seals which has to be overcome before the motor/pump will turn.

For a particular solar radiation level the maximum power avalable from the PV array occurs at the 'knee' or 'maximum power point' of the I-V curve. (Point N shown in Fig.2.1 for inclined radiation =GI). For a range of radiation levels the maximum power occurs along line M-N. It can be seen from Figure 2.1, for GI that the operating point for the motor/pump occurs at Point C, with less power being drawn than is available.

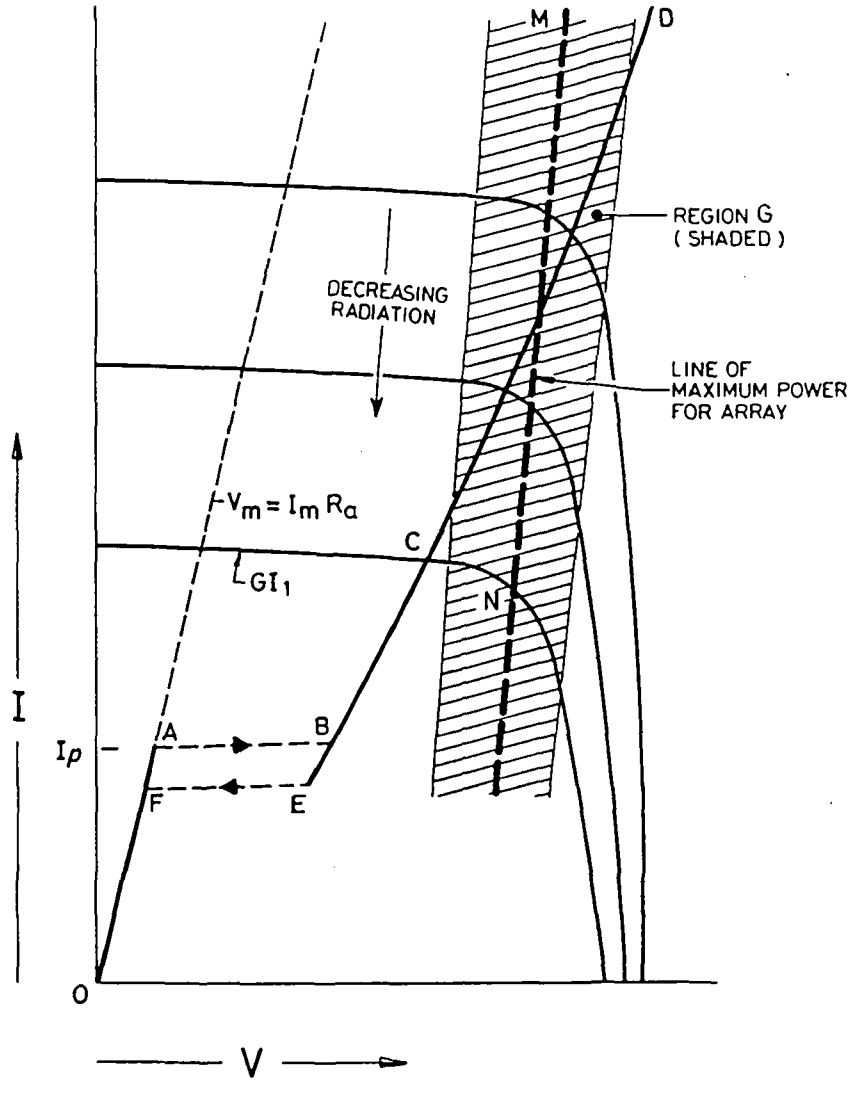

I - V CURVE FOR MOTOR / PUMP

Figure 2.1

The optimum match between motor/pump and PV array occurs when line B-C-D lies on or close to line M-N. The maximum power points vary with cell temperature as well as radiation. To account for this variation and to make the match between motor/pump and PV array realistic, a region can be defined,G, (Fig 2.1) wherein matching is considered to be good.

Roger (13) has identified two conditions which should be satisfied to ensure a good match between the motor/pump and PV array.

a) The operating curve must be as vertical as possible, that is, dIm/dVm must be as large as possible for all values of the rotation speed.

From Eqn16

$$\frac{dI_m}{dV_m} = \frac{1}{R_a} + \frac{1}{K_e \phi} \frac{dI_m}{dn} \qquad -20.$$

and Eqn 17

$$\frac{dT}{dn} = K\phi \frac{dI_m}{dn} \qquad -21.$$

combining

$$\frac{dI_m}{dV_m} = \frac{1}{R_a} + \frac{1}{K K_e \phi^2} \frac{dT}{dn} \qquad -22.$$

Therefore, to satisfy the above criterion for a good match, dT/dN , should be as large as possible.

For a centrifugal pump, the relationship between torque and speed is a polynomial one, where, except for initial starting, torque and dT/dN increase with speed. Therefore, from Equation 22, dIm/dVm also increases with n. Thus for a good match a pump, such as a centrifugal is required where the torque increases rapidly with speed in the region G.

As a comparison, a positive displacement pump has a torque which is virtually constant, independent of speed, giving

$$dT/dn=0$$

and

$$dIm/dVm=1/Ra$$

The positive displacement pump requires a high torque, and high current, right from the start, resulting in a horizontal I-V curve, which is a very poor match to the PV

array.

b) For low speed outside the operating region, G, dT/dn should be low. This ensures that as soon as there is sufficient current to turn the motor/pump, the unit accelerates quickly to reach the operating region G. So considering the equation

$$Tm-Tp=J\times 2\pi\times dn/dt \qquad -23.$$

For the speed to increase quickly to the region G, Tm> Tp for low speeds, Tm increases with solar radiation, therefore Tp should be low for low speeds. So dt/dn should be small for low speeds outside the region G and increase rapidly for speeds within the region.

It is not always possible to get a good match between motor/pump and PV arrav. One way to improve the match is to fit a device between the motor and PV array which matches their impedance. Such a device is commonly called a maximum power point tracker. Roger (14) discusses two devices which can be used.

2.2.4 Maximum Power Point Tracker (MPPT)

The device is essentially a D.C. to D.C. transformer which attempts to hold the PV array voltage close to its maximum power point, but allows the motor voltage to vary in accordance with the torque/speed requirements of the pump.

A MPPT is essential if a positive displacement pump is to be operated with any reasonable efficiency from a PV array.

Figure 2.2 shows a typical I-V curve for a motor/pump.

The motor/pump , under radiation GI_1,without a MPPT, would operate at Point 1 and the PV array at voltage V1,

under available power P1. But with a MPPT fitted the array operating point would become Point 2, and the array voltage ,V2, would be the voltage at maximum power P2.

The MPPT holds the power from the array constant at P2 (less losses in the MPPT) and allows the motor voltage and current to vary, therefore Vm=V3 and Im=I3.Therefore the increase in power available to drive the motor/pump is P2-P1, less power losses in the MPPT.

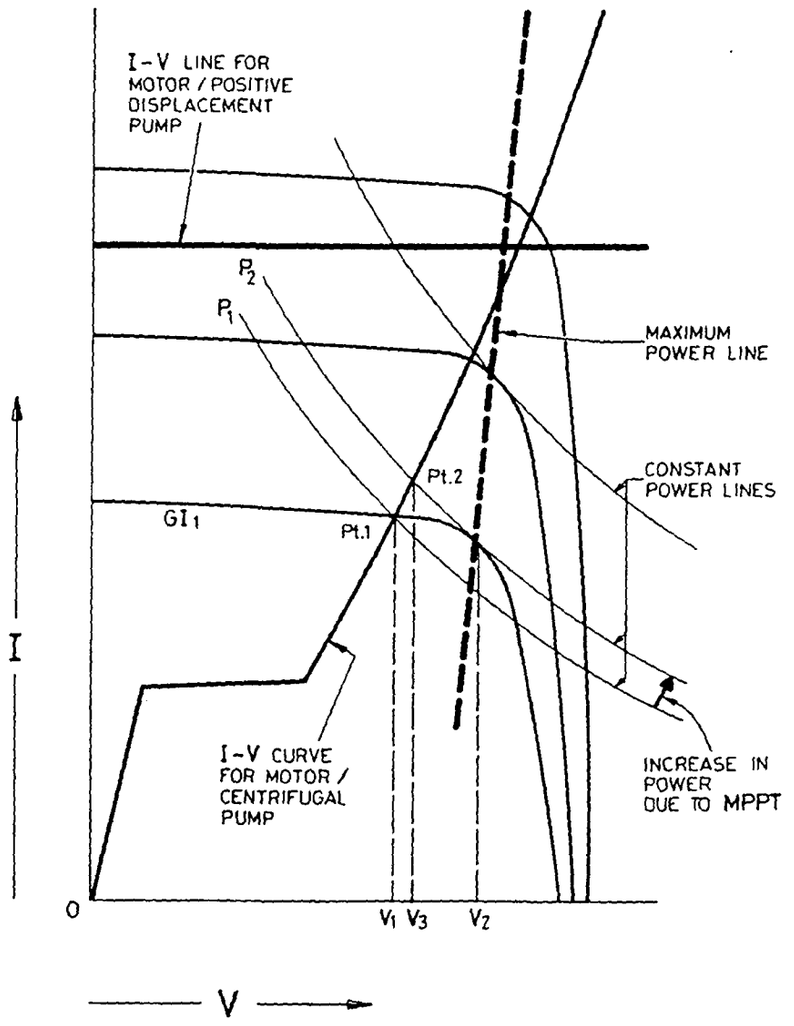

I-V CURVE FOR MOTOR / PUMP WITH MPPT.

Figure 2.2

The power at the output of the MPPT is Pout, which includes losses within the MPPT.Halcrow (9) has assumed a power loss of 10%.

From the basic relationship for power

$$Pout=0.9xP2=VmxIm \qquad -24.$$

P2 is held relatively constant by the MPPT and Vm and Im may vary to suit the motor requirements.

MPPTs are classified as either 'buck','boost' or 'buck-boost'. A buck is used when the voltage required by the motor/pump is less than the maximum power point voltage, and a boost is used when it is higher. A form of buck MPPT is used in this thesis project.

A typical circuit diagram for a MPPT is shown in Figure 2.3 , from Roger(14).

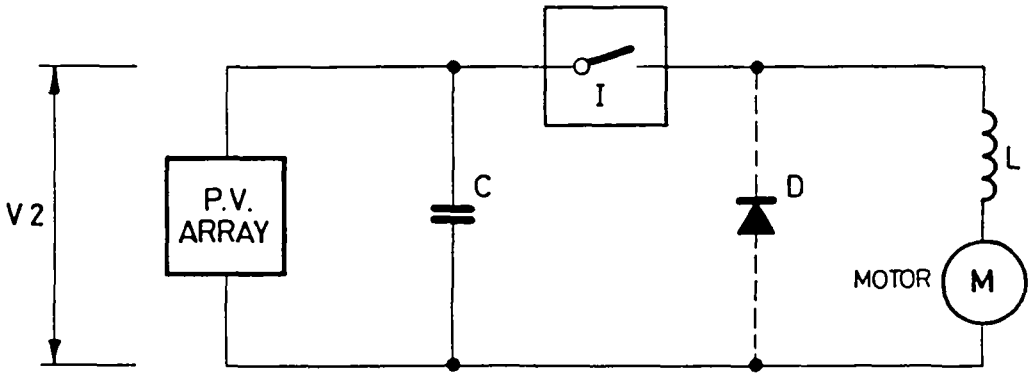

SCHEMATIC OF
MAXIMUM POWER POINT TRACKER CIRCUIT

Figure 2.3

The voltage at Maximum Power, V2, is either:

a) predetermined by the manufacturer this is only an approximate determination as V2 varies with radiation and cell temperature,

b) determined by a pilot cell attached to the array which monitors open circuit voltage for the given radiation and temperature conditions and varies V2 accordingly (15).

c) controlled by feedback from the array output power (16).

The electronic switch, I, is open and closed at a certain rate to ensure the array voltage is held at V2, the output voltage and current being allowed to vary to meet the needs of the motor/pump.

2.2.6 Characteristics of Pipeline Losses.

Hydraulic losses within the pipeline are the result of:

- pipe friction losses in the suction and discharge lines.
- entry and exit losses for the pipe line
- loss of velocity pressure
- losses in fittings including the strainer and flowmeter.

The flow in the pipe is turbulent therefore pipe friction losses are a function of the square of the flow velocity. Likewise entry and exit losses, velocity pressure and losses in fittings can be considered as proportional to the flow velocity squared.

Therefore $\text{Losses} \propto V^2$

or $\text{Losses} = kQ^2$

where k is a constant for the pipe line.

Therefore with a static head,HS, the total pumping head H is

$$H = HS + kQ^2 \qquad -25.$$

2.2.7 Characteristics of a Centrifugal Pump

As shown, the characteristics of a centrifugal pump are well suited to photovoltaic operation. In order to model a centrifugal pump, however, these characteristics must be defined mathematicallv.

As one of the aims of this project was to model an existing solar pump it was considered preferable to base the model for the centrifugal pump on the manufacturer's data for the actual pump installed, rather than work from the first principles of pump theory and develop a model.

Two relationships were selected to define the performance of the centrifugal pump.

$$H=fn(Q,n) \qquad -26.$$

and

$$T=fn(Q,n) \qquad -27.$$

Stepanoff (17) has indicated that relationship 26 above can be expressed as

$$H=An^2+BnQ+CQ^2 \qquad -28.$$

By selecting various points on the H-Q curve the constants A,B &C can be found. This relationship is dependent on friction and shock losses within the pump and is therefore specific to the pump being considered.

Unfortunately no equation could be found to express relationship 27 above, so an equation was developed to fit the data.

The form chosen was

$$T=Dn^2+EnQ+FQ^2 \qquad -29.$$

The constants D, E & F are found from the Power-Capacity (P-Q) curve where

$$T=P_{IN}/n \qquad -30.$$

CHAPTER 3

DETAILS OF THE SOLAR PUMP TEST RIG

3.1 SETTING UP THE TEST RIG

A Solar powered water pump was purchased by the Department of Water Resources in 1984. The object was to install the pump in an irrigation area of N.S.W., monitor its performance and make this information available to the public, especially the farming community.

Tenders were called and four quotations received to design and supply the solar pump. The pump was required to deliver 60000 litres/day against a total head of 4 metres for a total daily solar radiation on the horizontal plane of 18 MJ/m2. A copy of the specification is included in Appendix A.

The successful tenderer offered to supply a centrifugal pump, mounted on a pontoon and driven by a D.C. electric motor powered by Solarex panels and fitted with a maximum power point tracker.

The highly saline water required careful selection of pump materials and fittings.

Because of the remote location the pump is required to operate completely unattended for long periods. Also because the pump loses prime every time it stops, it was necessary that the pump be either a self-priming type or a submersible or floating centrifugal with the inlet submerged. The pump

was incorporated into part of the Department's Subsurface Drainage Scheme at Wakool, approximately 600 km south-west of Sydney (60km west of Deniliquin). It is required to pump water from a drain surrounding an evaporation basin back into the basin (the drain being fed by seepage from the evaporation basin).

The pump was installed in December 1984 however, a few weeks later strong winds combined with wave action in the drain capsized the pump. A subsequent investigation found the pontoon was poorly designed. The manufacturer repaired the pump and improved the pontoon's flotation. The pump was recommissioned with monitoring equipment on the 4th October 1985.

3.2 SITE DETAILS

Sketches showing the plan and cross-section of the installation are in Appendix B. Photographs of the installation are included in Appendix C.

From the levels given in the cross-section, it can be seen that the water level in the Peripheral Drain can vary between the levels R.L. 70.8 to R.L. 72.2, with the pipe discharge at approximately 74.7m. Therefore the static head varies between 2.5 and 3.9 metres. The Department tries to keep the level of the drain as low as possible.

The discharge line is 35 metres long, comprised of 10 metres of 50mm diameter flexible hose and 25 metres of 50mm diameter P.V.C. pipe.

It can be seen from the plan that the array faces north, and there are no trees or poles etc. to cast shadows over the array. The pontoon is positioned in the drain by 4

slack cables. The Peripheral drain is nearly 1 km long in an East-West direction and under certain conditions a fairly strong swell can develop and rock the pontoon.

Department personnel check the installation every few days. The surface of the array is cleaned approximately every month. The data loggers are changed every month.

3.3 SOLAR POWERED WATER PUMP

The water pump is connected via a timing belt drive to a 24 volt D.C. electric motor. The motor receives its power via a patented solar controller, from 12 solar panels each capable of 40 peak watts. 20 metres of cable connects the pump to the solar array.

The pump motor and solar controller are mounted on an angle iron frame supported in the water by two fibre glass (polystyrene filled) floats to form a pontoon. A sketch of the pump is in cluded in Appendix D.

A canopy covers the motor and controller to protect them from direct sun light and driving rain. The pump discharges into 50mm diameter flexible hosing leading to a rigid P.V.C. pipe on the shore.

Solar pump performance data and meteorlogical data is collected and logged every half hour into a solid state memory. Appendix E contains a summary of the Solar pump details.

3.3.1 Pump

The pump is a conventional centrifugal pump with a 50 mm suction and a 40 mm discharge and a 159 mm diameter impeller, mounted on its side with the inlet and eye of the impeller below water level ensuring the pump is always self

priming.

The pump has zinc-free bronze impeller and casing, and a mechanical seal and roller ball bearings. A manufacturer's data sheet of pump curves are included in Appendix F.

3.3.2 Motor

The motor is a .75 kw, 24 volt D.C. 2400 RPM electric motor manufactured by Honeywell, series BA 3637. The motor is marketed as being suitable for linking to solar arrays. A manufacturer's data sheet is included in Appendix G.

The solar pump manufacturer has guaranteed that the motor would not be damaged at low radiation levels when there is insufficient power to turn the rotor resulting in heating of the motor.

3.3.3 Maximum Power Point Tracker (MPPT)

The MPPT is a patented device designed by the solar pump manufacturer. It is connected between the solar array and the motor and is mounted on the pontoon.The MPPT requires cooling which is provided by water discharged from the pump flowing through a heat sink in the MPPT.

The manufacturer states that the function of the MPPT is to maintain the voltage at the array around 29.5 volts , ie the peak power point of the array. This ensures, it is claimed, that the pump will deliver more water at low radiation values and therefore improve the over-all efficiency of the solar pumping unit. Unlike more sophisticated MPPT devices, this one does not vary the voltage set point to follow the peak power point of the array.

It is possible for the MPPT to be disconnected from the circuit and the pump perform without it.

3.3.4 Cable

The cable is 16mm2 copper cable suitable for submersible applications and outdoor use. The resistance of the cable is 1.15 mOhms/m .The loop length of the cable is 40 metres.

3.3.5 Photovoltaic Array

The PV array was manufactured by Solarex. There are 12 panels Solarex type X100G. Each panel is made of 36 silicon solar cells and can deliver 40 peak watts at 16.2 volts under an intensity of 1000watt/m^2 at a cell temperature of 25 ° C. (Manufacturer's data sheets are included in the Appendix H) The panels are mounted in an aluminium frame bolted to a concrete slab. Each panel is wired in series with another to form a pair. The resulting six pairs are wired in parallel.

The array can be tilted through a variety of angles between 10° and 60°. Presently the array is a 34 degree(latitude tilt).

To suit the Department's requirements and prevent damage to the silicon backing by cockatoos, a wire gauze covers the back of the panels. It is anticipated that this gauze may increase the cell temperature of the arrav.

3.4 MONITORING EQUIPMENT

Two data loggers have been installed at site. One records voltage and current at the array, cell temperature of the array, flow rate, static pressure at the pump and solar radiation on the tilted plane. The second collects

data from a meteorological mast 10 metres high and records wind speed, maximum wind speed, wind direction, ambient temperature and solar radiation on the horizontal plane.

The loggers are changed once a month by Department personnel and sent by courier to Sydnev.

The Energy Authority of N.S.W. supplied and installed some of the transducers and provides computer facilities to interegate the data loggers.

The wind data is mainly for the Energy Authorities' use.

See Appendix E. for a summary of the monitoring equipment.

3.4.1 Data Loggers

The loggers are supplied by Unidata in Perth. They have a 16k capacity memory and powered by their own batteries. They have been programmed to access all transducers every 5 seconds, average the data over 1/2 an hour and log the result.

3.4.2 Pressure transducer

The pressure transducer is a Unidata type 6512A Piezo-resistive type with an error of -+5% of Full Scale Deflection with a range of 0-50kPa.

This type of pressure transducer was chosen because its non-metallic diaphragm and base would not be affected by the corrosive water being pumped.The unit is mounted on the discharge pipe of the pump, 0.3 metres above water level. Therefore 0.3 metresH_2o or approximatelv 3kPa has to be added to all pressure readings.

3.4.3 Flowmeter

The flowmeter is a 'Signet Flosensor' supplied by Tempress Controls, Sydney type MK515PO.

It is an inferential type of flowmeter. Four paddles mounted on a titanium spindle are each fitted with ceramic magnets.The paddles rotate past a coil and generate an alternating current. Both the frequency of the current and the amplitude of the signal are directly proportional to the flowrate. The error is +-1.0% of Full Scale Deflection with a range of 0.3 to 12.0 lit/sec.

Unfortunately because of the low flows a 32mm dia flowmeter was required, necessitating 32/50mm dia reduction and expansion joints adding extra head loss to the system.

The data logger counts the number of pulses per unit time and logs the average.The Energy Authority's computer later coverts this to flowrate.

The flowmeter was calibrated prior to installation at the Department's Hydraulics laboratory at Manly. A calibration curve was developed. The error in the meter was found to be linear and this is allowed for when processing the data.

3.4.4 Pyranometers

The pyranometer mounted on the solar array at the same angle as the array is an Eppley Black and White, with a millivolt output. This voltage is directly proportional to the solar radiation.

The pyranometer on the horizental plane is a flat silicon cell supplied by Unidata.

3.4.5 Voltage and Current Measurements

The voltage and current measurements are taken at the solar array, the current is measured using a shunt. It was originally intended to also have a voltage tapping on the electric motor side of the solar controller in an attempt to see the actual effect of the solar controller. However difficulties were encountered at site and this had to be abandoned.

3.4.6 Cell Temperature Transducer

A temperature sensitive transistor was placed in the silicon cover on the back of one of the solar panels. It was not possible to place the transistor right at the back of the photovoltaic cell.

The transistor was placed as close as possible to the back of the photovoltaic panel but not touching the panel. It was feared that the cell might be damaged if any attempt was made to directly bring the transistor into contact with the cell.The 'cell temperature' readings therefore are not true cell temperature values. However it is considered that the relationship between the 'true cell temperature' and the actual reading would probably be linear and therefore give a good indication of the effect of cell temperature variation on panel performance.

3.5 PROCESSING OF DATA

The data loggers are sent directly to the Energy Authority of N.S.W. who interegate the loggers, apply the appropriate conversion and calibration factors and then record the data on floppy 5 1/4 discs in ASCII format. The floppy discs are then forwarded to the Department of Water

Resources.The data is later transferred to the UNSW VAX Computer and into a format which can be directly read by the simulation package TRNSYS.

A typical printout of the data is included in AppendixI.

3.6 DIFFICULTIES ENCOUNTERED IN THE OPERATION AND MONITORING OF THE SOLAR PUMP

3.6.1 Capsize of Pump

The pump was installed and commenced operation in December 1984, but after 3 weeks of operation the pump capsized and the motor, solar controller and pump bearings were damaged.

The pump capsized due to poor stability and faulty floats. The Manufacturer repaired the pump and it was recommissioned in early October 1985 with monitoring equipment added.

3.6.2 Blockage of Pump Inlet

In late January 1986 the strainer was found to be completely blocked by slime and vegetation. It is evident that the strainer needs to be checked every few weeks to ensure that this does not recurr.

When the suction is blocked there is a possibility that the mechanical seal may be damaged due to the higher suction pressures in the casing, resulting in poor performance when the suction is cleared. Fortunately this did not occur.

3.6.3 Flowmeter

Over the months August to November 1986 a fault devoloped between the flowmeter and data logger resulting in incorrect flows being recorded. After replacement of the flowmeter and checking of the data logging equipment, the

fault was found to be in the wiring to the logger.

3.6.4 Incorrect Calibration of Flowmeter

During a site check of the pump's flowrate in January 1987 it was found that the measured flowrate did not match the flowrate calculated by the Energy Authority's computer, from pulse rates recorded by the data loggers. The error was eventually found to be with the flowmeter calibration factor used in the Energy Authority's computer to convert pulse rate to flowrate. Fortunately the error was simply rectified by multipying all flowrates since October 1985 by 0.6 using the TRNSYS simulation package. Accordingly the pipeline friction constant ,k, was significantly increased.

3.6.5 Faulty Data Loggers

During a one month period October to November 1986, all data was lost due to faulty loggers.

3.6.6 Overload of Data Loggers

With the removal of the MPPT in November 1986, the flowrate increased with a subsequent increase in the number of pulses per unit time from the flowmeter.Over the five second recording period this overloaded the pulse counter in the Data Logger and it zeroed and started recording again, resulting in apparently low flows under high radiation levels. From analysis of the data it appears the problem occurred for flowrates above 2.4 lit/sec.Flow data over this period was therefore corrected, based on the static pressure readings, which were not affected.

CHAPTER 4

DEVELOPMENT OF THE COMPUTER MODEL OF THE SOLAR PUMP

4.1 THE CONTROL PROGRAM

The computer model for the solar pump was divided into separate modules, one for each component of the solar pump. The modules were the PV array, MPPT (optional), motor, pump and pipeline as shown in the Figure 4.1 below.

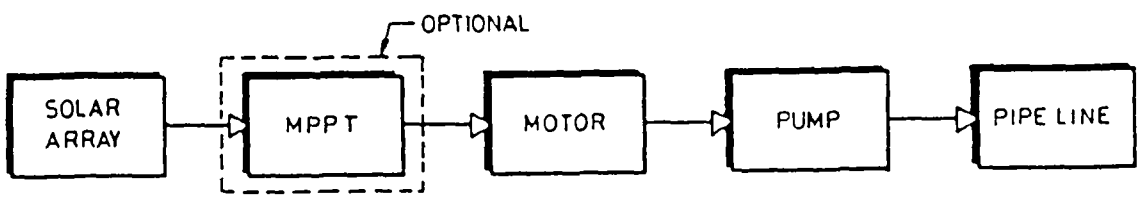

Figure 4.1

These modules were then combined under the transient simulation program TRNSYS (18), developed by the University of Wisconsin and the University of N.S.W.. TRNSYS is specifically designed for the simulation of solar energy systems. It has a modular structure, which allows other modules, written in the FORTRAN language, to be incorporated within it.

Data collected at site (eg meteorological), over a selected period of time, can be input to TRNSYS with the resultant output being either for the same time interval or totalised over a specified period.

The input data required for the model is radiation on the plane of the arrav, cell temperature, static head,the pipeline friction constant and resistance of the cable. The resultant output is flowrate: however other values can also be predicted, namely: total head, torque, speed, voltage and current.

The basic program flow chart is shown in Figure 4.2 on the next page.

The program for the PV array is titled TYPE34.FOR, a simplified flowchart for the program is in Appendiv J.

The programs for the Motor, Pump, MPPT and Pipeline are combined under the one program TYPE351.FOR, the program for the solar pump without a MPPT is titled TYPE35.FOR; simplified flowcharts for both programs are in Appendix J.

The theoretical basis for each of the modules shown in Figure 4.2 was discussed in Chapter 2 , specific details for each of the modules used in TRNSYS are discussed below.

4.2 PHOTOVOLTAIC ARRAY

4.2.1 TRNSYS Model of PV Array

An attempt was initially made to use the PV Array model incorporated in TRNSYS. This model was developed for concentrator PV arrays with liquid cooling of the cells. However, even after extensive testing and modification of the model it could not satisfactorily simulate the PV performance data provided by the array manufacturer, SOLAREX.

The greatest discrepancies were

(a) the knee of the I-V curve simulated by the model was too 'sharp'.

(b) the slope of the I-V curve between the 'knee' and

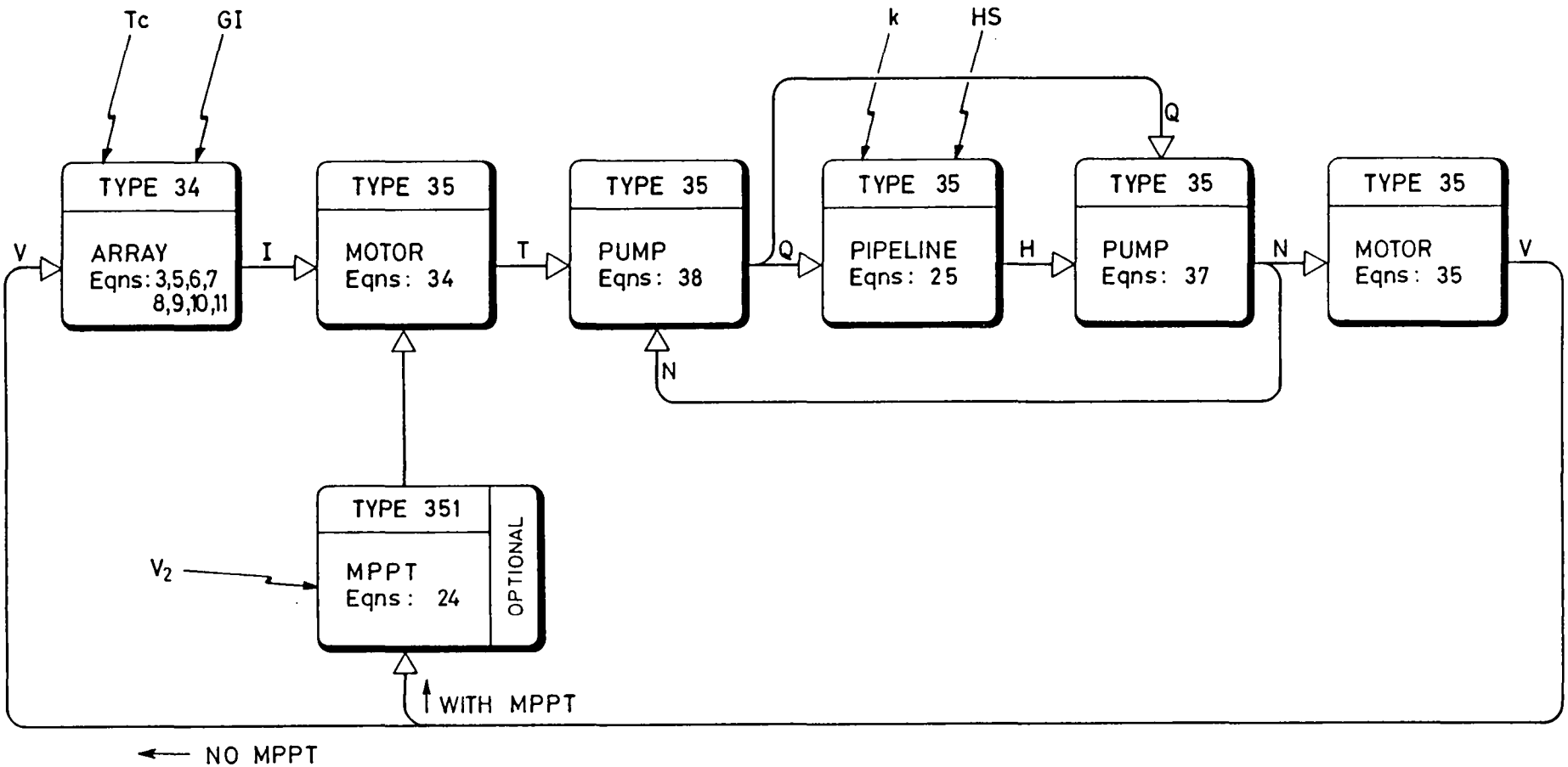

SIMPLIFIED FLOW-CHART FOR SOLAR PUMP COMPUTER MODEL

Figure 4.2

open circuit voltage was too steep.

It was therefore decided to use the alternative array model developed by Singer et al.The theoretical basis for this model was discussed in Chapter 2.

4.2.2 PV Array Model Used in Solar Pump Program.

In Chapter 2 six parameters were mentioned, which can define the performance of a PV array, namely Voc,Isc,Pm,α, γ, & β .

At the time of commissioning at the Solarex factory, values were recorded for Isc (15.6 amps) and Voc (33.1 V) under inclined radiation of GI=935 watts/m^2 and an estimated cell temperature Tc = 58°C.

Unfortunately the uncertainty in the value for Tc (Section 3.4.6) and the inability to determine Pm, meant these values could not be used in the computer model.

Therefore the values provided by Solarex for one panel, have been used. These values have an accuracy of +- 10%. No information has been given by Solarex on expected reduced performance when the panels are wired to form an array. To provide some account of this in the computer model the Peak Power (Pm) has been reduced by 5%.

Data provided by Solarex (data sheet included in Appendix H), at Standard conditions of Tc=25°C and GI=1000W/m^2

Gives :

Voc = 40.0V

Isc = 15 amps

Pm =440W-5% =420W

also from the data sheet

α =25uA/°C/cell area cm^2

each cell is 100 cm^2 (100mm x 100mm)

therefore α = 2.5mA/°C

and γ =2.4mV/°c/(No. of cells in series) ,

there are 72 cells in series (36 per panel),ieN=72

No value is given for β in the data sheet. Singer suggests a value of 0.5 , however 0.4 appears reasonable when compared against the graphs of cell performance for various radiation levels based on Solarex data.

These parameters are incorporated into the program defining the PV array performance, TYPE34;FOR.

4.3 MODEL OF THE PERMANENT MAGNET DC MOTOR

The initial model for the motor was based on characteristics provided by the motor supplier Honeywell. The efficiency of the model was found to be significantly greater than the motor at site. Honeywell therefore requested detailed information from the motor manufacturer Pacific Scientific, and different characteristics were provided, (see Appendix G). The new model, based on these new characteristics, showed the motor to be less efficient, which more closely matched the motor at site.

This example highlights the difficulties in basing a computer model of a solar pump solely on data provided by component suppliers or manufacturers.

The following equations are based on the new motor characteristics.

From the equations defined in Section 2.2.2 and using data provided by the motor manufacturer, the various motor

constants can be determined.

Firstly from Equation 18

$$T = K\phi (Im - B) \qquad -31.$$

The constant $K\phi$ is the slope, given as 0.755 lbin/amp or 0.0853 Nm/amps.

At stall torque, n=0

$$I = 185 \text{ amps}$$

$$T = 138 \text{ lb. in.}$$

giving B = 2.22 amps

and from Equation 16

$$Vm = Em + Ia\,Ra \qquad -32.$$

at zero speed the back EMF, Em, is zero,

therefore $Ra = Vm/Ia$

and from stall torque conditions

$$Ra = 24/185 = 0.130 \text{ ohms.}$$

Note, performance data is given at the rated voltage of 24 volts

and Ra is a constant for the motor.

Thus, Equation 16 may be written as

$$n = \frac{Vm - 0.13\,Im}{Ke\,\phi} \qquad -33.$$

The constant $Ke\phi$ has been given by the manufacturer as $Ke\phi = 0.00893$ V/rpm (This can also be determined from the performance charts).

The two equations defining the performance of the motor are thus

$$T = 0.0853(Im - 2.22) \qquad -34.$$

and

$$n = \frac{Vm - 0.13\ Im}{0.00893} \qquad -35.$$

These equations are incorporated into the program TYPE35;FOR which models the motor, pump and pipeline.

4.4 MODEL OF THE MPPT

The MPPT supplied with the solar pump is of 'Type A' mentioned in Section 2.2.4. The manufacturer states the voltage V2 should be held at 29.5 volts, however voltage readings recorded at the array, indicate this voltage is actually about 31.8 volts.With the MPPT removed the voltage never rises above 27 volts. Obviously V2 has been incorrectly set in the factory.

The model of the MPPT involves determining array output current, I2, (from the PV model) for the voltage V2 = 31.8 volts, for a given radiation and cell temperature.

The output power of the array is then calculated from

$$P_2 = I2 \times V2 \qquad -36.$$

It is assumed that on average there are 10% losses through the MPPT, resulting in power to the motor, Pm.(equation 24)

$$Pout = 0.9\ P_2 = Vm \times Im$$

For a given radiation and cell temperature Pout is held constant, while Vm and Im are allowed to vary.

Data provided by the manufacturer indicates that losses within the MPPT under stall torque conditions(ie high current),vary between 27% and 40% for current 15 to 28 amps. Unfortunately no information is available on losses for the normal operating range of the solar pump used in this

project, although the manufacturer expects a loss of about 7% for a 750 watt array. A loss of 10% has been assumed by Halcrow (9).

4.5 MODEL OF THE PIPELINE

As shown in Section 2.2.6 the head and flow relationship for the pipeline can be defined by Equation 25 as

$$H = HS + kQ^2$$

The static head, HS, varies, depending on the level of water in the peripheral drain in which the solar pump floats. The level varies with rainfall and seepage from the evaporation ponds. No record is taken of the level in the drain, therefore static head must be calculated from the pressure readings recorded at the pump. The pressure transducer is mounted on the discharge line, 0.3 metres above the water level, so 0.3 metres or (3 kpa) must be added to all pressure readings. The measurement is discharge pressure only and does not include pressure losses in the suction side of the pump, but these are considered to be negligable.

The constant, k, is independent of static head and flowrate. It only varies with frictional changes in the pipeline such as scaling on the walls of the pipe, or kinking or damage to the flexible hose or pipe. k can be determined when the measured head, H, is plotted as a function of Q^2.

Soon after installation in October, 1985, when the internal surface of the PVC pipe was clean, k was found to be 0.2 (metres /(litres/sec)^2). When the PVC pipe was

checked in March, 1987, the internal surface was badly scaled (Photo in Appendix C) and k was 0.25. For ease of calculation it has been assumed that k varies linearly with time over the 18month period from October, 1985, to March 1987.

The constants HS and k can be determined from various plots of $H=fn(Q^2)$.The resulting straight line has a y intercept HS and a gradient of k. A simple computer program has been written to scan the data and determine HS at weekly or fortnightly intervals. Because of the capacity of the drain, level changes occur slowly making weekly or fortnightly values for static head acceptable.

However one caution must be observed when processing the data: during periods of low radiation the pump may be turning and generating pressure but not enough to overcome the static pressure and pump water, and during a same half hour recording period the pump may deliver water for only a few minutes. When the head and flowrate are averaged for the half hour period and the values recorded, the relationship $H = fn(Q^2)$ for the average values does not applv. This difficulty is overcome by using only data which indicates continuous flow for the whole half hour period. The resulting static head is averaged over the weekly or fortnightly period.

4.6 MODEL OF CENTRIFUGAL PUMP

Two equations have been given in Chapter 2.2.5 which describe the performance of the pump over its normal operating range. Equation 28 describes the relationship between flow, head and speed. From pump performance curves

provided by the manufacturer, three points can be chosen. From the solution of three simultaneous equations the constants A, B and C can be determined. They are

$$A=\frac{6.0}{n_o^2} \qquad B=\frac{0.67}{n_o} \qquad C=-0.20$$

giving

$$H=\left[\frac{6.00}{n_o^2}\right]n^2 + \left[\frac{0.67}{n_o}\right]nQ - 0.20Q^2 \qquad -37.$$

where n_0 = 1300 rpm

Likewise for Equation 29

$$D=\left[\frac{0.65}{n_o^2}\right] \quad , \quad E=\left[\frac{0.94}{n_o}\right] \quad , \quad F=-0.055$$

giving

$$T=\left[\frac{0.94}{n_o^2}\right]n^2 + \left[\frac{0.65}{n_o}\right]nQ - 0.055Q^2 \qquad -38.$$

CHAPTER 5

PERFORMANCE OF THE SOLAR PUMP AND COMPARISION WITH THE COMPUTER MODEL

5.1 PHOTOVOLTAIC ARRAY

5.1.1 The I-V Curve

Values of voltage and current, for selected radiation and cell temperatures,have been plotted in Figure 5.1. The conditions of 900-930 Watts/m^2 at 50° C is frequently recorded during summer around midday. 495-515 Watt/m^2 at 25° C is typical of early morning conditions during winter and is often the conditions existing when the pump starts to deliver water. The figure shows a) the manufacturer's specified performance curve (based on one panel) b) the data recorded at site and c) data predicted by the model. There are only two operating voltage ranges: approximately 30-33 volts (to the right of the knee) for performance with the MPPT and 21-25 volts (to the left of the knee) for performance without.

5.1.1.1. Performance of Site Array

The recorded data compares well with the manufacturer's data for operation without the MPPT under the low radiation and reasonably well under the higher radiation.

Performance with the MPPT is significantly lower than expected for both radiation conditions. This may be the result of wiring and connection losses within the array,

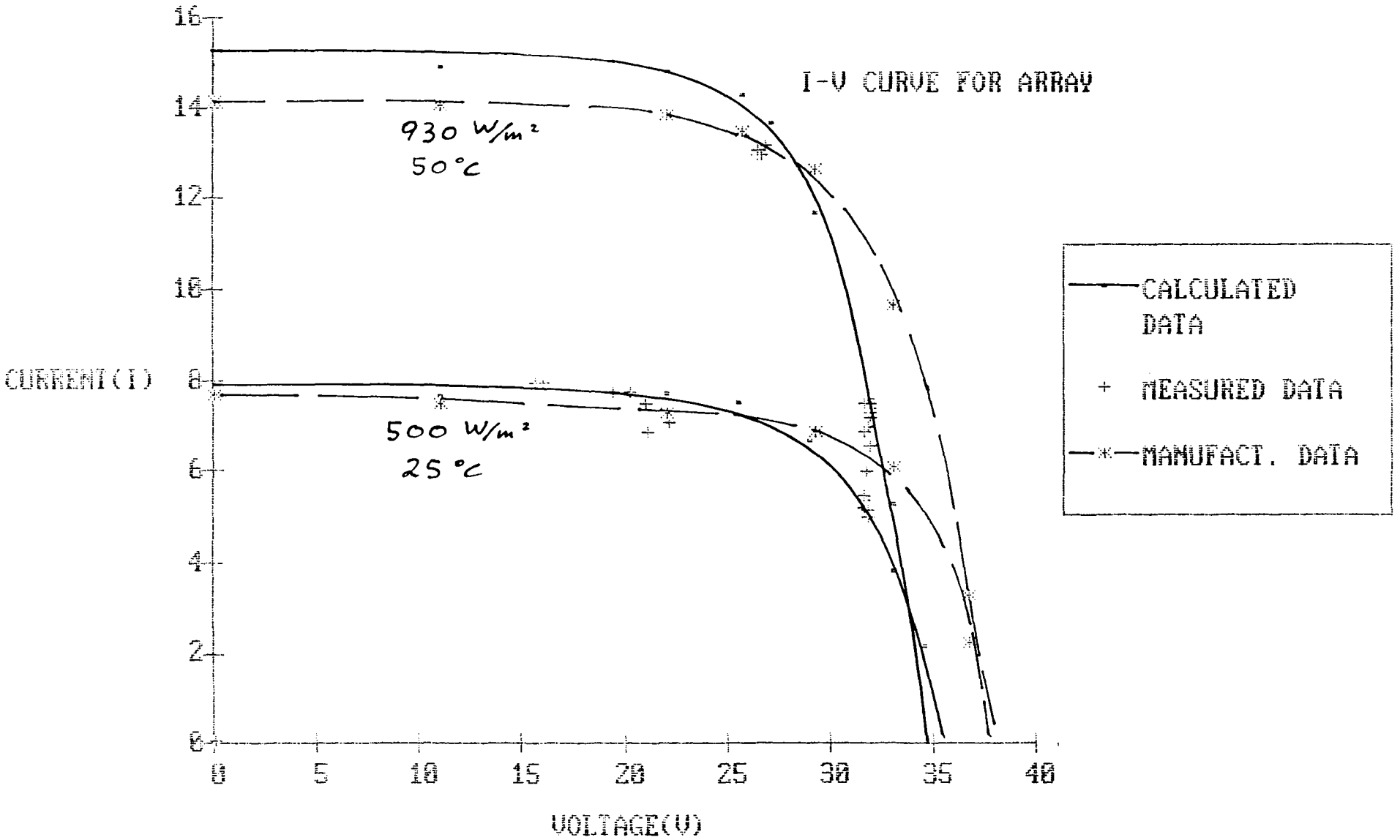
I-V CURVE FOR ARRAY
930 W/m²
50°C
500 W/m²
25°C
CALCULATED DATA
MEASURED DATA
MANUFACT. DATA
CURRENT(I)
VOLTAGE(V)
0
2
4
6
8
10
12
14
16
0
5
10
15
20
25
30
35
40

FIGURE 5·1

which would have a more noticeable effect at higher voltages. The manufacturer's data does not indicate what allowance, if any, should be made for wiring losses, nor is any indication given of the effect of variation in individual panel performance on the over-all performance of the array.

This reduced array performance with the MPPT would have a drastic effect on the solar pump's performance being well below that expected by the solar pump manufacture.

5.1.1.2. Performance of the Model

The model closely simulates the site array's performance with the MPPT but it over-estimates the array performance without the MPPT.

Although the model is based on manufacturer's data it does not adequately model the manufacturer's curve except under low radiation conditions without the MPPT. An attempt was made to "fine tune" the constants used in the array model but this was unsuccessful due to the number of constants and the range of cell temperature, radiation and voltage which the site array experienced.

5.1.2. Over-all Array Efficiencv

Figures 5.2 and 5.3. show the plot of Over-all Array Efficiency (OAE) as a function of inclined radiation for various values of cell temperature.

The OAE is defined as

$$OAE = \left. \frac{V \times I \text{ (measured at array)}}{\text{Total Area of Array} \times GI.} \right|_i \qquad -39.$$

where i is a 1/2 hour recording period.

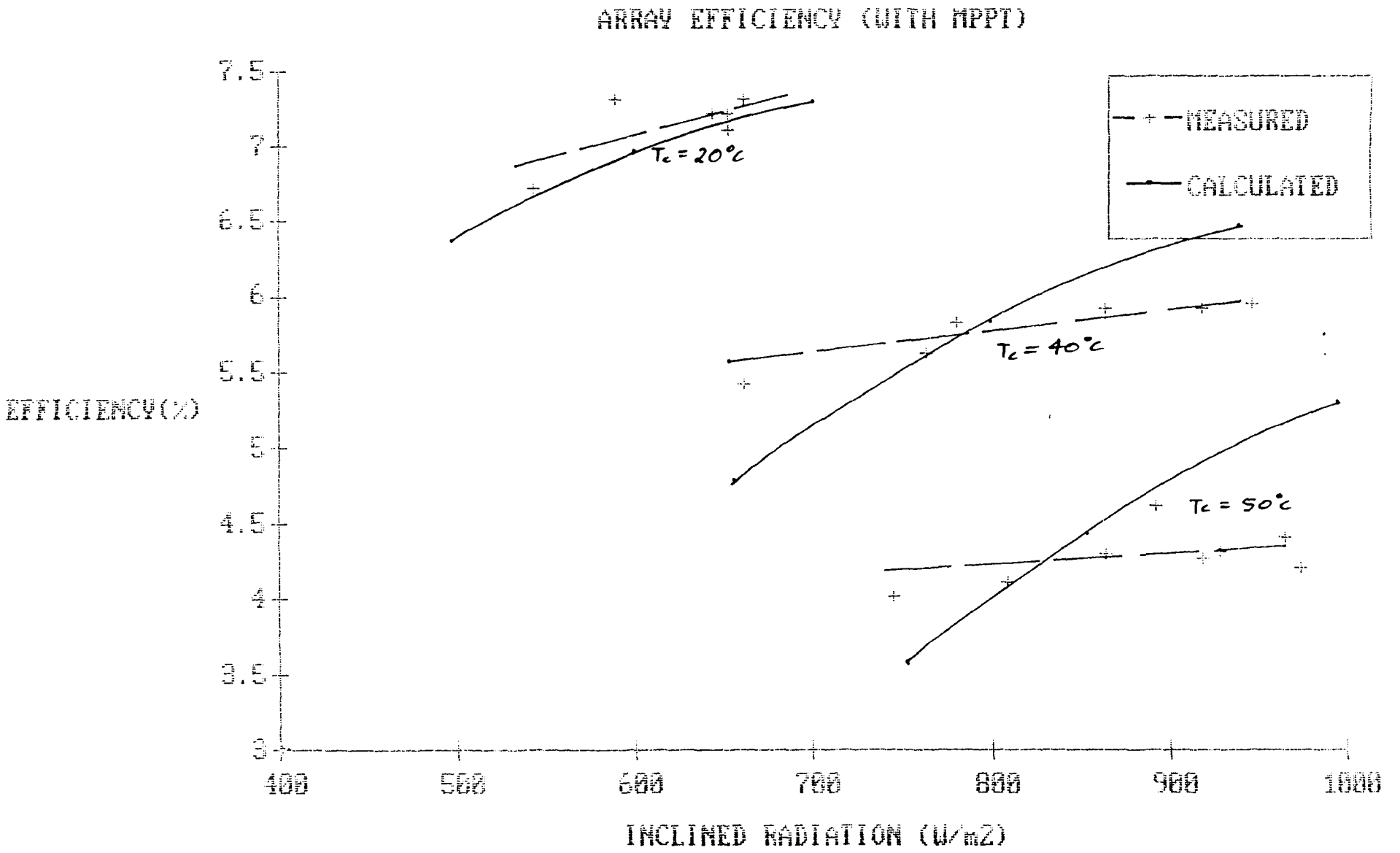
ARRAY EFFICIENCY (WITH MPPT)
EFFICIENCY(%)
7.5
7
6.5
6
5.5
5
4.5
4
3.5
3
400
500
600
700
800
900
1000
INCLINED RADIATION (W/m2)
MEASURED
CALCULATED
Tc = 20°C
Tc = 40°C
Tc = 50°C

FIGURE 5·2

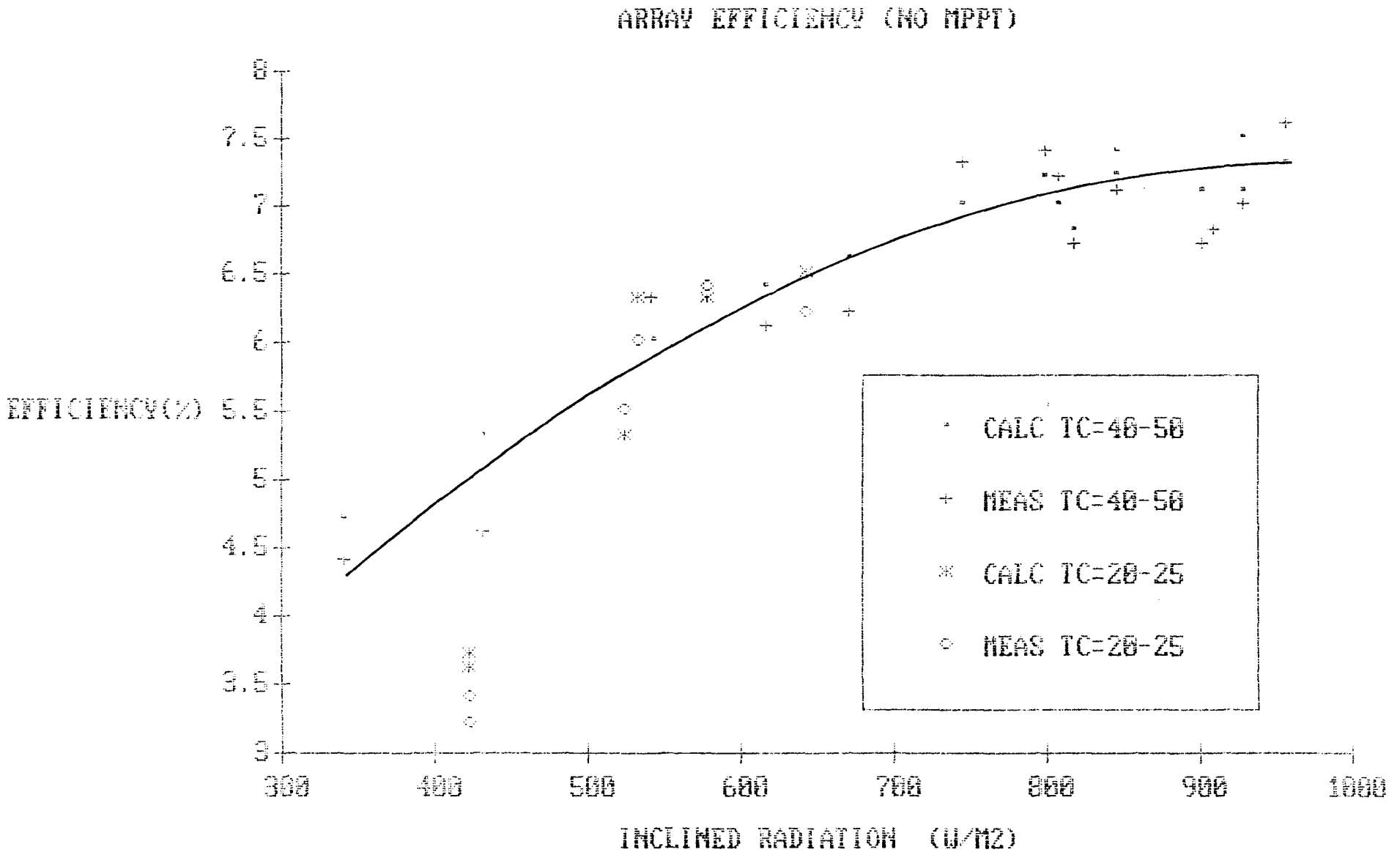
ARRAY EFFICIENCY (NO MPPT)
EFFICIENCY(%)
8
7.5
7
6.5
6
5.5
5
4.5
4
3.5
3
300
400
500
600
700
800
900
1000
INCLINED RADIATION (W/M2)
CALC TC=40-50
MEAS TC=40-50
CALC TC=20-25
MEAS TC=20-25

FIGURE 5·3

With the MPPT (Figure 5.2) the OAE is a strong function of the cell temperature, which is to be expected considering the pump operates at a voltage which is to the right of the "knee" (Figure 5.1) where the open circuit voltage is related to cell temperature. A small increase in cell temperature therefore leads to a large drop in current.

Reducing the set point voltage held by the MPPT to a value nearer the "knee" or to the left of it, diminishes the effect of cell temperature on the OAE. This effect can be seen in the performance of the array without the MPPT (Figure 5.3).

Without the MPPT, efficiency increases with radiation while cell temperature has little effect on the OAE: this is contrary to operation with the MPPT. The variation of the OAE with radiation is directly related to the match between the motor/pump and the array. From Figure 5.1 it can be seen that the operating point moves away from the "knee" as the radiation decreases. The closer the operating point to the "knee" the better the match between motor/pump and array. Without the MPPT under radiation less than 500 Watt/m2 the OAE is shown to increase with cell temperature. This is due to a characteristic of photovoltaic panels whereby short circuit current increases with cell temperature. Under low radiation conditions the operating point is well to the left of the "knee" where this effect is significant.

With the MPPT removed the maximum OAE is 7.5%, based on array area ;or 9.2% based on cell area. This is less than the target figure of 11% (based on cell area) suggested by

Halcrow (9). A better match between motor/pump and array would result in a higher efficiency than 9.2%.

5.2. MAXIMUM POWER POINT TRACKER

In discussing the development of the MPPT model in Chapter 4, it was mentioned the setpoint voltage is determined by the manufacturer and the MPPT ensures the array operates at this voltage. An analysis of measured data for pump operation with the MPPT however indicates this is not the case. The voltage varies from 31.0 to 32.2 volts. The limitations of the electronic circuitry may make it impossible to reduce this voltage variation, but such a variation can have a dramatic effect on the power output of the array as shown in Figure 5.1. The increase in voltage from 31.5 to 32.2 can reduce the power output by 25%. Reducing the set point voltage to the 29-30 volt range would cause the array to operate in a more stable region of the curve, close to the "knee" or just to the left of it.

The model of the MPPT does not allow for this variation in voltage and hence it is difficult to determine the power output of the array with a MPPT when operating to the right of the "knee". A typical value of 31.8 volts was chosen for the model. This generally results in the power output for the model being less than the measured data.

An efficiency of 90% was initially chosen for the MPPT (Section 4.4) model, but this consistently resulted in flowrates far in excess of those measured. The model of the array is known to underestimate power output and from measured data, without the MPPT, the model of the motor/pump is considered satisfactory. Therefore the problem probably

lay with the MPPT: with an efficiency of 90% being too high.

It is not possible to directly **measure** the efficiency of the MPPT, all that can be determined is the total efficiency of the combined MPPT,motor & pump. However, the efficiency of the MPPT can be **estimated** if this efficiency is divided by the efficiency of the motor/pump for performance without the MPPT, provided under both conditions the efficiencies for the motor/pump are similiar.

Thus

$$\text{Efficiency MPPT} = \frac{\text{Eff. MPPT,motor \& pump [with MPPT]}}{\text{Eff. motor \& pump only [withOUT MPPT]}} \quad -40.$$

This can be achieved by ensuring the pump is operating at similiar values of hydraulic head and flowrate for both conditions. Figure 5.4 shows the calculated efficiency of the MPPT.

The months of November 1985 (with MPPT) and November 1986 (without MPPT) are used in the graph. There were very few points with similiar flowrates and head. It can be seen that the efficiency of the MPPT is approximately 72%. This compares with the results supplied by the manufacturer for stall torque conditions. It also may explain why the manufacturer was very concerned, when the pump was installed, that the MPPT was adequately cooled. An array output of 400 watts would result in 110 watts energy dissipated in the MPPT!!

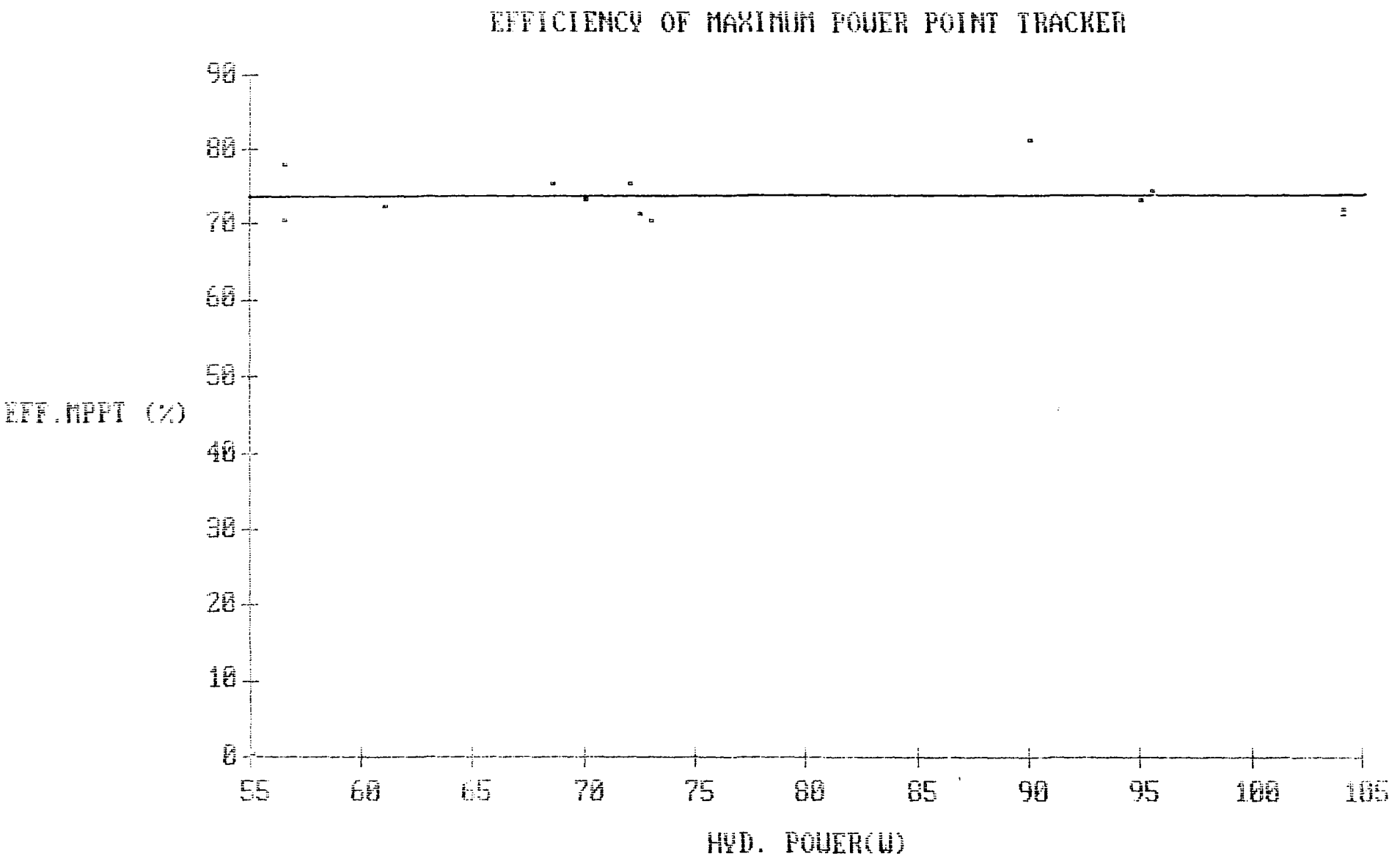
EFFICIENCY OF MAXIMUM POWER POINT TRACKER
EFF.MPPT (%)
90
80
70
60
50
40
30
20
10
0
55
60
65
70
75
80
85
90
95
100
105
HYD. POWER(W)

FIGURE 5.4

5.3.MOTOR AND PUMP

Most discussion in this section regarding the motor and pump performance is based on results taken in November and December 1986 when the MPPT had been removed and the current and voltage entering the motor can be recorded.

The peak efficiency for the combined motor and pump is 47%. This exceeds the target efficiency of 45% suggested by Halcrow (9).

It is not possible to individually check the motor or pump as torque and speed in the motor drive shaft is not measured at site. However, some speed tests of the drive shaft, taken at site using a tachometer, along with voltage and current readings, indicate the model predicts within 2% the speed of the shaft for a given voltage and current, although the accuracy of this result may be due more to good luck than good modelling.

An indication of the pump's performance can be gained if the equations defining motor performance are considered to be reasonable. Then, using these equations, plus the voltage and current measured at site, an estimate of the torque and speed at the pump shaft can be made. This is the basis for the following section.

5.3.1 The Pump

A torque/speed curve based on manufacturer's data, model results and measured data is shown in Figure 5.5, for a static head of 3.6 and a friction constant of 0.245 for the pipe line.

The plot of manufacturer's data is combined with information supplied by Karassik et al (19). Karassik

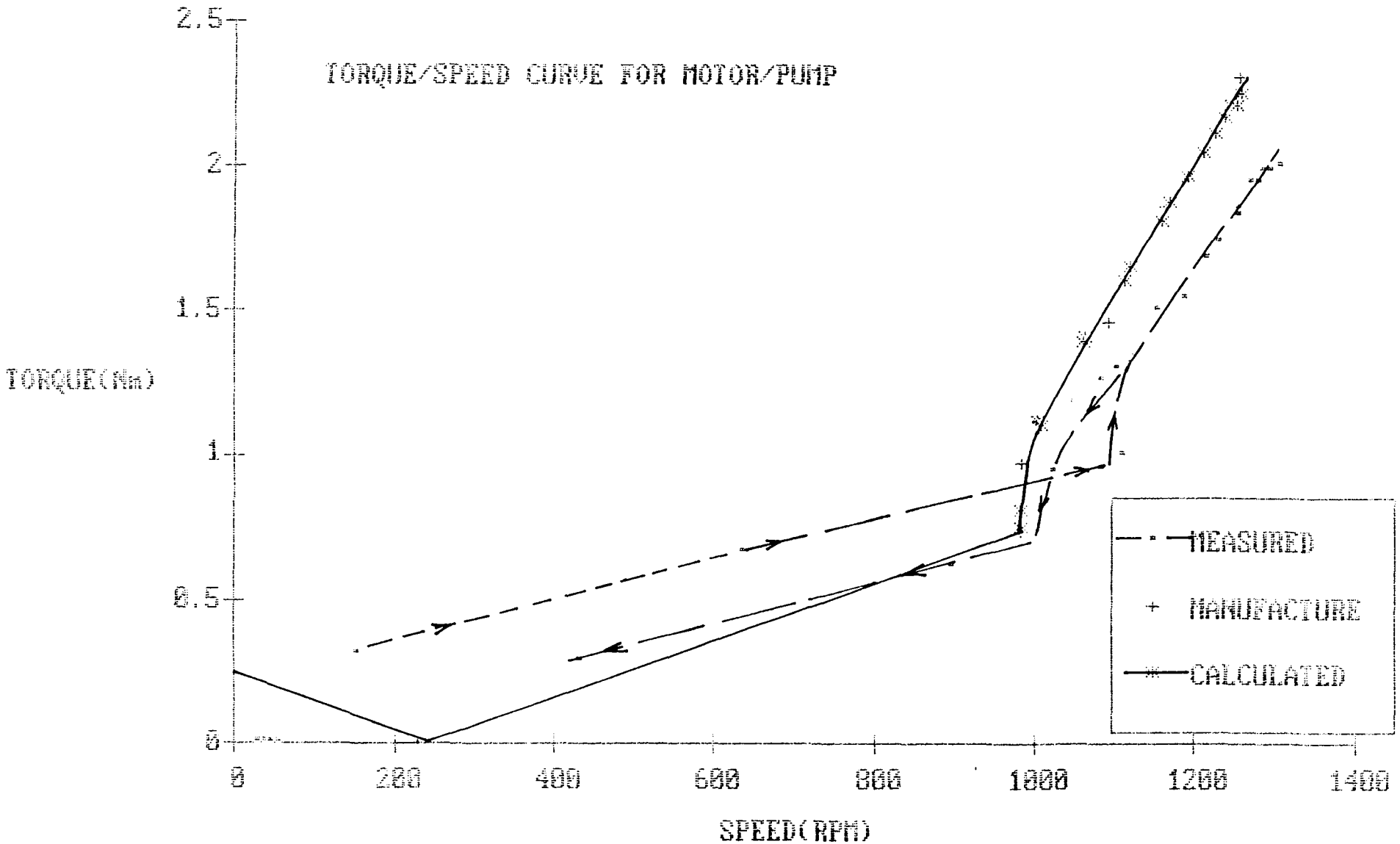
TORQUE/SPEED CURVE FOR MOTOR/PUMP
TORQUE(Nm)
2.5
2
1.5
1
0.5
0
0
200
400
600
800
1000
1200
1400
SPEED(RPM)
MEASURED
MANUFACTURE
CALCULATED

FIGURE 5·5

suggests a "breakaway" torque (i.e. torque at which pump starts to turn) of about 10% of normal operating torque to overcome static friction in bearings and seal. This breakway torque then decreases linearly with speed to nearly zero when the speed is 15-20% of normal operating speed. Beyond this point torque increases again due to hydraulic losses within the pump until a point is reached where pumping commences and the torque increases rapidly.

It can be seen that all three plots have a similar shape. There are no model predictions of pump performance under 'no flow' conditions as the model does not simulate pump performance in the 'no flow' region.

The following points emerge from an analysis of the torque /speed curves:

a) The model and manufacturer predict that flow will commence at 980 RPM whereas the measured data shows flow occurs at 1,100 RPM. This discrepency may be due partly to inaccuracies in the motor equations used to determine the torque and speed to the pump.

b)The sudden increase in torque at the commencement of flow is related to the flat Head/Discharge curve (Appendix F) for the pump at low flows. In this region, as flow increases, there is little change in speed but an increase in power and hence torque into the pump. The instabilitv,however, which is a charactertistic of conventional pump systems operating in this region, is not present as the input power is limited to one value by the I-V ~haracteristics of the photovoltaic array.

From the measured data it can be seen that the pumo

stops pumping at lower torque and speed values than when it commenced. This hysteresis effect is due to reduced friction in the pump and motor bearings and pump seal after a period of operation , combined with the inertia of fluid in the pipeline and the inertia of the pump and motor.

5.3.2. Combined Pump and Motor Operation.

The combined operation of the pump and motor in relation to the array characteristics is shown in the voltage/current plot, Figure 5.6, for the model and measured data; for static head, HS= 3.6m and friction constant,k = 0.245.

The plot reveals the following details about the operation of the motor/pump.

5.3.2.1. Region O-A, Where Speed=0

It can be seen that the current initially rises rapidly to about 4 amps at 2.5 volts. In this region the motor is not turning and so Vm & Im are directly related by Ohms law to the armature resistance of the motor (Ra) and the cable and connection losses between the measuring point and the motor.

The slope gives an indication of this total resistance, R=2.5/4.0 = 0.6ohms. Cable resistance is 0.046 ohms, therefore the remaining resistance is comprised of motor resistance (0.13 ohms based on mnf data) and connection losses. It is likely that the connection losses and armature resistance are higher than expected. Deterioration of brushes would result in increased armature resistance. When these results were recorded in Nov/Dec 1986 the pump had been operating for 14 months without the brushes being

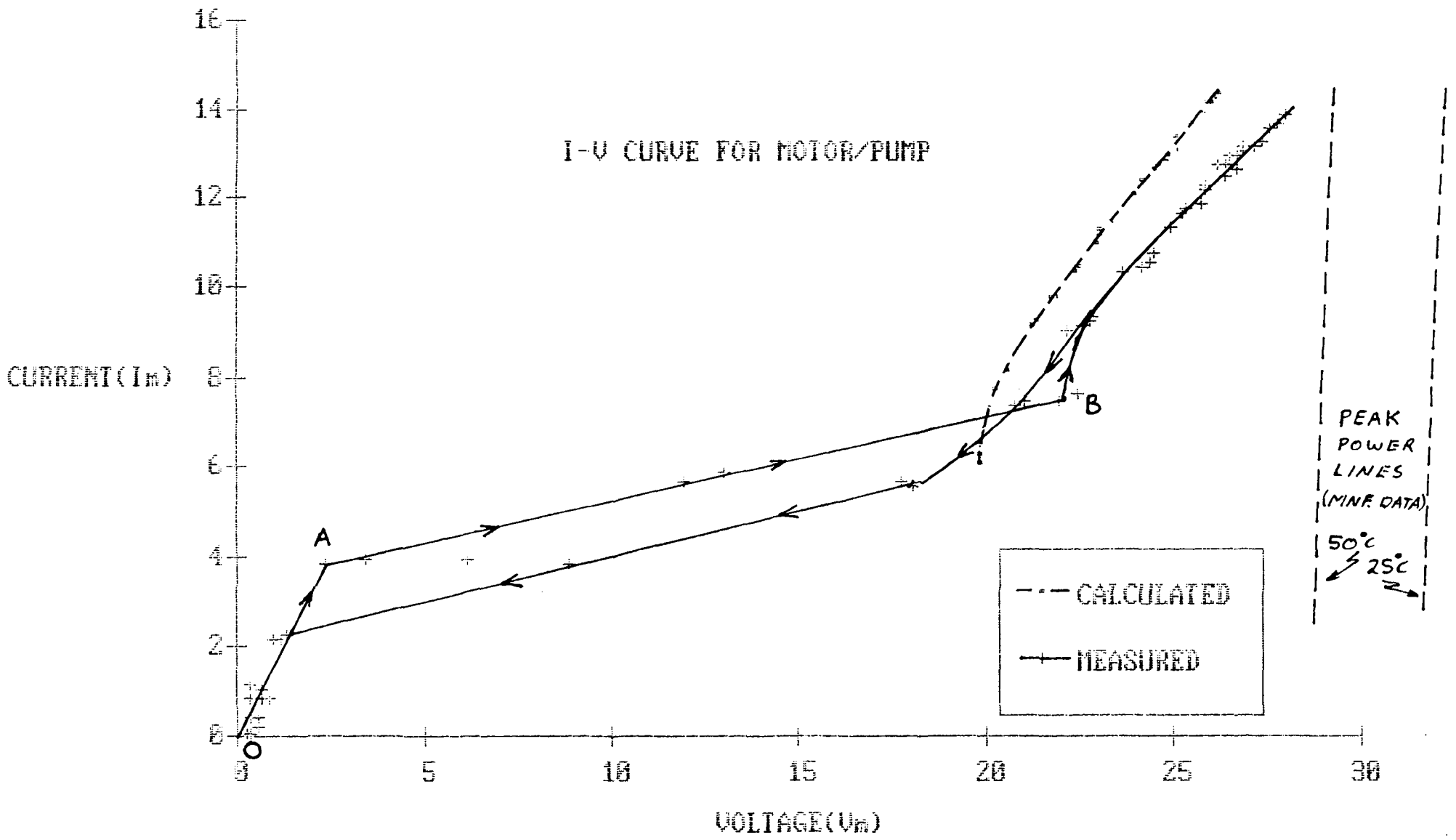
I-V CURVE FOR MOTOR/PUMP
CURRENT(Im)
VOLTAGE(Vm)
0
2
4
6
8
10
12
14
16
0
5
10
15
20
25
30
A
B
O
t
CALCULATED
MEASURED
PEAK
POWER
LINES
(MINE DATA)
50°C
25°C

FIGURE 5·6

changed.

As the current rises above 4 amps sufficient torque is generated to overcome initial stiffness in the bearings and seals, then the motor and pump start to turn. Based on the model for the motor, 4 amps results in 0.33 Nm torque, which is close to the 'break away' torque predicted by Karassik and shown in Figure 5.5.

Improved performance of the solar pump could be achieved by ensuring the electrical losses in brushes,cable and connections are kept to a minimum and the static friction of bearings and seals reduced.

5.3.2.2. Region A-B, Where Flow=0

Once the motor starts to turn, back EMF is generated and the voltage rises rapidly, until the pump starts to deliver water.

In the region between the motor starting to turn (Pt.'A' Figure 5.6) and the pump delivering water (Pt.'B'),the degree of slope indicates the amount of energy consumed in overcoming inertial effects and dynamic losses in the motor and pump. As mentioned in Section 2.2.3. the smaller the slope the quicker the pump reaches speed and commences to deliver water. This slope can be kept to a minimum by reducing dynamic friction in the motor and pump bearings and the pump seal. For this particular pump a ceramic seal is used which has much lower friction than a stuffing box, so there is little chance of improvement in seal friction for this pump. Further reduction can be achieved by reducing the inertia of the rotating parts, although, other than reducing the weight of the belt

sheaves, there is little that can be done without incurring high costs.

Once flow commences the slope of the curve increases as the torque required to turn the pump increases. Over this region the comparison between the modelled and measured data is good although once again, as for the Torque/speed curve the model commences pumping at a lower voltage than measured.

5.3.2.3. Comparison With Peak Power Line For Array

Also shown on Fig 5.6 is the peak power line for the array both for the manufacturer's data and the model.

The closer the I-V curve for the motor/pump approaches the peak power line for the array, the better the match between the motor/pump and the array. Also, as mentioned in Section 2.2.3 the steeper the slope of the I/V curve, the better the match.

It can be seen that the match is not very good.

The match could be improved, resulting in more water pumped if:

a) The slope of the I/V curve for the motor/pump was increased. This can be achieved by:

i) reducing the armature resistance, Ra, and keeping line losses to a minimum (see Equation 22 , Section 2.2.3). One simple improvement is to ensure motor brushes are in good condition and terminal connections are clean and secure.

ii) increase dT/dn (see Equation 22). Achieved by keeping the system curve for the pipeline flat, by keeping the pipeline friction to a minimum.

Further improvement could be obtained using a different pump with a flatter Head/Discharge curve, such as a pump with radial or forward curved vanes.

iii) ensuring the motor constants K and Ke are kept to a minimum, as long as this can be achieved without sacrificing some other aspect of motor performance.

b) The I/V curve was moved closer to the Peak Power line.

This could be achieved by:

i) allowing the motor to increase in speed but maintaining the original pump speed through increasing the pulley ratio.

ii) using a pump with a lower starting torque and higher efficiency, or a motor with a greater output torque for a given current and less speed for the given current and voltage.

c) A Maximum Power Point Tracker is fitted.

5.3.2.4. Performance Improvements

In the above sections 5.3.2.1 to 5.3.2.3.,a number of comments have been made regarding possible ways of improving the match between the motor/pump and the array. Using the computer model it is possible to alter various parameters and check the validity of these comments. This is investigated further in Section 5.7.

5.4 SOLAR PUMP PERFORMANCE

5.4.1 Monthly Performance

5.4.1.1 Monthly Flows Measured at Site

Flows for the fifteen month period, October 1985 to December 1986, are shown in Figure 5.7. No flow data is

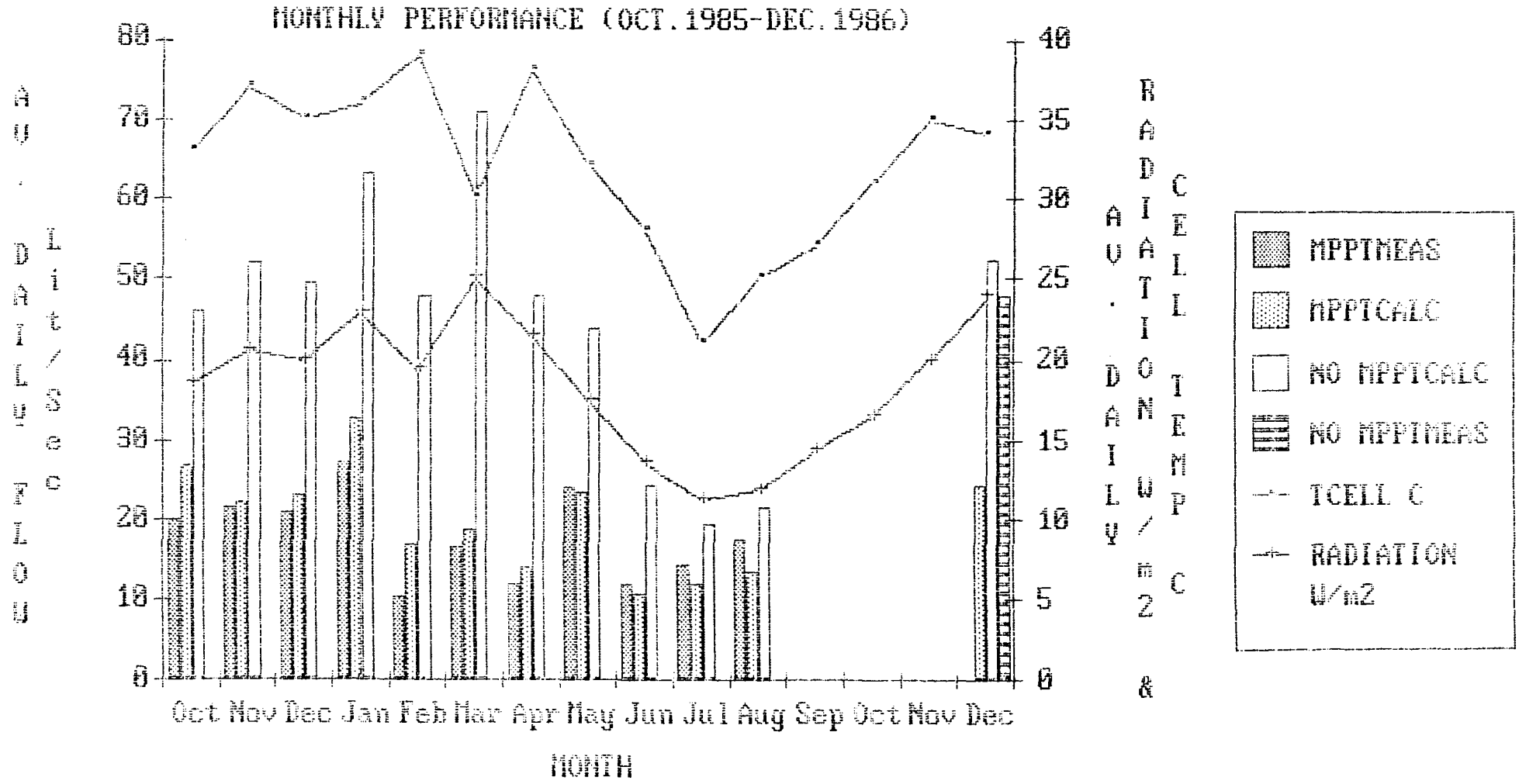
MONTHLY PERFORMANCE (OCT.1985-DEC.1986)
AV. DAILY WATT-HOURS
Watt-Hours
AV. DAILY RADIATION W/M2 & CELL TEMP C
MPPTMEAS
MPPTCALC
NO MPPTCALC
NO MPPTMEAS
TCELL C
RADIATION W/M2
Oct Nov Dec Jan Feb Mar Apr May Jun Jul Aug Sep Oct Nov Dec
MONTH

FIGURE 5·7

available for the period September to November 1986 due to problems with the data logger (Section 3.3).

For the whole period, the performance of the pumps at site is well below the performance specified in the original tender 60,000 litres per day under 18MJ/m^2 on the horizontal surface. For example, in October 1985 & May 1986, with daily inclined irradiation of 18.6 & 17.5 MJ/m^2 respectivelv, the average daily flow was 20,000 litres and 24,000 litres respectively. Removal of the MPPT (in Dec 86) certainly improved the flow but performance is still only 47,000 litres/day for a daily inclined irradiation of 24 MJ/m^2.

These results are abismal considering the solar pump was supplied to the Department by a reputable pump manufacturer who is marketing solar pumps. Clearly the manufacturer has no reliable method of sizing a solar pump system to meet a particular duty. It is also disturbing to note that the MPPT was added to the solar pump to improve the performance.

The effect of the MPPT is further highlighted when the Over-all Monthly Efficiency (OME) is considered.

$$OME = \frac{\sum_{MONTH} HYDRAULIC\ POWER}{\sum_{MONTH} GI \times AREA\ OF\ ARRAY} \qquad -41.$$

For two months with similar total radiation on the horizontal plane and average monthly cell temperatures: January 1986(with MPPT) and November/December 1986-(no MPPT)

For January 1986, with the MPPT,

OME =0.78%

for November/ December 1986 without the MPPT

OME =1.79%

Removal of the MPPT more than doubles the efficiency of the pump.

5.4.1.2 Monthly Flows Predicted by Model

The model predictions for this same period are also shown in Figure 5.7.

Model predictions of solar pump performance with the MPPT are not as good as predictions of performance without the MPPT.On average, model flows with the MPPT are higher than measured flows by 16% whereas model flow without the MPPT is only 7% higher.The discrepancy between model flow and measured flow WITHOUT the MPPT is mainly the result of:

a) the model over-estimating the current output of the array for performance to the left of the "knee" of the I-V curve,

b) the tendency for the model to over-estimate flow on cloudy days: this is discussed further in Section 5.4.4.

c) inherent errors in recording flowrate, radiation, cell temperature etc; and margins of error in component specifications provided by manufacturers.

For performance WITH the MPPT the discrepancy is due to:

a) the difficulty in modelling the steep slope of the I-V curve to the right of the knee (with the MPPT added, the pump always operates to the right of the "knee").

b) the difficulty in modelling the setpoint voltage, which for the actual pump varies from approximately 31.0 to 32.2 volts. The model assumes a constant voltage of 31.8V.

c) the tendency for the model to over-estimate flow on cloudy days.

d) inherent errors in recording flowrate, radiation, cell temperature etc; and margins of error in component specifications provided by manufacturers.

5.4.2 Typical Daily Performance

5.4.2.1 Daily Flows Measured at Site

Solar pump performance for four typical days are shown in Figures 5.8.1 to 4. It can be seen that for the two virtually clear days (Figures 5.8.1 & 5.8.3) the measured flowrate closely follows the radiation, commencing about 8pm and finishing about 4pm. The pump performance is significantly improved when the MPPT is removed.

The influence of cloud appears as sharp troughs in the radiation profile (Figures 5.8.2 & 5.8.4) with a resulting dramatic reduction in flowrate.

For performance both with and without the MPPT there is a threshold radiation of about 500 W/m2 below which no water is pumped.

Peak Efficiency is defined as

$$PE = \frac{\rho g Q_i H_i}{GI_i \times \text{AREA OF ARRAY}} \qquad -42.$$

where Q_i & H_i are the maximum flow and pressure occurring on a particular day under the irradiation value GI_i.

Over-all Daily Efficiency (ODE) is defined the same as OME, Equation 41, except the period is daily, not monthly.

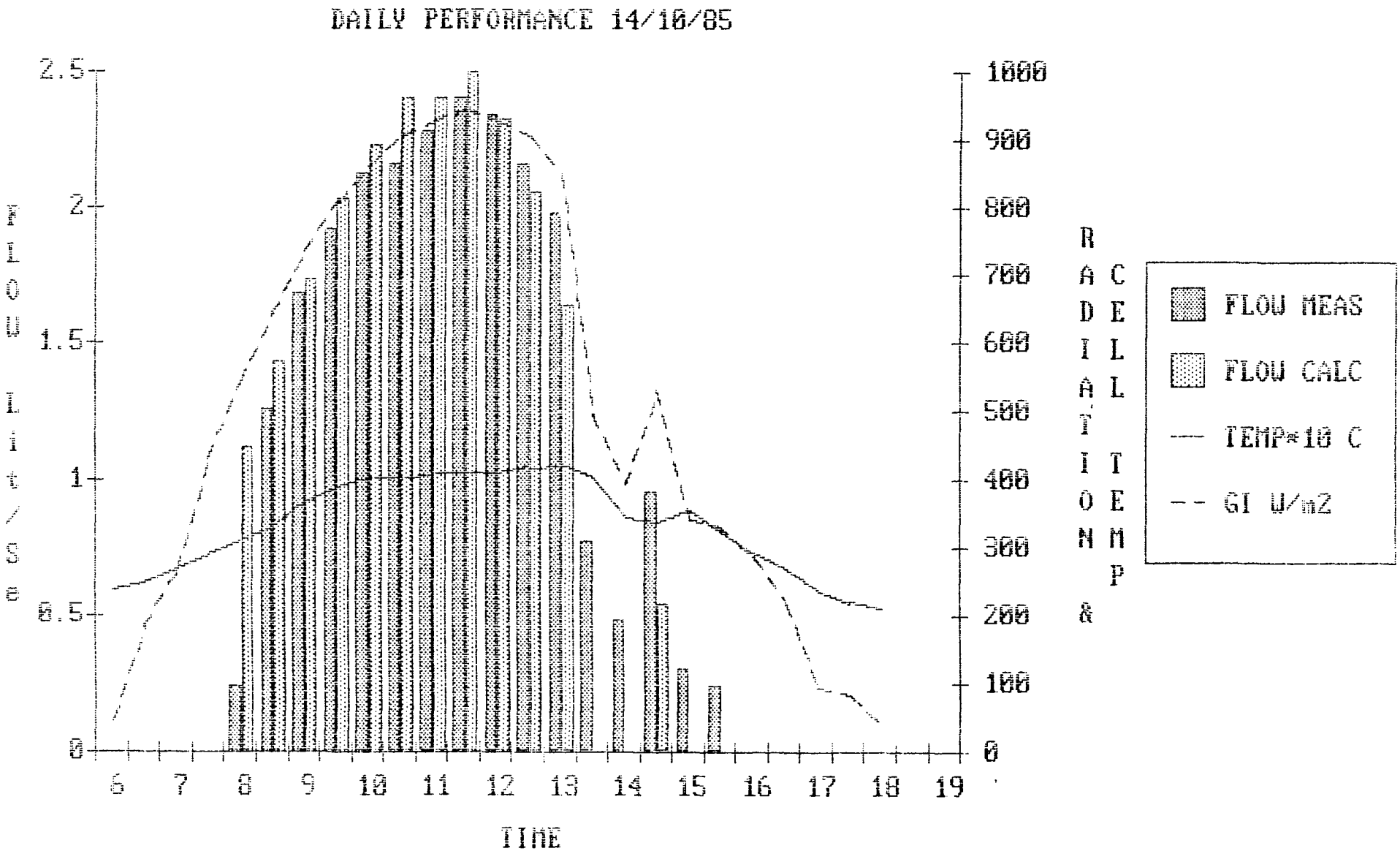
DAILY PERFORMANCE 14/10/85
FLOW L/min
RADIATION & CELL TEMP
TIME
FLOW MEAS
FLOW CALC
TEMP*10 C
GI W/m2
2.5
2
1.5
1
0.5
0
1000
900
800
700
600
500
400
300
200
100
0
6
7
8
9
10
11
12
13
14
15
16
17
18
19

FIGURE 5·8·1

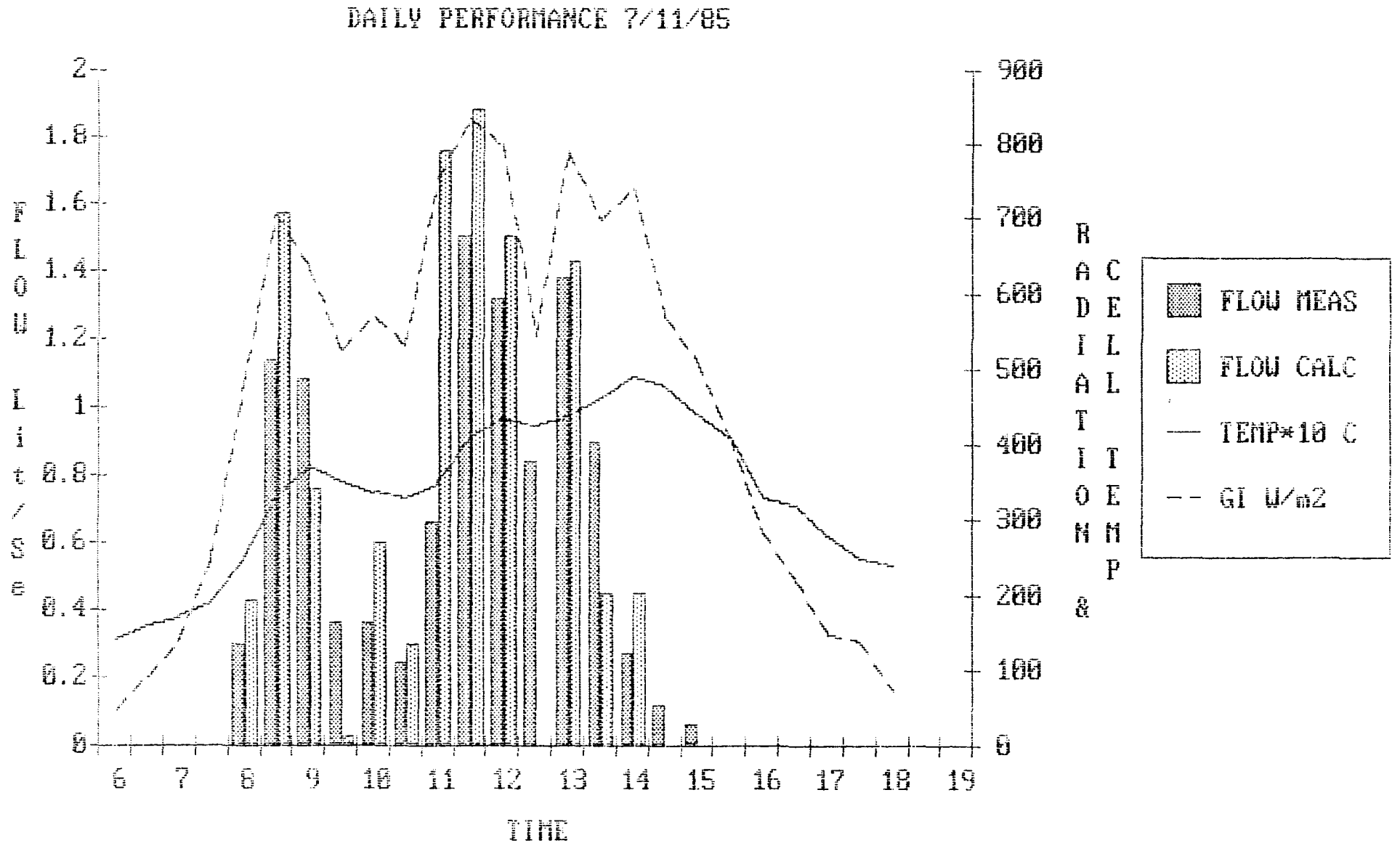
DAILY PERFORMANCE 7/11/85
FLOW GPM
RADIATION & CELL TEMP
TIME
FLOW MEAS
FLOW CALC
TEMP*10 C
GI W/m2
0
0.2
0.4
0.6
0.8
1
1.2
1.4
1.6
1.8
2
100
200
300
400
500
600
700
800
900
5
6
7
8
9
10
11
12
13
14
15
16
17
18
19

FIGURE 5·8·2

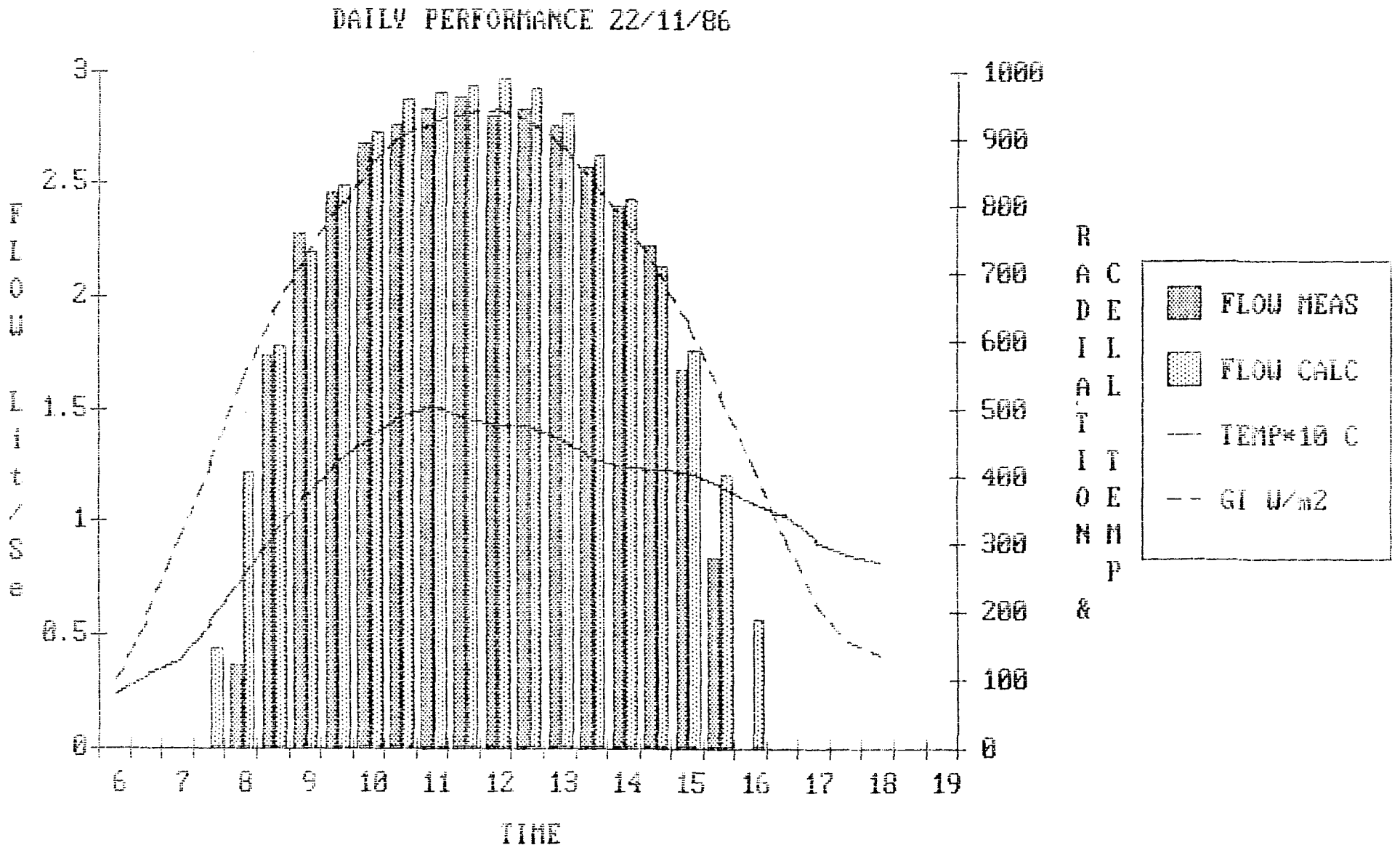
DAILY PERFORMANCE 22/11/86
FLOW l/s
RADIATION & CELL TEMP
TIME
0
0.5
1
1.5
2
2.5
3
100
200
300
400
500
600
700
800
900
1000
6
7
8
9
10
11
12
13
14
15
16
17
18
19
FLOW MEAS
FLOW CALC
TEMP*10 C
GI W/m2

FIGURE 5·8·3

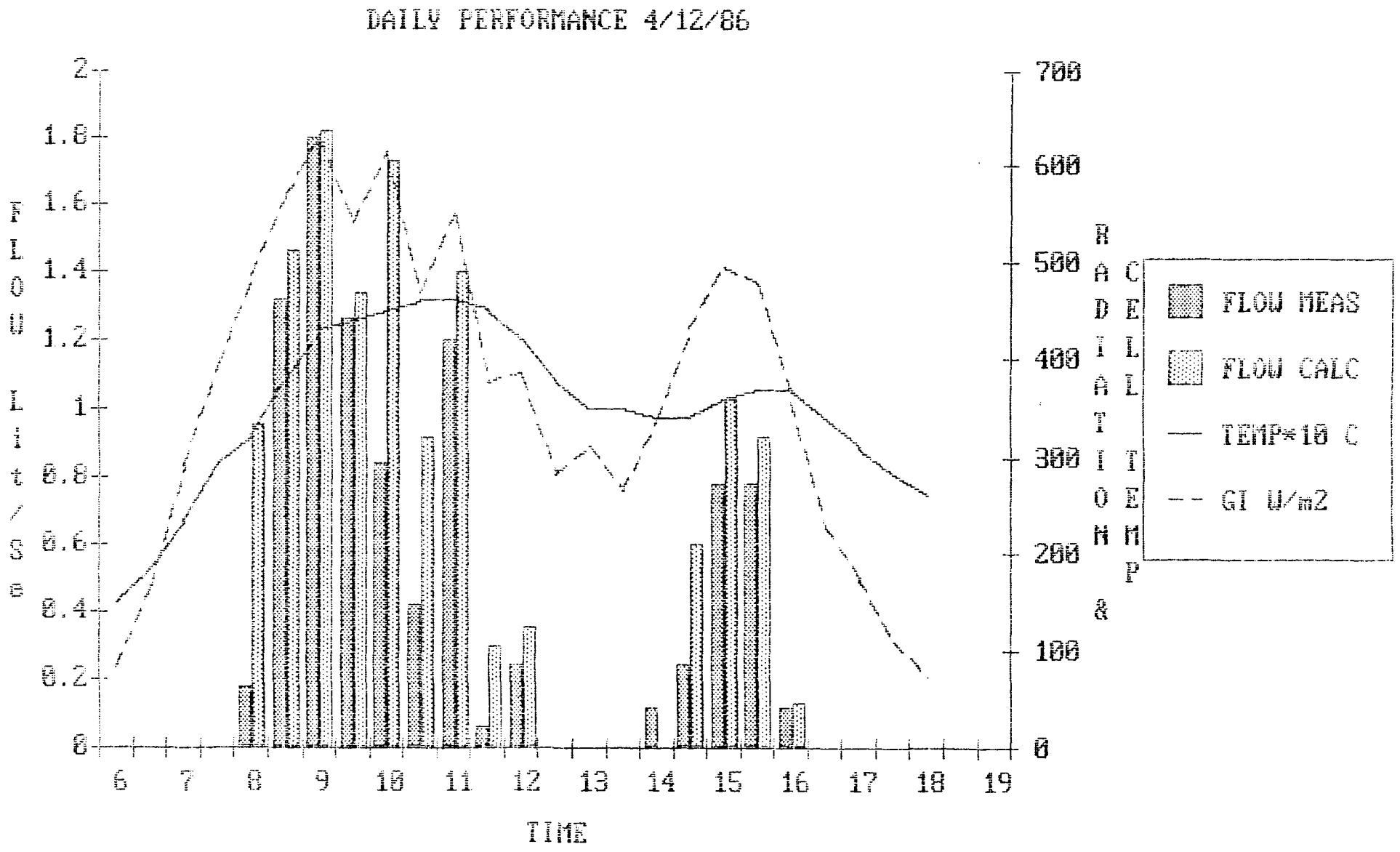
DAILY PERFORMANCE 4/12/86
GPM
RADIATION & CELL TEMP
TIME
FLOW MEAS
FLOW CALC
TEMP*10 C
GI W/m2
0
0.2
0.4
0.6
0.8
1
1.2
1.4
1.6
1.8
2
100
200
300
400
500
600
700
6
7
8
9
10
11
12
13
14
15
16
17
18
19

FIGURE 5·8·4

Performance of the pump at site **with** the MPPT has an ODE=1.0% under total inclined irradiation of 27.5 MJ/m^2, with a peak efficiency of PE=1.9% at $930W/m^2$. Under a total inclined irradiation of 21.5 MJ/m^2: ODE=1.1% and PE=1.3%.

Performance **without** the MPPT under 27.5 MJ/m^2 has ODE= 2.2% and PE=3.2% at 930 W/m^2. Consequently, Over-all Daily Efficiency was more than doubled when the MPPT was removed.

This performance, without the MPPT, compares favourably with results reported by Halcrow (9) for their most efficient solar pump which had an ODE=1.8% under irradiance of 21.6 MJ/m^2, and a peak efficiency of PE= 2.7% at 1000 W/m^2.

5.4.2.2 Daily Flows Predicted by Model

From Figures 5.8.1 & 5.8.3, the model satisfactorily predicts flowrate for clear conditions. However under cloudy conditions the model's predictions are very inaccurate, see Figures 5.8.2 & 5.8.4. This is due to two factors:

a) the model inaccurately predicts flow under low radiation and during cloudy days there are often periods of low radiation

b) The non-linear relationship between flowrate and radiation. The effect of this non-linearity is discussed in the next section.

5.4.3 Relationship Between Flowrate and Radiation

Flowrate as a function of radiation is shown in Figures 5.9.1 and 5.9.2, for performance on clear days with and without the MPPT respectively.:- it can be seen that the relationship between flowrate and radiation is a non-linear one, with pumping commencing once a threshold radiation

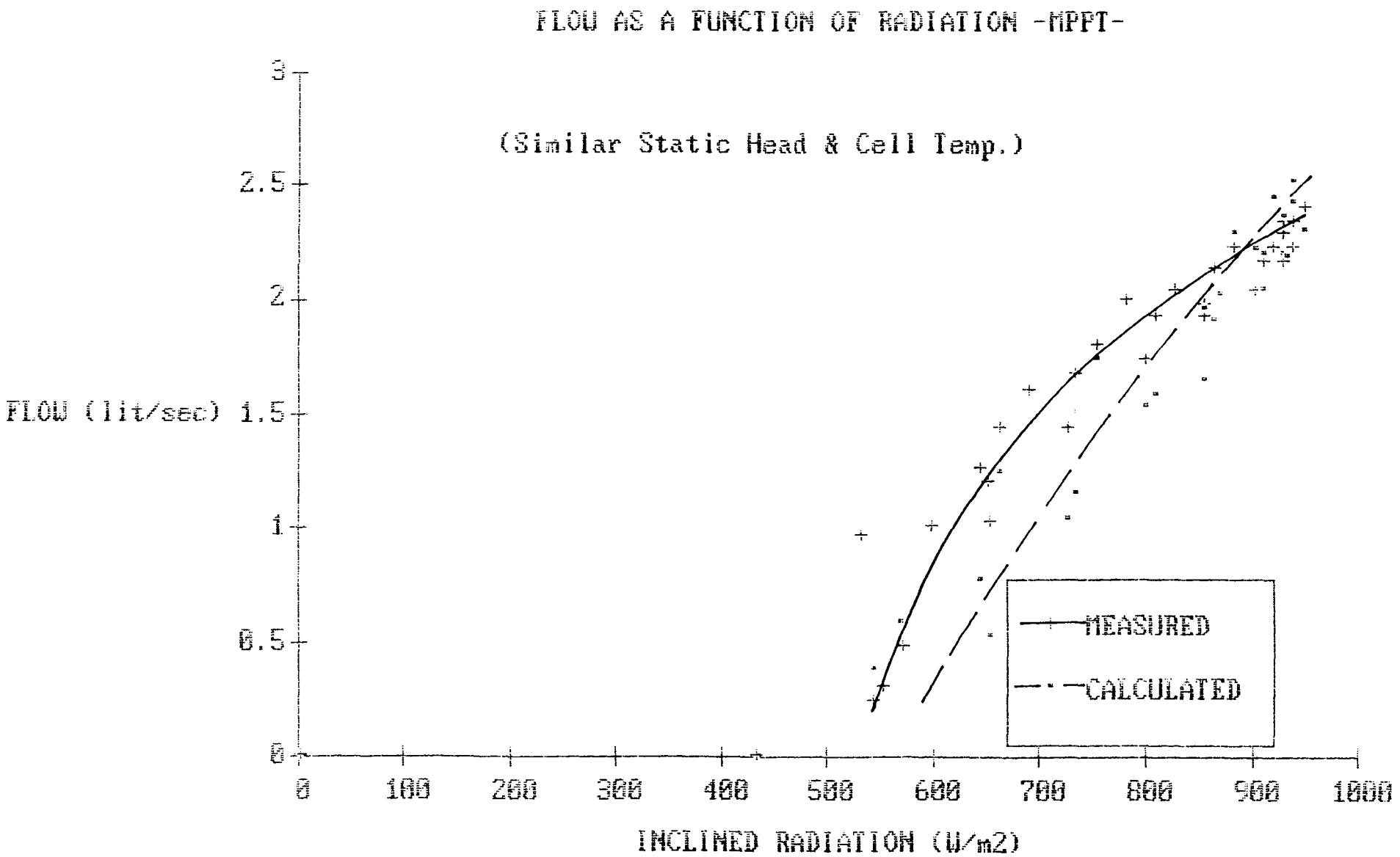
FLOW AS A FUNCTION OF RADIATION -MPPT-
(Similar Static Head & Cell Temp.)
FLOW (lit/sec)
3
2.5
2
1.5
1
0.5
0
0
100
200
300
400
500
600
700
800
900
1000
INCLINED RADIATION (W/m2)
MEASURED
CALCULATED

FIGURE 5·9·1

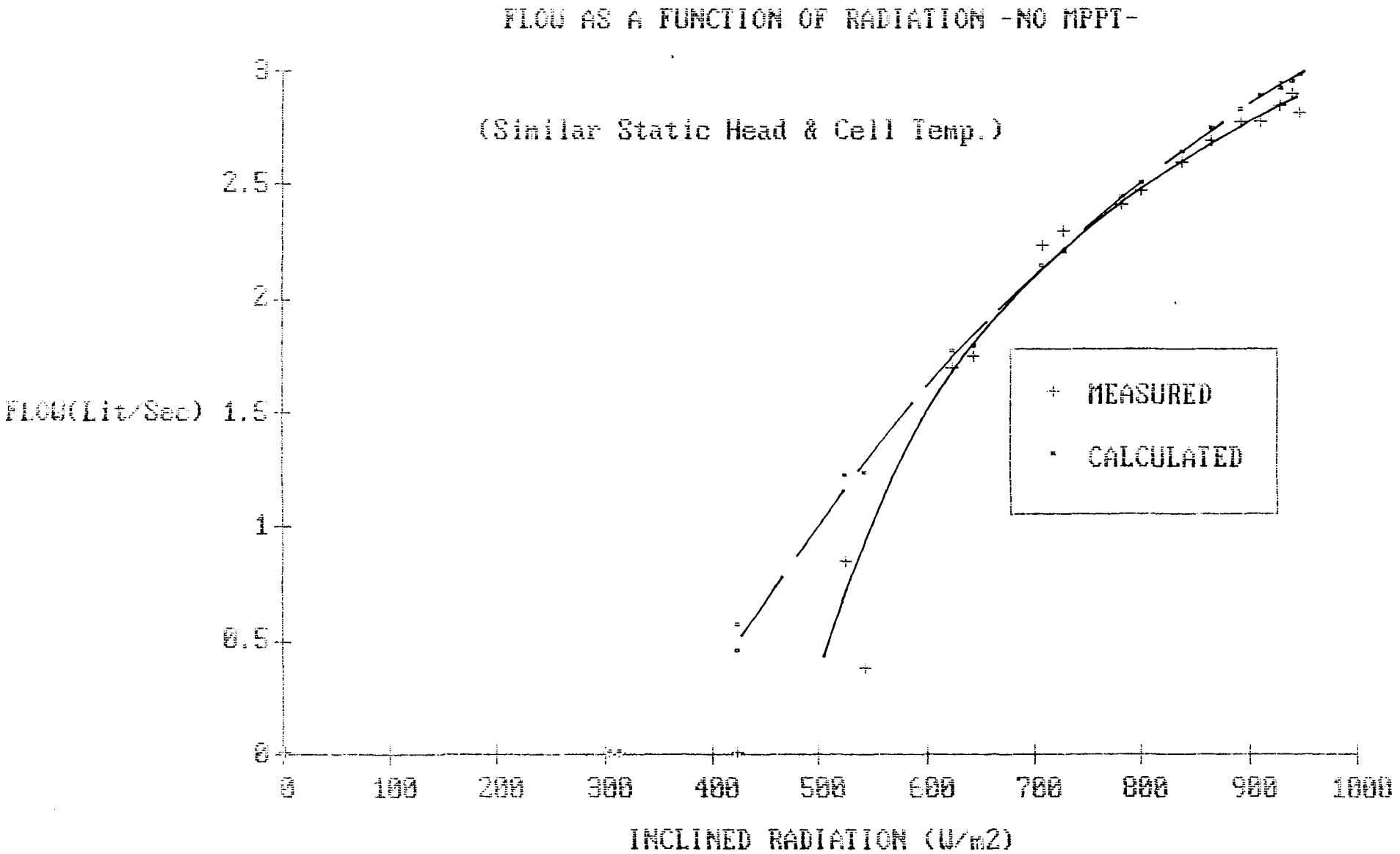
FLOW AS A FUNCTION OF RADIATION -NO MPPT-
(Similar Static Head & Cell Temp.)
FLOW(Lit/Sec)
3
2.5
2
1.5
1
0.5
0
0
100
200
300
400
500
600
700
800
900
1000
INCLINED RADIATION (W/m2)
MEASURED
CALCULATED

FIGURE 5·9·2

value of about 500 $W.m^2$ is reached.

The use of average radiation data hides the peaks and troughs that may occur over the recording period, giving a false indication of flow. This is obviously not a problem on clear days but is definately a problem when predicting flow on cloudy days. The larger the recording period, the greater the discrepancy between predicted flow and actual flow.

For example, the average radiation for a recording period may be 600 W/m^2, comprised of two 900 W/m^2 peaks and the remainder of the period less than 500W/m^2. For the average of 600 W/m^2 the model would predict water pumped for the whole period, where in fact the pump would only have pumped for the two brief periods of 900 W/m^2. The model would have over estimated flow for this period.

The averaging period for the Wakool Solar pump is 1/2 an hour. Reducing this period or using a program to simulate radiation under cloudy conditions should overcome this problem.

These results show, that a manufacturer should be careful sizing a solar pump for a particular region, using only average monthly radiation data. Account must be taken of cloud cover in the region.

5.5 THE EFFECT OF CELL TEMPERATURE ON PUMP PERFORMANCE

The effect of cell temperature on the pump's performance can be seen in Figure 5.10 where Over-all Daily Efficiency is graphed as a function of cell temperature for days with similar total irradiation.

For performance both with and without the MPPT, the Over-all Efficiency decreases as the cell temperature

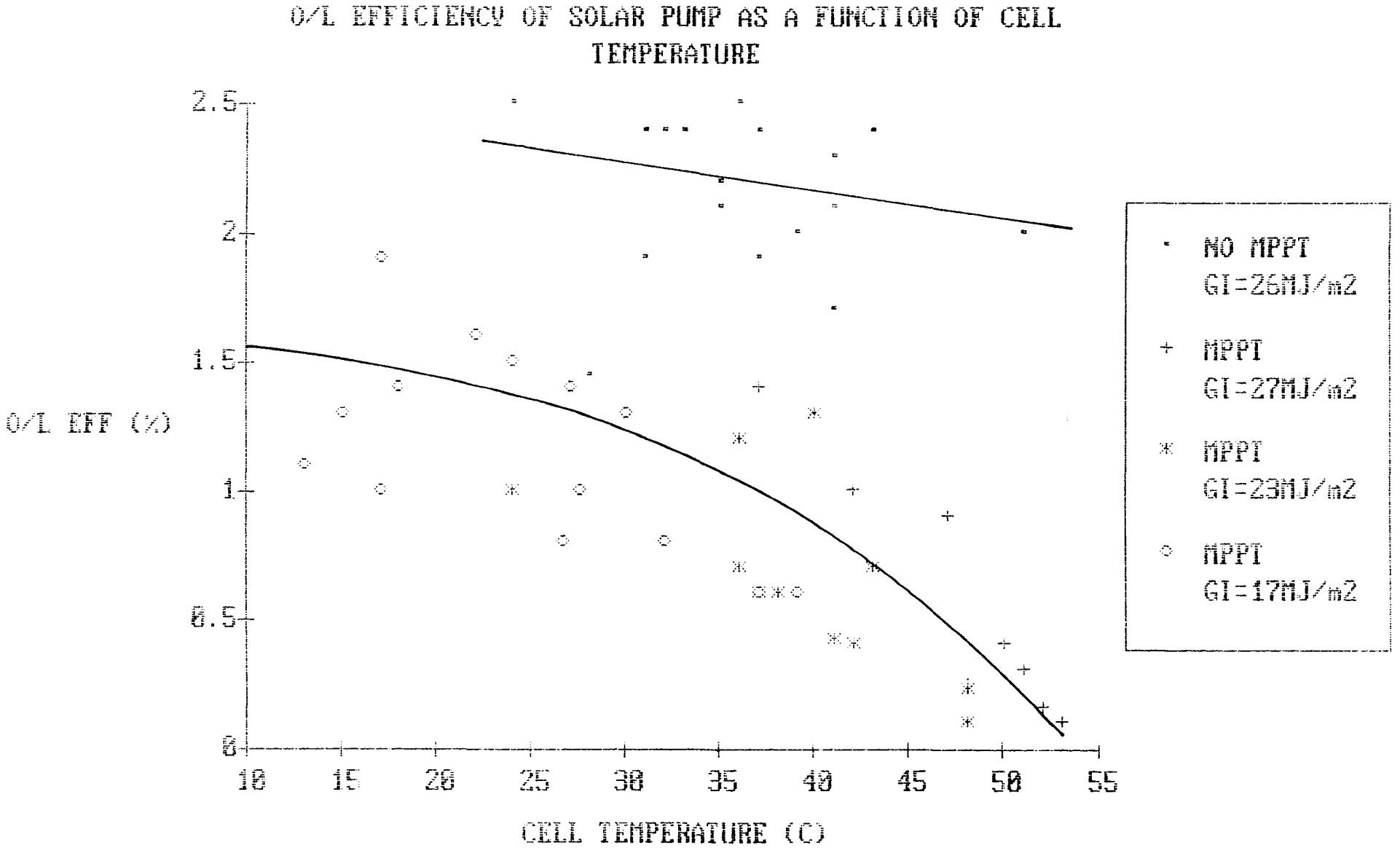
O/L EFFICIENCY OF SOLAR PUMP AS A FUNCTION OF CELL TEMPERATURE
O/L EFF (%)
2.5
2
1.5
1
0.5
0
10
15
20
25
30
35
40
45
50
55
CELL TEMPERATURE (C)
NO MPPT
GI=26MJ/m2
MPPT
GI=27MJ/m2
MPPT
GI=23MJ/m2
MPPT
GI=17MJ/m2

FIGURE 5·10

increases. This reduced efficiency is a direct result of reduced array performance at higher cell temperatures. However, as expected, the trend is more noticeable for performance with the MPPT as current output for the array is a strong function of cell temperature for operating voltages to the right of the 'knee'.

5.6 EFFECT OF STATIC HEAD ON PUMP PERFORMANCE

Over the 15 month recording period the static head at site ranged between 2.7m and 3.9 metres. From the model's predicted performance the Over-all Efficiency varied between 2.15% and 1.75% respectively for no MPPT. The efficiency reaches a peak at around 1 metre head, Figure 5.11.

The model indicates the efficiency is fairly sensitive to static head variation for heads greater than about 2 metres.

According to the model the solar pump has been incorrectly matched to the static head at site. Probably this match could be improved by varying the pulley ratio.

5.7 EFFECT OF VARYING PARAMETERS ON THE OVER-ALL EFFICIENCY OF THE SOLAR PUMP

5.7.1 Pipeline Friction

The effect of varying the friction constant k,from 0 to 1.5 is shown in Figure5.12.A maximum Over-all Efficiency of 2.03% is attained with k=0.05, equivalent to a pipe diameter of 80 mm.As expected, as the diameter is reduced, the Over-all Efficiency is reduced.

Scaling of the discharge pipe over the 18month period to March 1987, with k increasing from 0.2 to 0.25, has decreased the Over-all Efficiency by only 0.03%.

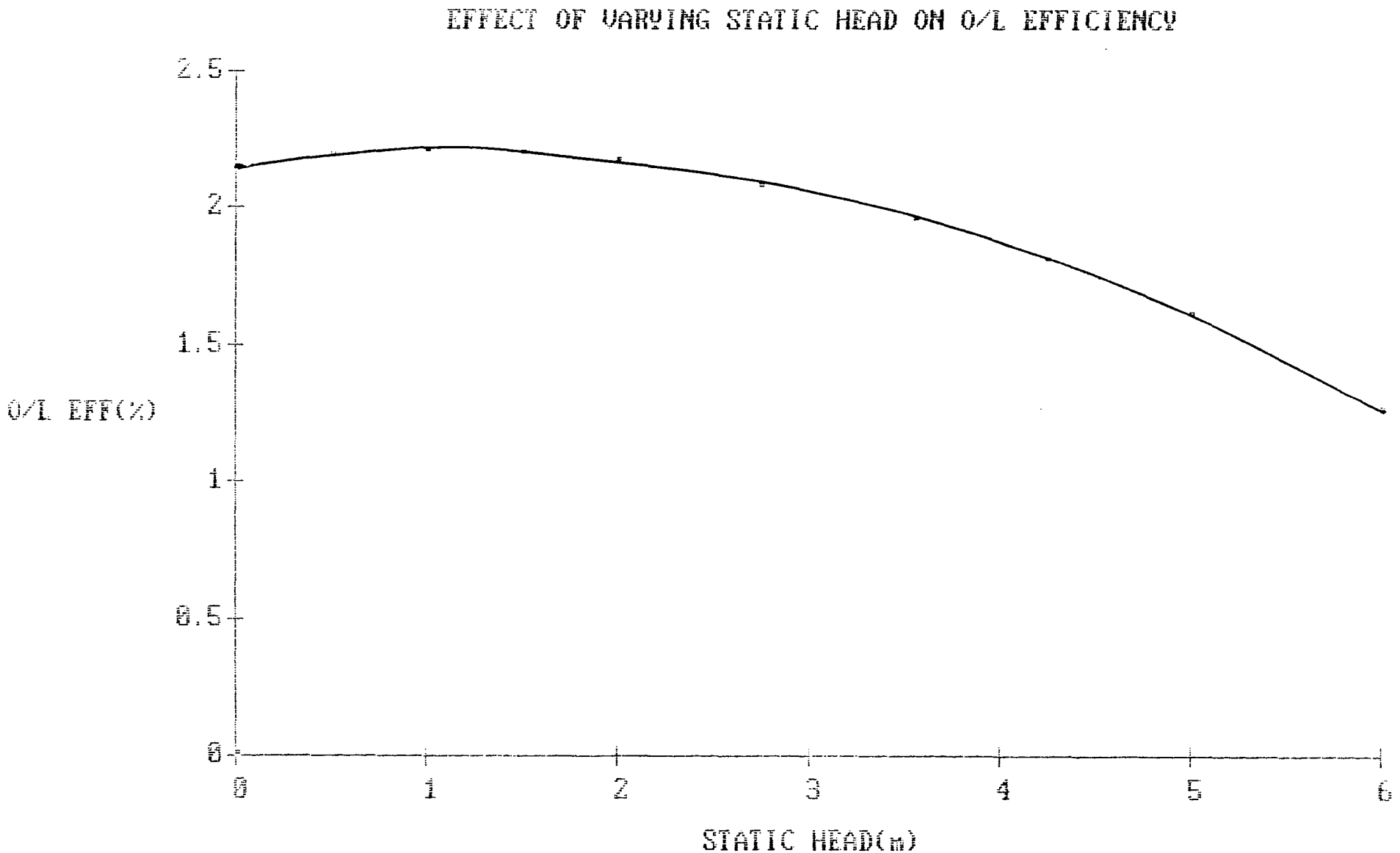
EFFECT OF VARYING STATIC HEAD ON O/L EFFICIENCY
O/L EFF(%)
2.5
2
1.5
1
0.5
0
0
1
2
3
4
5
6
STATIC HEAD(m)

FIGURE 5·11

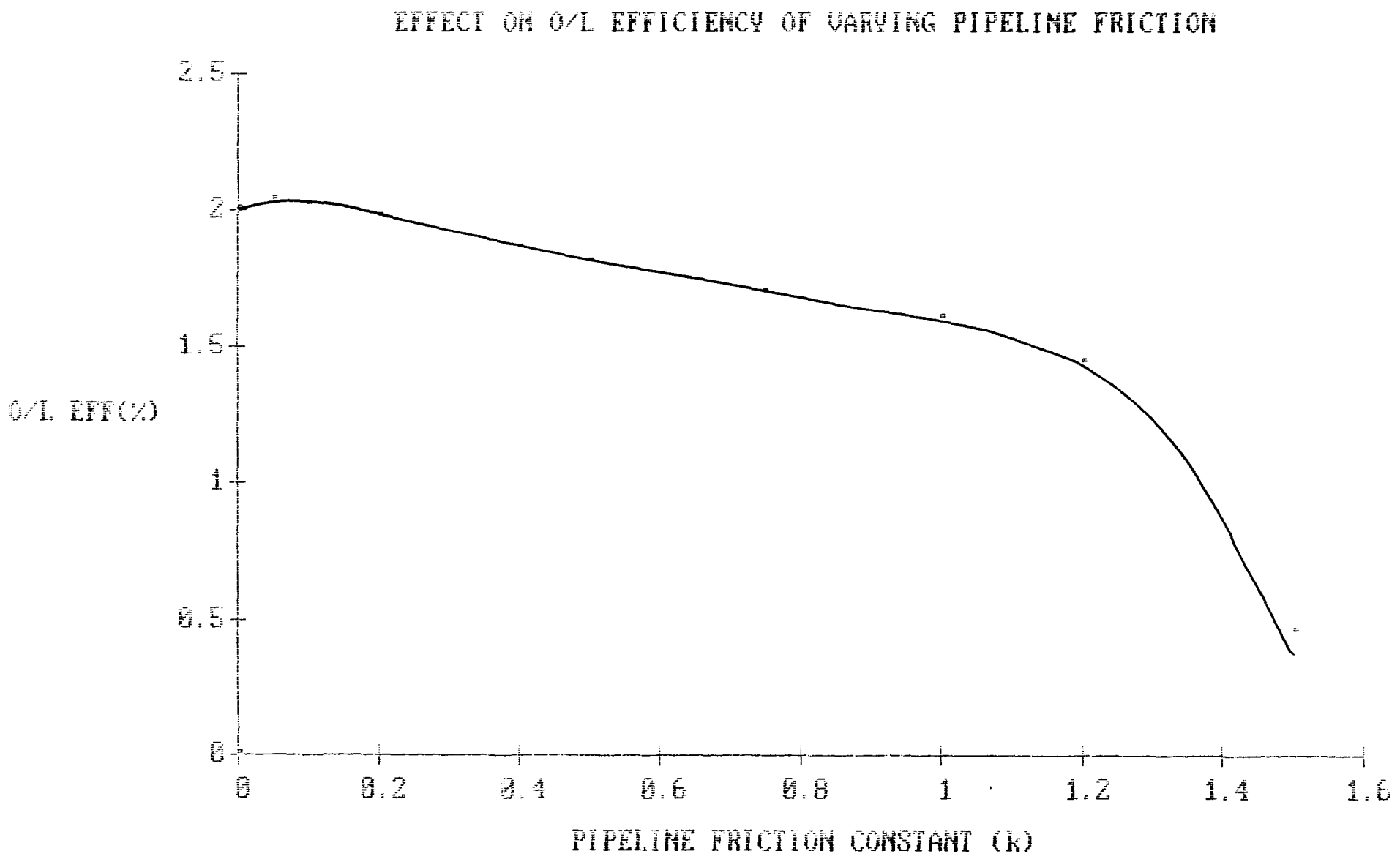
EFFECT ON O/L EFFICIENCY OF VARYING PIPELINE FRICTION
O/L EFF(%)
2.5
2
1.5
1
0.5
0
0
0.2
0.4
0.6
0.8
1
1.2
1.4
1.6
PIPELINE FRICTION CONSTANT (k)

FIGURE 5·12

Any gain in efficiency achieved by using a larger pipe has to be compared with the extra capital cost involved in the pipe and fittings.

5.7.2 Armature Resistance and Cable Losses

The total resistance across the array terminals is the sum of the armature resistance and the losses in the cabling, including connection losses.The present total resistance based on manufacturers' data is 0.176ohms.

Figure 5.13 shows there is little advantage in trying to reduce this total resistance, at best a 0.05% increase in efficiency could be achieved.However it does highlight the effect of increased resistance due to incorrect sizing of cable, wear of motor brushes, poor contacts etc.

Unfortunately the model does not converge to a solution for total resistance greater than about 0.4 ohms, because of the sensitivity of array current to voltage variation for solutions to the right of the 'knee'.This is discussed further in Section 5.7.5.

5.7.3 Motor Parameter, B

This parameter is used in Equation 18 defining the torque produced by the motor.

From the graph supplied by the motor manufacturer, Appendix G ,it can be seen that B is the y intercept. Considering the magnitude of the y scale there is potentially a fairly large error in determing the value of B.

The Over-all Efficiency is strongly dependent on the value B.(Figure 5.14).The accuracy of the model is therefore very sensitive to the value chosen.

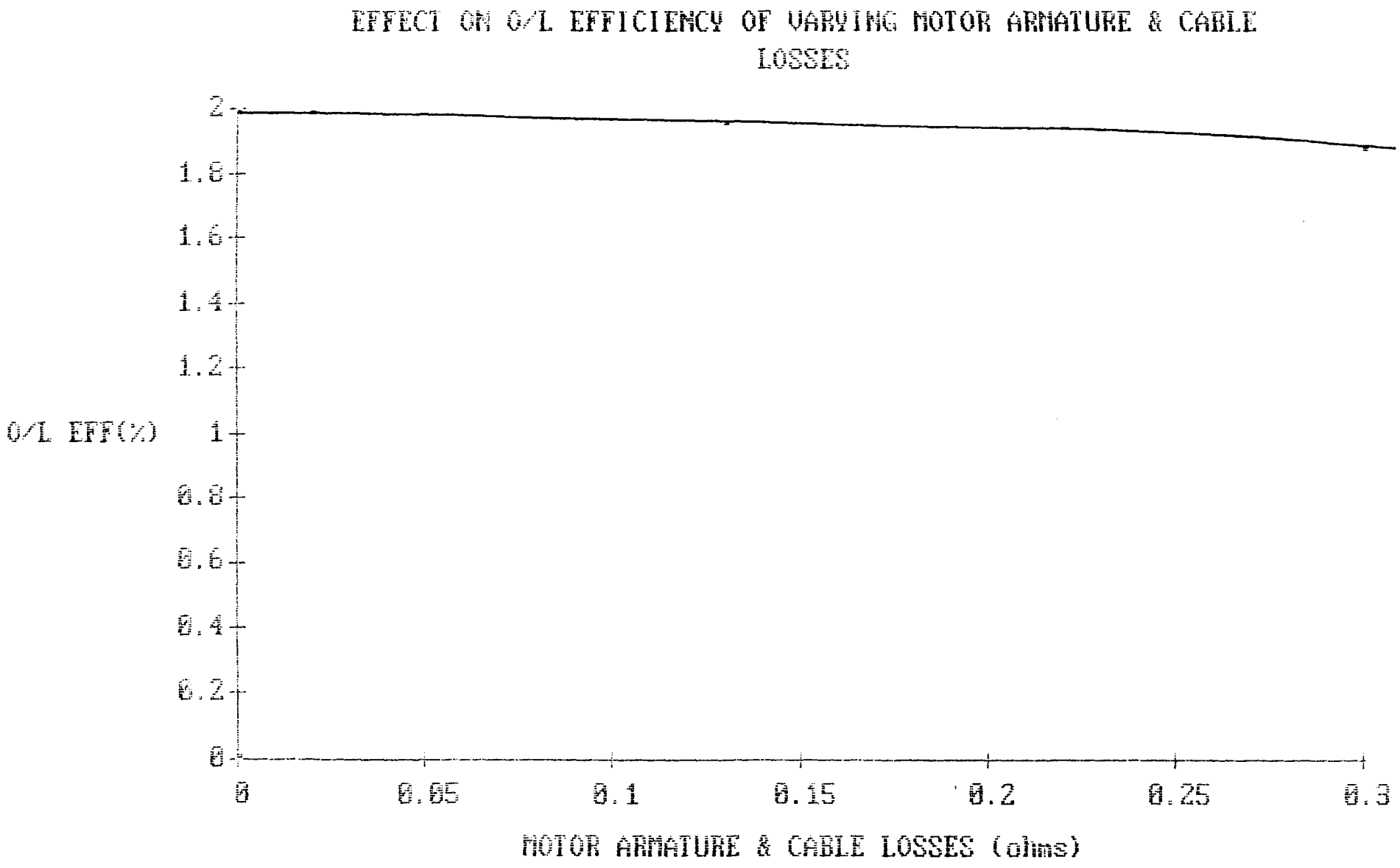
EFFECT ON O/L EFFICIENCY OF VARYING MOTOR ARMATURE & CABLE LOSSES
O/L EFF(%)
2
1.8
1.6
1.4
1.2
1
0.8
0.6
0.4
0.2
0
0
0.05
0.1
0.15
0.2
0.25
0.3
MOTOR ARMATURE & CABLE LOSSES (ohms)

FIGURE 5·13

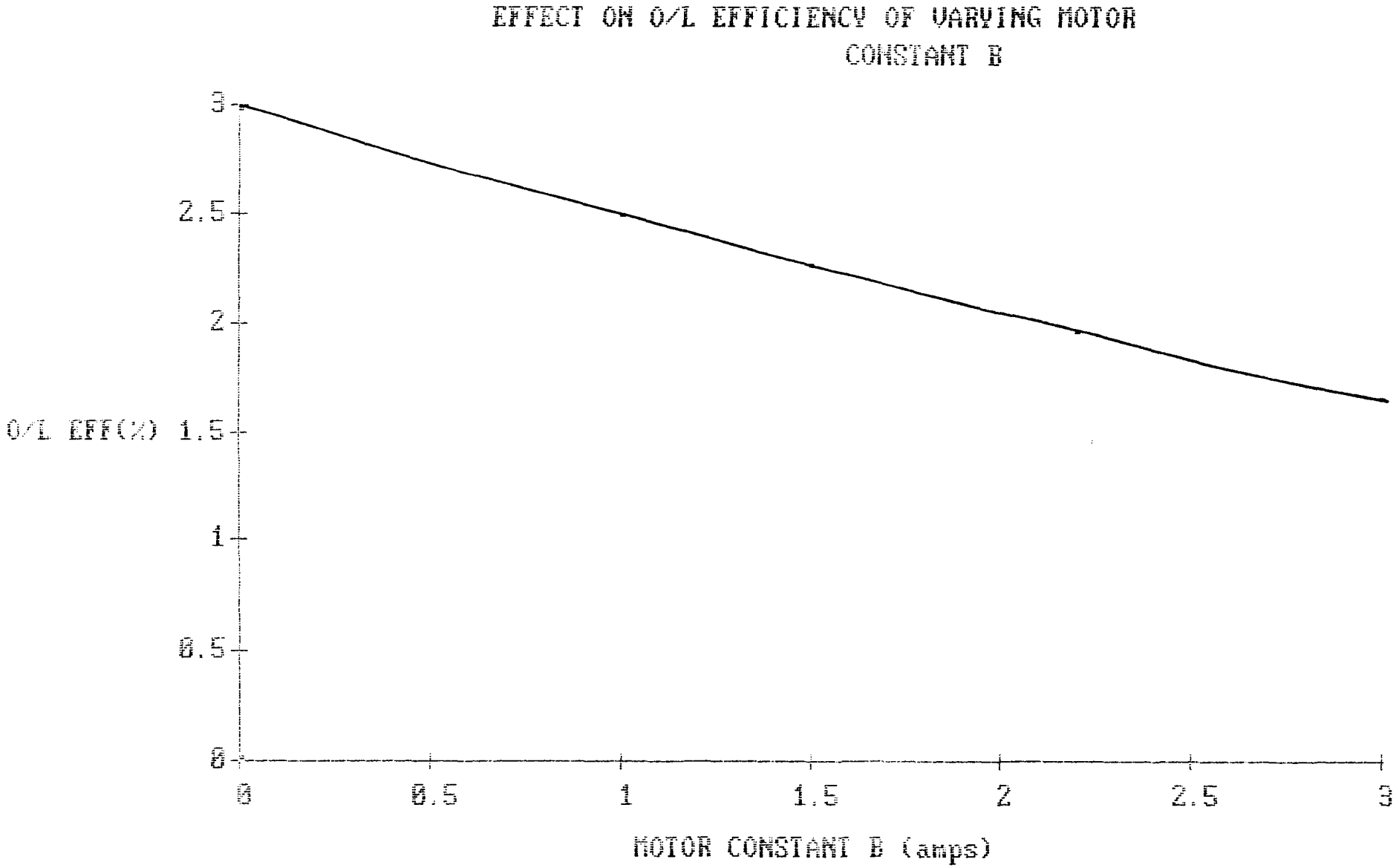
EFFECT ON O/L EFFICIENCY OF VARYING MOTOR CONSTANT B
O/L EFF(%)
3
2.5
2
1.5
1
0.5
0
0
0.5
1
1.5
2
2.5
3
MOTOR CONSTANT B (amps)

FIGURE 5·14

B is probably related to mechanical and electrical losses within the motor, and any attempts to reduce these losses are worthwhile. For instance, improved roller bearings and a lighter rotor and shaft, would reduce frictional and inertial losses. However any improvements in motor performance and hence Over-all Efficiency, have to be weighed against the costs involved in the improvements.

5.7.4 Motor Parameters K,Ke & ϕ

The parameters K & Ke relate to the size of the permanent magnet and wound rotor. ϕ is related to the strength of the magnetic flux and hence permanent magnet.They appear in the motor Equations16 & 18 as either Kϕ or Keϕ .In Equation 22 defining the slope dIm/dVm they appear as KKeϕ^2.

I have not sought to analyse how they relate to motor design, but rather I have tried to determine the sensitivity of the Over-all Efficiency to their variation.

The Figure 5.15 shows that any increase in KKeϕ^2 leads to a dramatic increase in Over-all Efficiency.This is contrary to the expectations of Equation 22, where it appeared that an increase in dI/dV would lead to improved efficiency.Probably any advantage gained through increasing dI/dV is out weighed by a reduction in efficiency through lower torque and increased speed. This would tend to move the I-V line for the motor/pump (Figure5.6 & discussed in Section 5.3.2.3) further to the left of the Peak Power Line for the array.

For this Thesis it did not seem worthwhile taking this analysis of motor parameters further. Rather the analysis

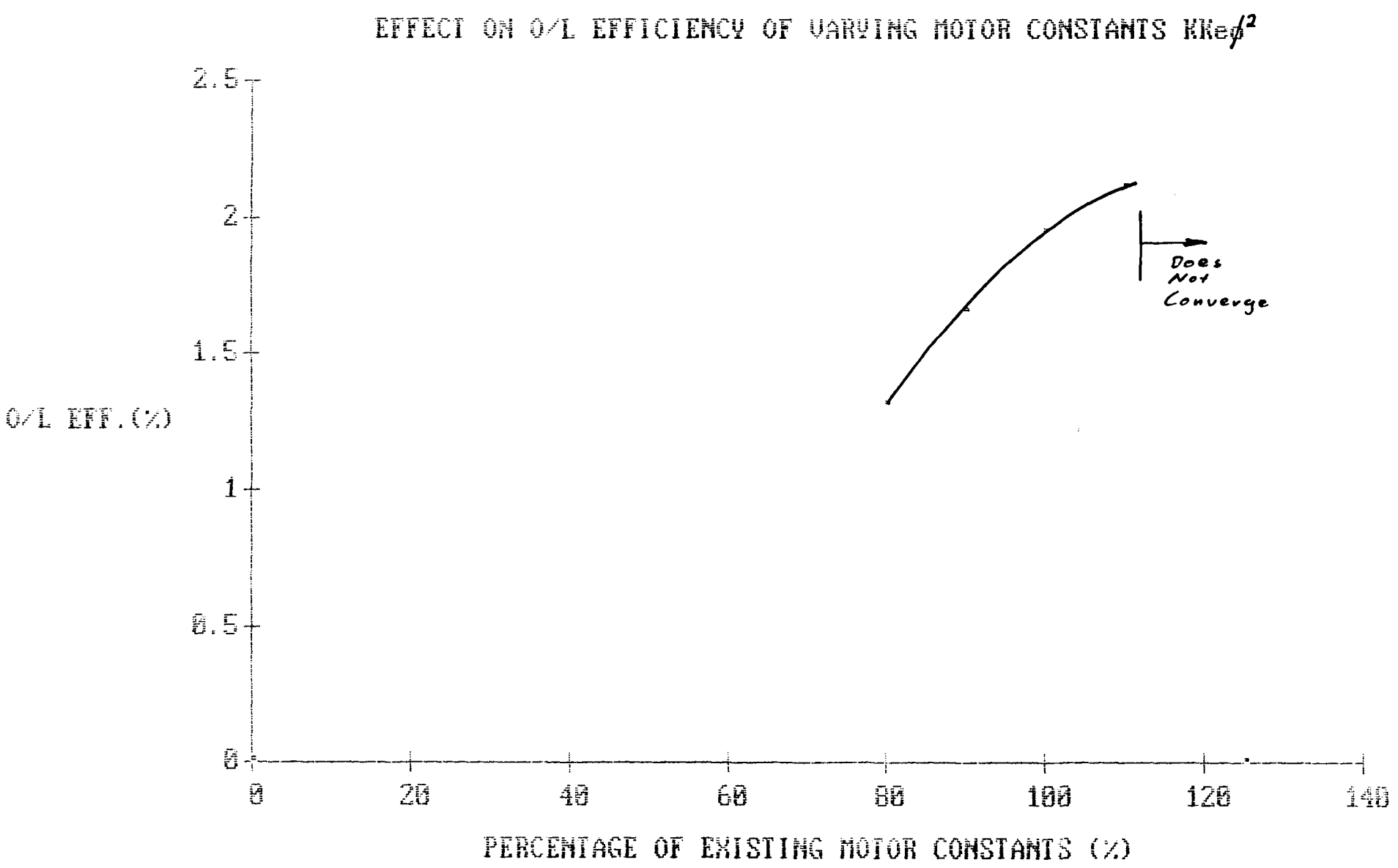
EFFECT ON O/L EFFICIENCY OF VARYING MOTOR CONSTANTS KKeϕ²
O/L EFF.(%)
2.5
2
1.5
1
0.5
0
0
20
40
60
80
100
120
140
PERCENTAGE OF EXISTING MOTOR CONSTANTS (%)
Does Not Converge

FIGURE 5·15

shows the influence these parameters have on over-all performance.

The analysis has also revealed a problem with the computer model. For values of $KKe\phi^2$ above 115% the model does not converge to a solution, because of the sensitivity of array current to voltage variation for solutions to the right of the 'knee'.This is discussed further in the next Section.

5.7.5 Pulley Ratio , RP

In Section 5.3.2.3 it was predicted that reducing the pulley ratio would improve the Over-all Efficiency. The model shows this to be the case., Figure 5.16.

Unfortunately the computer model does not converge for an RP less than 0.43. Because under this condition the intersection point of the I-V curve for the motor/pump and the I-V curve for the array occurs to the right of the knee. In this region array current is very sensitive to any variation in array voltage. Therefore with voltage as the iterative variable, as in the computer model, convergence does not occur.

The model highlights the sensitivity of the Over-all Efficiency to pulley ratio and therefore the need to carefully select the pulley ratio.

5.7.6 Pump Parameters

Unfortunately due to the nature of the equations defining pump performance used in the computer program, it is not possible to readily relate the constants in these equations to the shape and size of the pump. Therefore the program, in it's present form, cannot be used to optimize

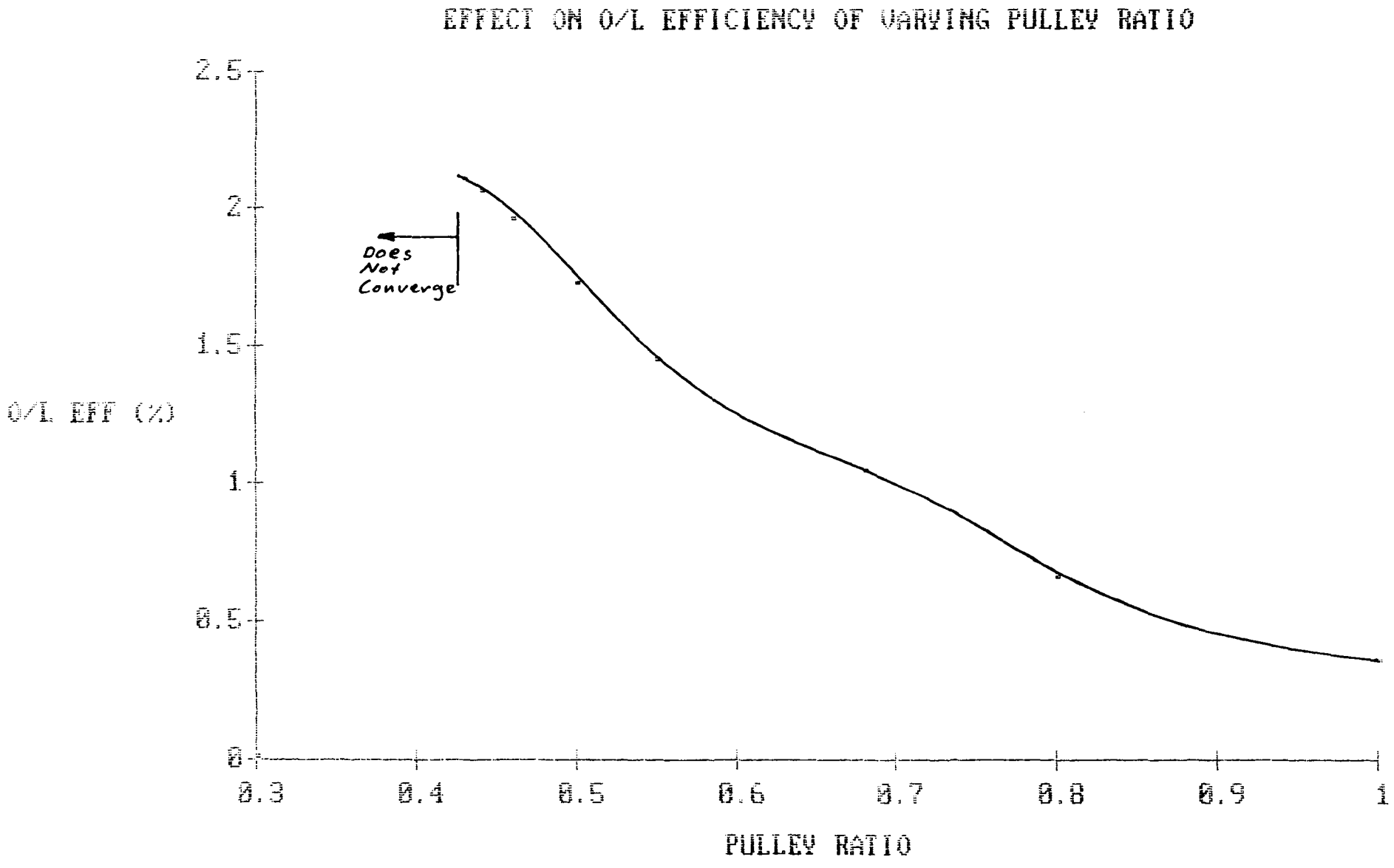
EFFECT ON O/L EFFICIENCY OF VARYING PULLEY RATIO
O/L EFF (%)
2.5
2
1.5
1
0.5
0
Does
Not
Converge
0.3
0.4
0.5
0.6
0.7
0.8
0.9
1
PULLEY RATIO

FIGURE 5·16

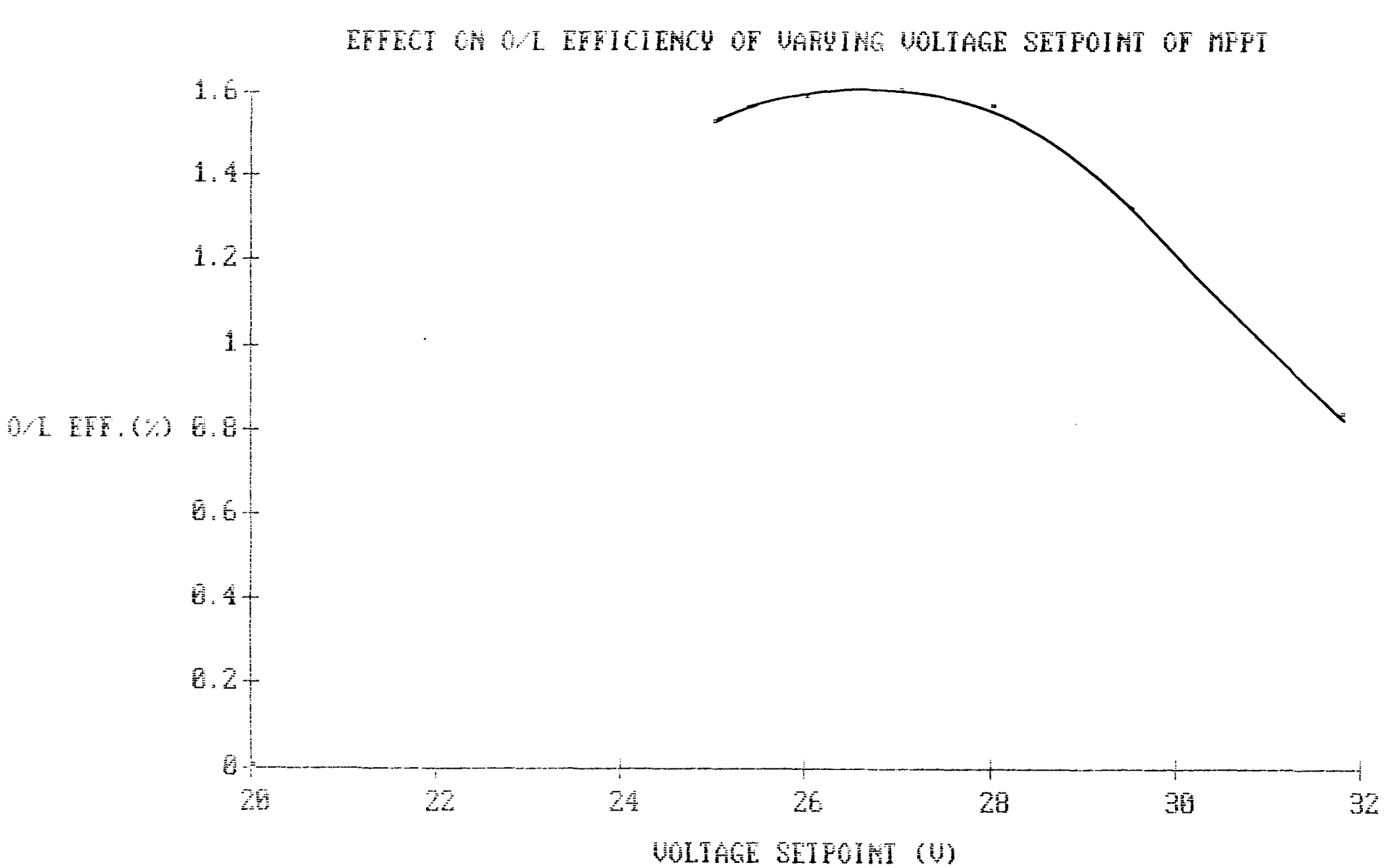
EFFECT ON O/L EFFICIENCY OF VARYING VOLTAGE SETPOINT OF MPPT
O/L EFF.(%)
1.6
1.4
1.2
1
0.8
0.6
0.4
0.2
0
20
22
24
26
28
30
32
VOLTAGE SETPOINT (V)

FIGURE 5·17

the design of the pump.

5.7.7 Voltage Setpoint, with MPPT.

The model indicates that with the MPPT added, Over-all Efficiency reaches a peak of 1.6% at a voltage setpoint of 27 volts(Figure 5.17).From the data provided by Solarex, Over-all Efficiency should be highest at around 29.5 volts. The discrepancy is due to the difficulty in modelling the "knee" of the I-V curve. Probably the setpoint voltage predicted from Solarex data is more accurate.

5.8 RELIABILITY

From the solar pump's installation in October 1985 through to the most recent site inspection in March 1987 there has been no noticeable deterioration in solar pump components.

The PV array has not shown any signs of physical deterioration. The pump, despite its operation in a corrosive environment, shows no signs of wear of bearings or seal. Likewise the motor appears satisfactorv.

There has been no maintenance of any kind apart from washing the arrav.

It is intended to dismantle the pump and motor in September 1987 and check the deterioration of brushes, seals and bearings.

The continuous performance of the solar pump over an 18 month period, in a harsh environment atests to the suitability of this design to remote area applications where reliability and low maintenance are critical considerations.

CHAPTER 6

CONCLUSION

The solar pump has been operating continuously for over 15 months and detailed meterological and pump performance data has been collected. The computer model has simulated the solar pump's performance over this period.

From an analysis of the data and running of the computer model the following points emerge:

6.1 PERFORMANCE OF THE SOLAR PUMP AT SITE

6.1.1 Analysis of this data shows the solar pump is performing below that specified by the Department of Water Resources and predicted by the manufacturer, which supports the view that manufacturers have no reliable method for the design and selection of solar pumps.

With the Maximum Power Point Tracker (MPPT) fitted the average flow is only 30% of that specified. The MPPT is shown to have an efficiency of only 72% and causes the pump to operate in a low power region of the photovoltaic array. Removal of the MPPT more than doubled the pump's performance but a poor match between the pump/motor and array characteristics still caused the pump to operate well below specification.

6.1.2 Despite the solar pump's apparent poor performance, it had an over-all efficiency of 1.8%, which was more efficient than most pumps tested in a project for the World Bank.

6.1.3 The pump has proven itself to be very reliable: it has been operating continuously, with no deterioration in performance for over 15 months in a harsh corrosive environment, with no maintenance of any components apart from washing of the PV array surface.

6.2 PERFORMANCE OF THE COMPUTER MODEL

6.2.1 The computer model successfully simulates the performance of the individual components of the solar pump. However the array model could be improved through better modelling of the following characteristics of the I-V curve: a) the region to the left of the 'knee' for high radiation values b)the maximum power point c)the region to the right of the 'knee' for high cell temperatures.

6.2.2 The computer model of the solar pump predicts, within 7%, the performance of the solar pump without the MPPT fitted and within 17% with the MPPT. The additional error associated with the fitting of the MPPT is because of inaccuracies in modelling: a) the array characteristics close to the open circuit voltage of the array b) the set point voltage of the MPPT.

6.2.3 The use of average radiation data to estimate a pump's performance can result in grossly over-estimated flowrates because of the non-linear relationship between flow and radiation. This results in the model over estimating flows on cloudy days.

6.2.4 The required cell temperature input to the model restricts the model's application. Further developments of the model should attempt to express cell temperature as a function of ambient conditions.

6.2.5 Basing the computer model for the solar pump solely on manufacturers' data sheets has the advantage of a simple model which can be easily adapted to 'off the shelf ' components, but has the disadvantages of: inherent errors in manufacturers' specifications; and limitations in using the model to design or optimize components.

6.2.6 The computer model predicts that the solar pump's performance could be improved by improving the match between the pump/motor and the arrav, achieved through reducing the pulley ratio and modifying some of the parameters associated with the electric motor design. Unfortunately the effect of modifying pump parameters could not be investigated.

Also the model has shown that reducing pipe friction and cable and connection losses has little effect on the solar pump's performance but if these losses increase, eg through scaling of the pipe walls or deterioration of motor brushes, then performance will deteriorate significantlv.

The monitoring of the solar pump at Wakool and the development of the computer model has shown that a solar powered photovoltaic water pump can be successfully modelled on computer and the model used to predict performance and optimize the design. With further development, computer models will assist both the manufacturer and purchaser of solar pumps in the design and selection of solar pumps for particular duties and locations, increasing their economic viability and market potential.

BIBLIOGRAPHY

1. 'Two Outback Settlements Get Combined Water Supply' IEA Magazine Oct/86

2. P. Longrigg 'Use of Solar Photovoltaics to Transport and Desalt Groundwater Supplies Using Brushless D.C. Motors' Solar Cells Vol 13 1985

3. J. Kenna et al 'The Prospects for Solar Water Pumping: Economic Case Studies of Agricultural and Water Supply Application in the Developing World' ISES Conf. 1983

4. C.Bhattacharjee 'Photovoltaic System for Mini Irrigation and Rural Electrification in Tribal Areas' Irrigation and Power July/85

5. Hobbs & Morrison 'Solar Photovoltaic Water Pumping System Performance & Design ANZSES Conf. 1986

6. G.Swanson 'Solar Pumps/ Getting Off the Ground' Water Well Journal Mar/85

7. Dept. Water Res. File no.83/12042 'Investigation of Alternative Power Sources for Pumping'

8. Dept. Water Res. 'Farm Water Supplies: Reola Station, Bourke' File no.A9096

9. Sir W. Halcrow 'Small-Scale Solar-Powered Irrigation Pumping Systems:Phase 1 Project Report' (1981) Report to UNDP

10.Braunstein & Kornfield; 'Analysis of Solar Powered Electric Water Pumps' Solar Energy Vol 27/3 1981

11.Hsiao & Bevins 'Direct coupling of Photovoltaic Power Source to Water Pumping System' Solar Energy Vol 32/4 1984

12.Singer et al 'Characterisation of PV Array Output Using a Small Number of Measured Parameters Solar Energy Vol 32/5 1984

13.J.Rogers 'Theory of Direct Coupling Between D.C. Motors & PV Solar Arrays Solar Energy Vol 23 1979

14.J.Roger 'Water & Photovoltaics in Developing Countries' Solar Cells Vol 6/3 1982

15.G.Hart et al 'Experimental Test of Open Loop Maximum Power Point Tracking Techniques for Photo-voltaic Arrays' Solar Cells Vol 14 1985

16.K.Daly 'The Modelling & Control of Solar Array AC/DC Converter/Battery Systems' ANZSES Conf. 1986

17.A.Stepanoff 'Centrifugal and Axial Flow Pumps' John Wiley & Sons, 1967

18.TRNSYS A Transient Simulation Program. University of Wisconsin/University of N.S.W.

19.I.Karassik et al 'Pump Handbook' McGraw Hill 1976

APPENDIX A.

WATER RESOURCES COMMISSION

SCHEDULE OF TECHNICAL DATA No. 83

WAKOOL - TULLAKOOL

SOLAR POWERED WATER PUMPING UNIT

1. Description of Work

(a) This Schedule of Technical Data covers the design, manufacture, supply and delivery to the Commission's Wakool Office of one solar powered water pumping unit comprising solar array, pump, motor, cable, associated controls and equipment. This Schedule does not include pipework or valves.

(b) Wakool is about 670 km south west of Sydney. It is served by the Victorian Railways, being linked by rail to Echuca and thence Melbourne. Freight for Wakool not completely occupying a rail waggon is transported by rail to Kerang and by road between Kerang and Wakool.

The station closest to Wakool on the New South Wales railway system is located at Finley approximately 110 km by road east of Wakool.

2. Application

(a) The pumping unit is required to pump saline water during daylight hours from the peripheral drain around the evaporation basin of the Wakool-Tullakool Sub-Surface Drainage Scheme.

(b) The unit shall be suitable for operating completely unattended.

(c) The pumping unit shall be capable of supplying a minimum of 60,000 litres per day at 4 metres total head with a daily global insolation of 18 MJ/m^2 day at an ambient temperature of 25°C.

3. Location of Pump and Motor

(a) The pump and motor unit shall be suitable for installing in one of two locations:

(i) Mounted on a concrete plinth on the bank of the channel. The base of the motor and pump shall be suitable for bolting directly onto the concrete plinth. Maximum total suction head (including losses in the pipe and foot valve) is three metres.

(ii) floating on the surface of the water in the drain.

Note: Alternative installations, if proposed in the tender, will be considered.

(b) It is estimated the total static head may vary ± 0.15 metres.

4. Description of Equipment

(a) Motor, Pump and Associated Controls.

(i) The motor and pump unit shall be suitably protected against pumping when the water level in the peripheral drain is inadequate for satisfactory operation.

(ii) The motor and controls shall:

1. be capable of withstanding continuous current flow through the armature, brushes and control wiring during low sunlight conditions when there is insufficient power to turn the motor/pump;

/2...

A.

2. be equipped with temperature protection and automatic reset.

3. be protected to AS1939 Class IP56 or equivalent.

(iii) The motor insulation shall be to AS1359 Class F or equivalent.

(iv) All wetted surfaces of the pump and motor shall be suitable for operating in saline water at 21°C as set out below:

Conductivity millimhos/cm	HCO_3^- mg/L	Cl^- mg/L	SO_4^{2-} mg/L	Ca^{2+} mg/L	Mg^{2+} mg/L	Na^+ mg/L	K^+ mg/L	pH
51.4 (30800 ppm)	135	22800	2405	1600	2190	10400	13.2	6.5

(v) The solar array shall not be short circuited under any operating condition of the pumping unit.

(vi) All components exposed to the atmosphere shall be of corrosion resistant materials or coated with suitable protective coatings and capable of resisting damage by intense sunlight.

(vii) The tenderer shall supply details of all materials in contact with the water.

(b) Solar Array.

(i) The solar array shall be of strong lightweight construction which can be readily installed by semi-skilled personnel.

(ii) The array shall be capable of withstanding winds of up to 200 kilometres per hour.

(iii) All components shall be of corrosion resistant materials or coated with suitable protective coatings and capable of resisting damage by intense sunlight.

(iv) The support frame shall be suitable for bolting directly onto concrete.

(v) Provision is to be made for tilting the panels at 15, 30, 45 and 60 degree angles relative to the horizontal.

(vi) The solar panels shall:

1. have toughened glass fronted surfaces or equivalent suitable for resisting hail stones and windblown sand. Silicone rubber surfaced panels are unacceptable.

2. be suitably constructed to allow easy cleaning

3. be totally enclosed and weatherproof. Electrical terminations shall be suitably sealed at entry to the solar panel

4. be suitable for operating at ambient temperatures of up to 50°C.

(vii) The back and the front (if necessary) surfaces of the solar panels shall be protected against damage by birds and animals. The top of the solar panels shall be fitted with serrated curved strip to prevent birds from alighting thereon.

/ 3...

(c) The cable and cable connections between the solar array and motor shall be weatherproof and shall not deteriorate under intense sunlight. A minimum of 20 metres of cable shall be provided between the solar array and motor.

(d) If the pumping unit is designed to operate at a nominal voltage exceeding 50 V d.c. notices warning of the voltage, shall be provided at the solar array and motor.

5. Performance Details

The tenderer shall supply all necessary performance charts and details for the solar pumping unit, to allow full assessment of the quotation.

6. Inspection

The completed pumping unit and solar array shall be inspected by the Commission's Inspector at the Contractor's works. The Contractor shall at his expense, do any work on the pump or other components which the Commission's Inspector may require during his inspection.

No item is to leave the Contractor's works until the Commission's Inspector is satisfied that the item complies in all respects with this Specification.

7. Assembly, Operating and Maintenance Instructions and Tools

The Contractor shall supply:

(a) instructions detailing full assembly of the solar array and pumping unit.

(b) three copies of the operation and maintenance handbook which shall contain at least the following information:

- Complete instructions for dismantling, examining, adjusting, reassembling and testing the pump/motor units, together with suggested regular maintenance instructions.
- A list of materials in the pump/motor units.
- A list of spare parts for the pump/motor units.

(c) one complete set of any special tools which will be required for the assembly and maintenance of the solar array and pump.

8. Packing

(a) The Contractor shall securely pack all items to ensure that the items are protected during transit from loss, damage or distortion to the satisfaction of the Commission's Inspector.

(b) The cost of packing shall be included in the quotation price and will not be paid as a separate item.

9. Delivery

The tenderer shall state the intended date of delivery to Wakool. Early delivery shall be favourably considered when assessing the quotations.

The Contractor shall be responsible for the safe delivery of all items to the Commission's Wakool Office. Any damage during transportation shall be repaired by the Contractor in a manner acceptable to the Engineer or replaced by new work.

/4...

A.

Maintenance

The Contractor shall guarantee the whole of the pump, electric motor, solar array and all other components against defective materials or workmanship for a period of 12 months from the date of delivery, or six months from commissioning, whichever is sooner.

11. Source of Manufacture

Preference will be given to goods manufactured in New South Wales over those manufactured in other States of Australia and to goods manufactured in Australia over those manufactured overseas. Approved New South Wales country manufacturers are also entitled to additional preference. Tenderers are to complete the attached schedule and include it with their quotation.

12. Quotations

(a) The lump sum quotation shall be accompanied by the following:

(i) A statement that the quotation complies with this Schedule of Technical Data. Alternatively, if the quotation does not fully comply with this Schedule of Technical Data, a statement listing those details which do not comply with the said Schedule.

(ii) A statement that the quotation is a firm price.

(iii) A statement that the delivery is firm.

(iv) Descriptive matter showing overall dimensions, performance and materials of construction of the items included in the offer as required by this Schedule.

(v) A list showing details, including location, of previously installed solar pumping units of similar capacity and construction to the one quoted in this tender.

(vi) A guarantee that the pumping unit will meet the capacity requirements of Clause 2(c) of this Schedule.

(vii) The completed Schedule for Source of Manufacture.

(b) The inclusion in the quotation or on any supplementary matter or printed letterhead accompanying the quotation of the Tenderer's standard general clauses or conditions may lead to rejection of the quotation.

APPENDIX C

APPENDIX B.

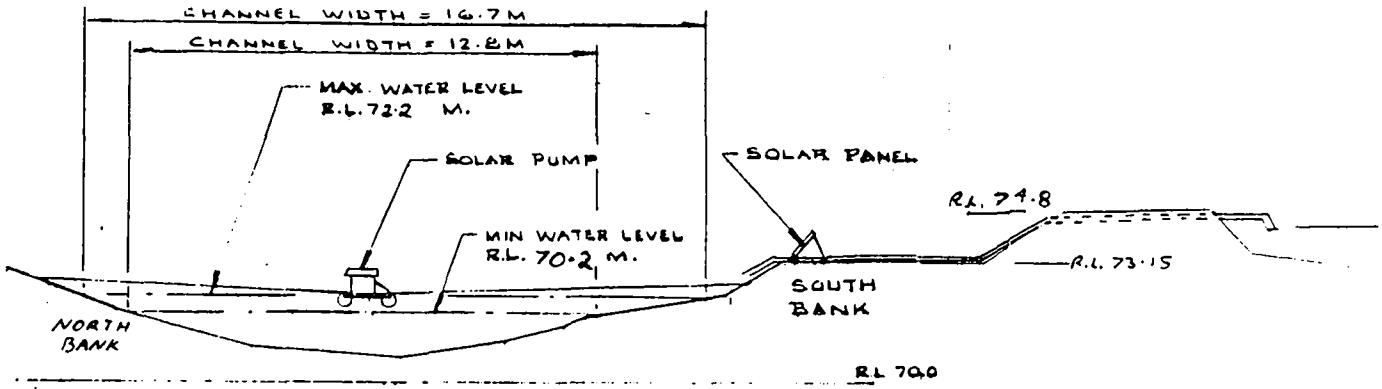

SECTION A-A

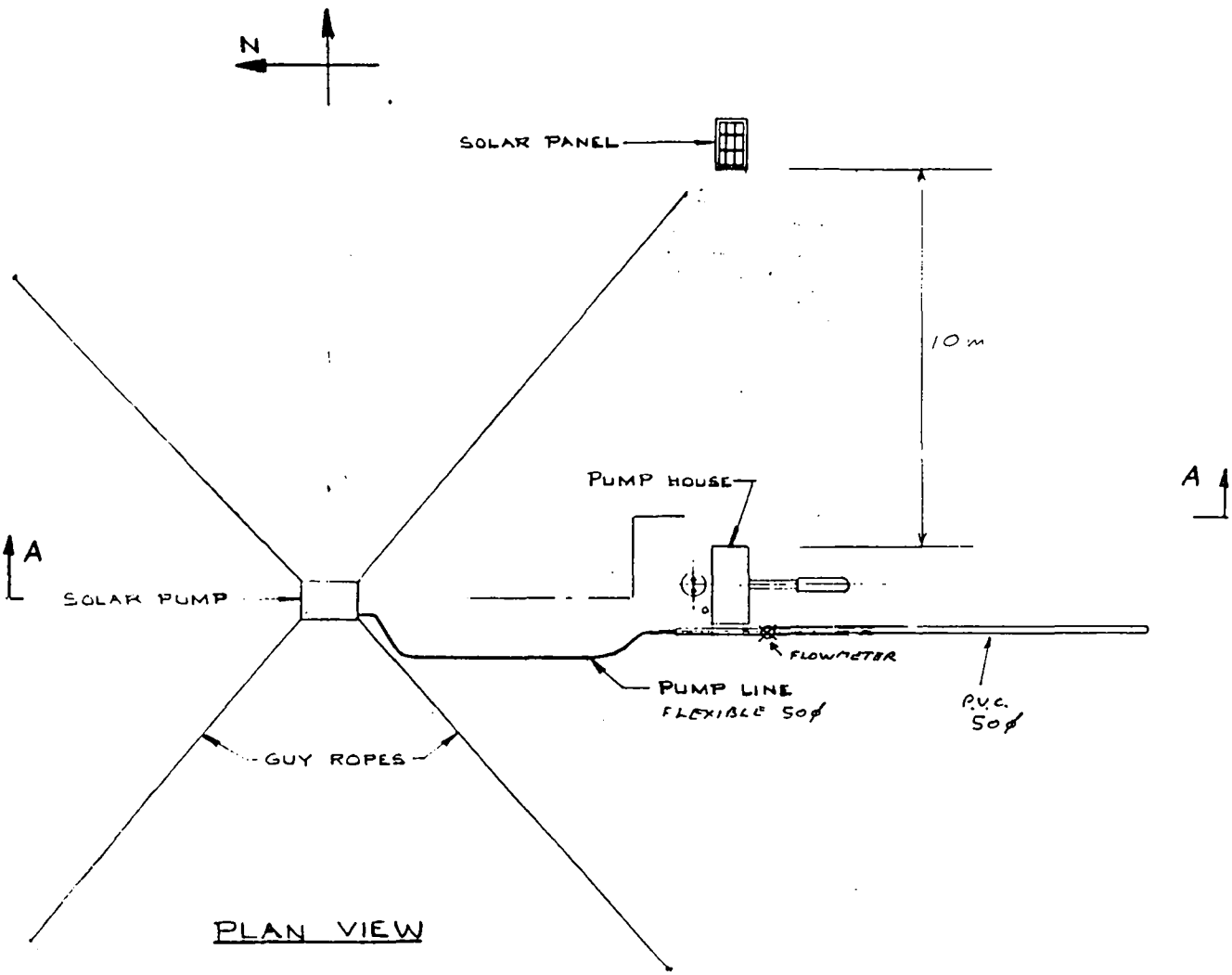

PLAN VIEW

SKETCH OF SOLAR PUMP INSTALLATION

WAKOOL - TULLAKOOL

APPENDIX C.


EVAPORATION BASIN
SOLAR PUMP
PERIPHERAL DRAIN

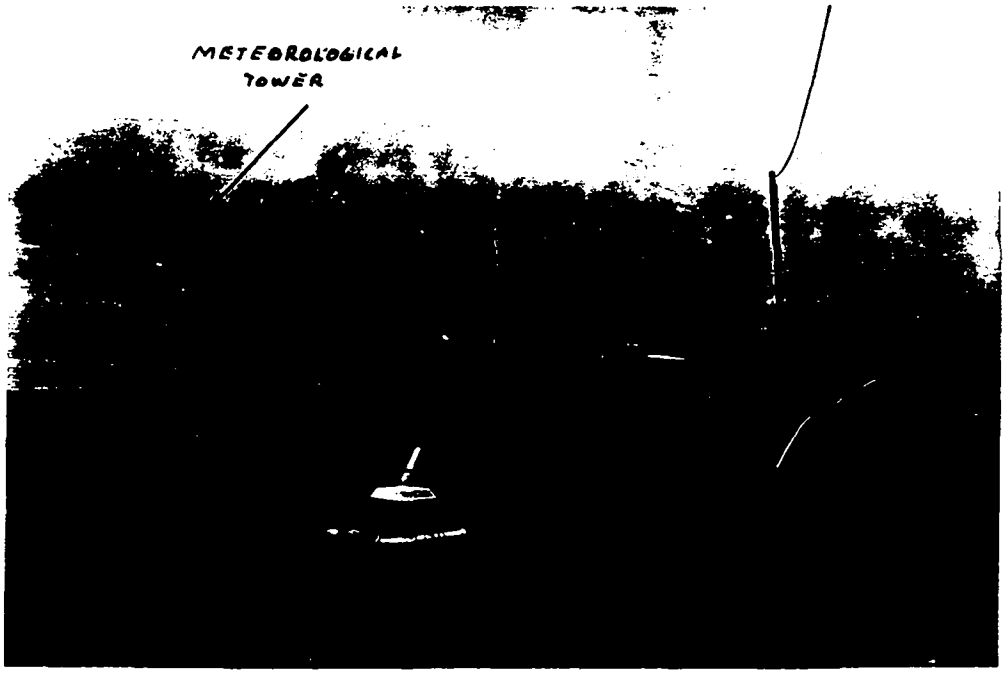
METEOROLOGICAL TOWER

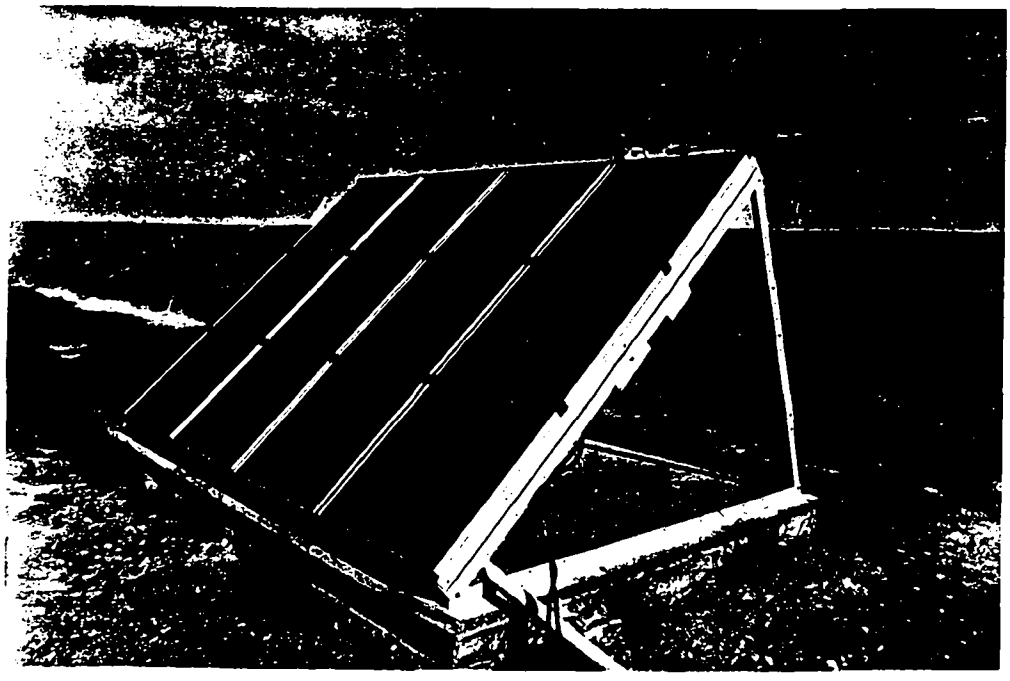
PYRANOMETER

SOLAR PUMP AFTER
18 MONTHS OPERATION

MINIMUM
DRAIN LEVEL

SCALING OF
PIPE
(MARCH/87)

INITIALLY
INTERNAL
PIPE SURFACE
WAS WHITE

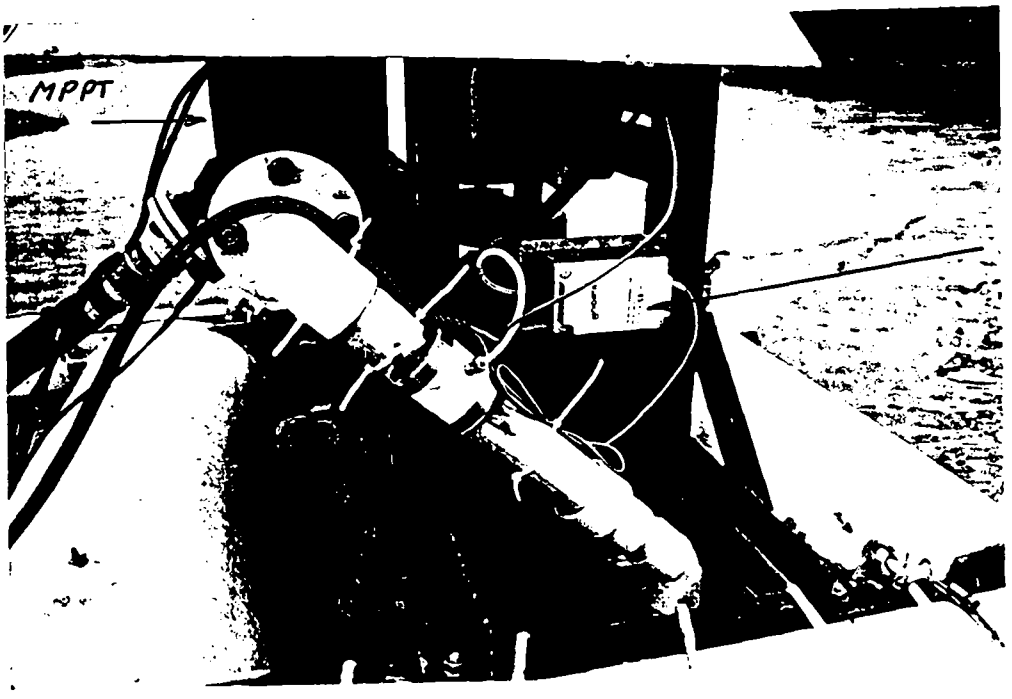

PRESSURE TRANSDUCER

DATA LOGGER FOR PUMP

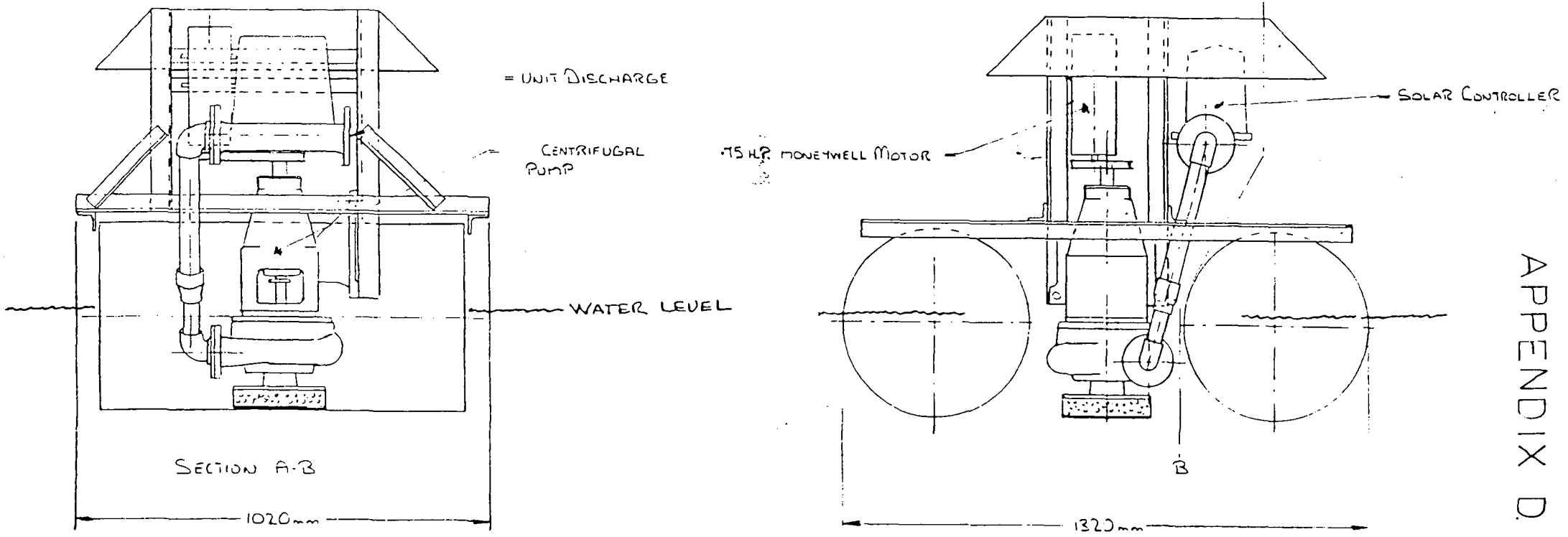
= UNIT DISCHARGE
CENTRIFUGAL PUMP
WATER LEVEL
SECTION A-B
1020mm
A
SOLAR CONTROLLER
.75 H.P. HONEYWELL MOTOR
B
1320mm

APPENDIX D.

TABLE I DETAILS OF SOLAR PUMP UNIT

COMPONENT	TYPE	DETAILS	COMMENTS
Pump	Centrifugal (Submerged suction)	50 mm Suction 159 mm Impeller Rated Speed 1300 RPM	Timing Belt Drive: Motor/Pump Ratio 0.46/1 Mechanical Seal
Motor	Permanent Magnet D.C. Motor	0.75 kw 24 volt D.C. 2400 R.P.M.	
Solar Array	Semicrystalline Silicon Solar Cells	12 Panels connected in series of two 40 Peak Watts at 1000 W/m^2 and 25° Cell Temperature	Mounted on Aluminium frame. Tilted at 34° Angle of tilt may be varied
Maximum Power Point Tracker		Rated to 0.9 kw	Heat Sink cooled by water discharged from pump
Cable		16 mm^2 Copper Cable 1.15 mohms/m	40 metres loop length

TABLE II DETAILS OF MONITORING EQUIPMENT

COMPONENT	TYPE	DETAILS	COMMENTS
Data Logger	Battery Powered CMOS	16 K Memory	Accesses all transducers every 5 seconds & logs data every ½ hour
Pressure Transducer	Piezoresistive	Range: 0-50 kPa ± 5% F.S.D.	Non-metallic diaphragm calibrated at Commission laboratory
Flow Meter	Inferential type with paddles	Range: 0.3-12 litres/sec ± 1% F.S.D.	Calibrated at Commission laboratory
Pyranometers			
Inclined	Eppley Black & White	± 3%	Mounted on Array
Horizontal	Silicon Flat Cell	Range: 0-1500 W/m^2 +5%	Mounted on 10 metre Tower
Anemometer & Wind Vane	Cup Anemometer	Range: 1.5-40 m/sec ± 2%	Mounted on 10 metre Tower
Temperature Transducers Ambient & Cell Temperature	Temperature Sensitive Transistor	Range - 10°C to 60°C ±0.5°C	Ambient transducer mounted on 10 metre Tower Cell Temperature Transducer fitted to back of a Photovoltaic Cell

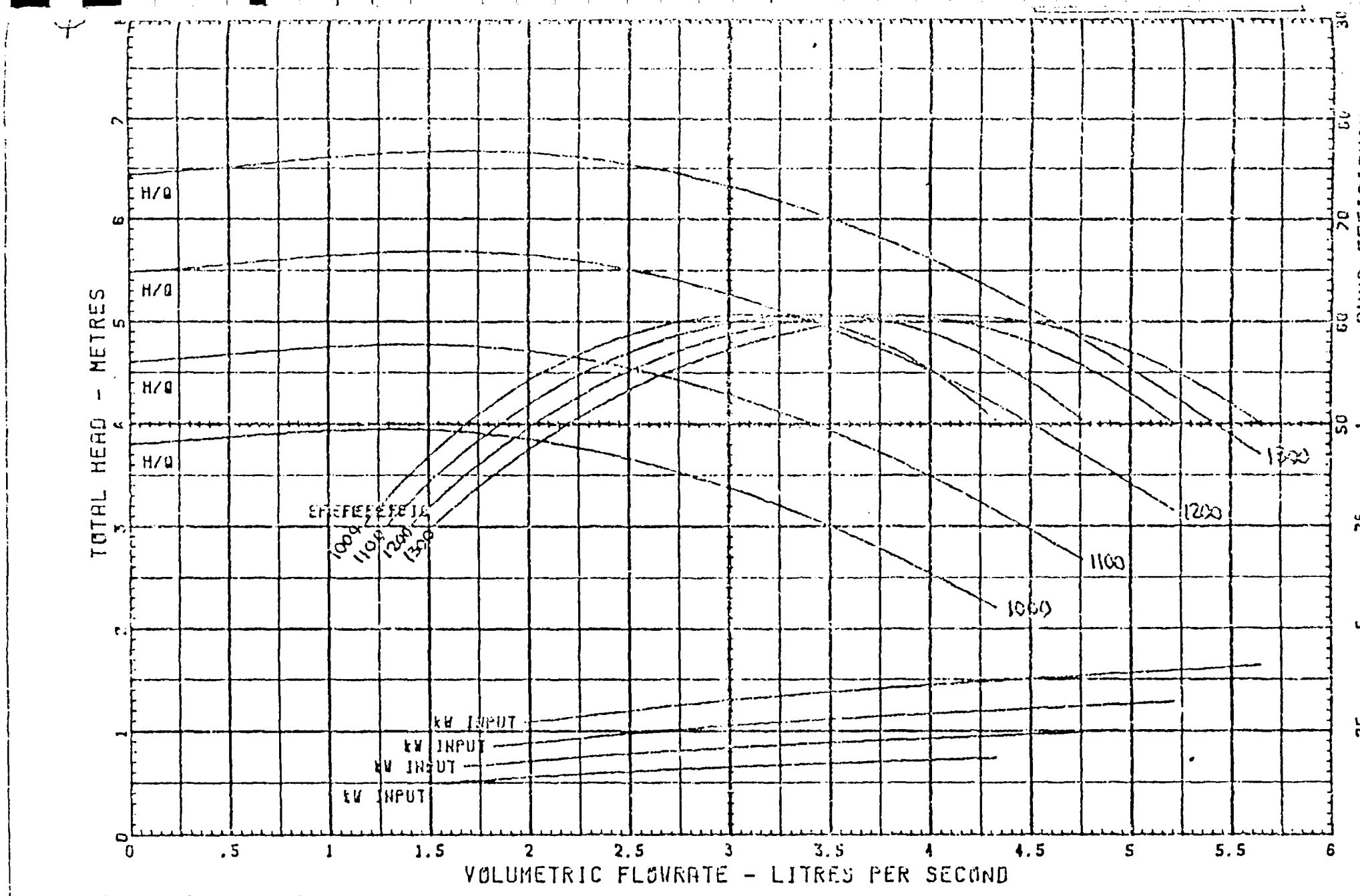

DATA REFER TO CLEAN COLD WATER

APPENDIX F

APPENDIX G.

FINAL MOTOR DATA

DATE: _____

CUSTOMER: Honeywell/Australia MOTOR#: BA3637-3501-568-

INPUT VOLTAGE: 24V AC (DC) RATED TORQUE: 20 LB-IN HP: 0.75

RATED SPEED: 2400 RPM NO LOAD SPEED: 2655 RPM RATED CURRENT: 28.7 AMPS

DUTY CYCLE: Intermittent FRAME TYPE: BA36 LENGTH: ~~ INCH

STALL TORQUE: 138 Lb-IN. STALL CURRENT: 185 AMPS

VOLTAGE CONSTANT: K_E 8.93 $\frac{V}{KRPM}$ TORQUE CONSTANT: K_T 0.755 $\frac{LB\text{-}IN}{AMP}$

COMMENTS: _____

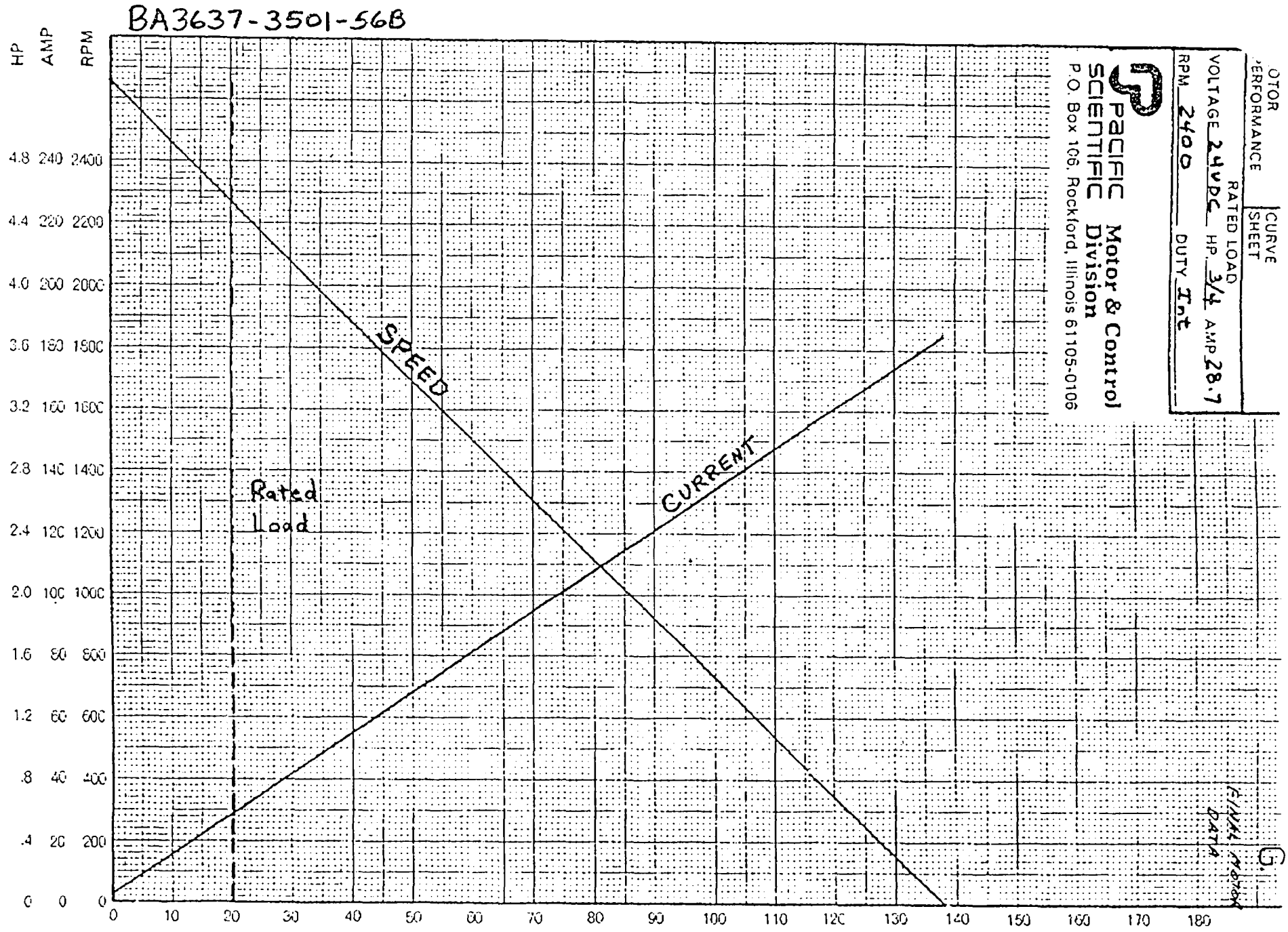
BA3637-3501-56B
HP
AMP
RPM
4.8 240 2400
4.4 220 2200
4.0 200 2000
3.6 180 1800
3.2 160 1600
2.8 140 1400
2.4 120 1200
2.0 100 1000
1.6 80 800
1.2 60 600
.8 40 400
.4 20 200
0 0 0
0 10 20 30 40 50 60 70 80 90 100 110 120 130 140 150 160 170 180
SPEED
CURRENT
Rated
load
MOTOR PERFORMANCE
CURVE SHEET
RATED LOAD
VOLTAGE 24VDC HP 3/4 AMP 28.7
RPM 2400 DUTY Int
Pacific Scientific Motor & Control Division
P.O. Box 106, Rockford, Illinois 61105-0106
FINAL MOTOR DATA
5.

G.

PC-8

MOTOR PERFORMANCE	CURVE SHEET 249A
RATED LOAD VOLTAGE 24DC HP 3/4 AMP 28	
RPM 2400 DUTY CONT.	

HONEYWELL MOTOR PRODUCTS
P.O. Box 106, Rockford, Illinois 61105

BA 3637-316-1

ORIGINAL
MOTOR DATA

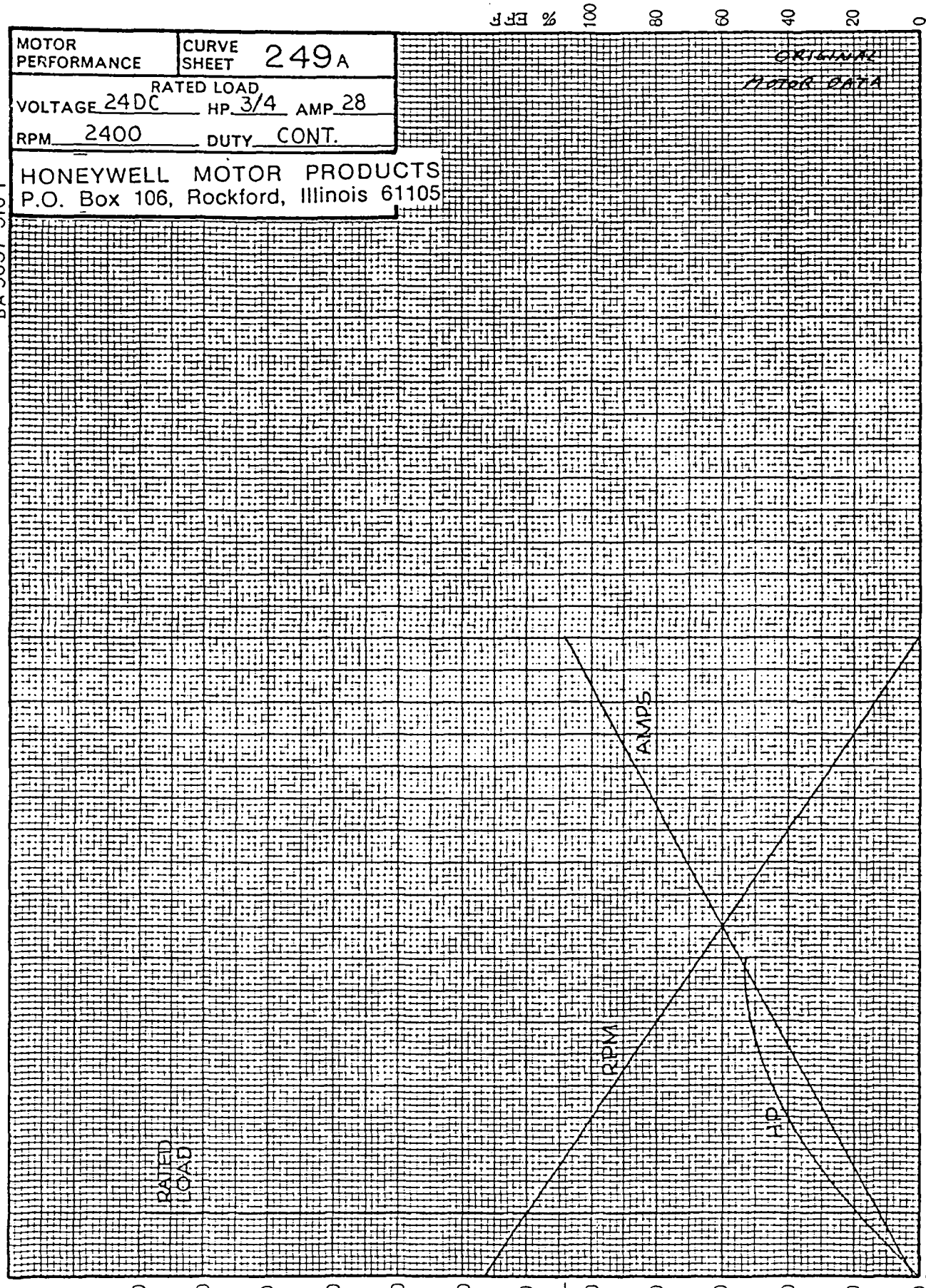

APPENDIX H.

SOLAREX UNIPANEL TYPE X100G

PERFORMANCE AT VARIOUS TEMPERATURES AT AM1(1kW/m²)

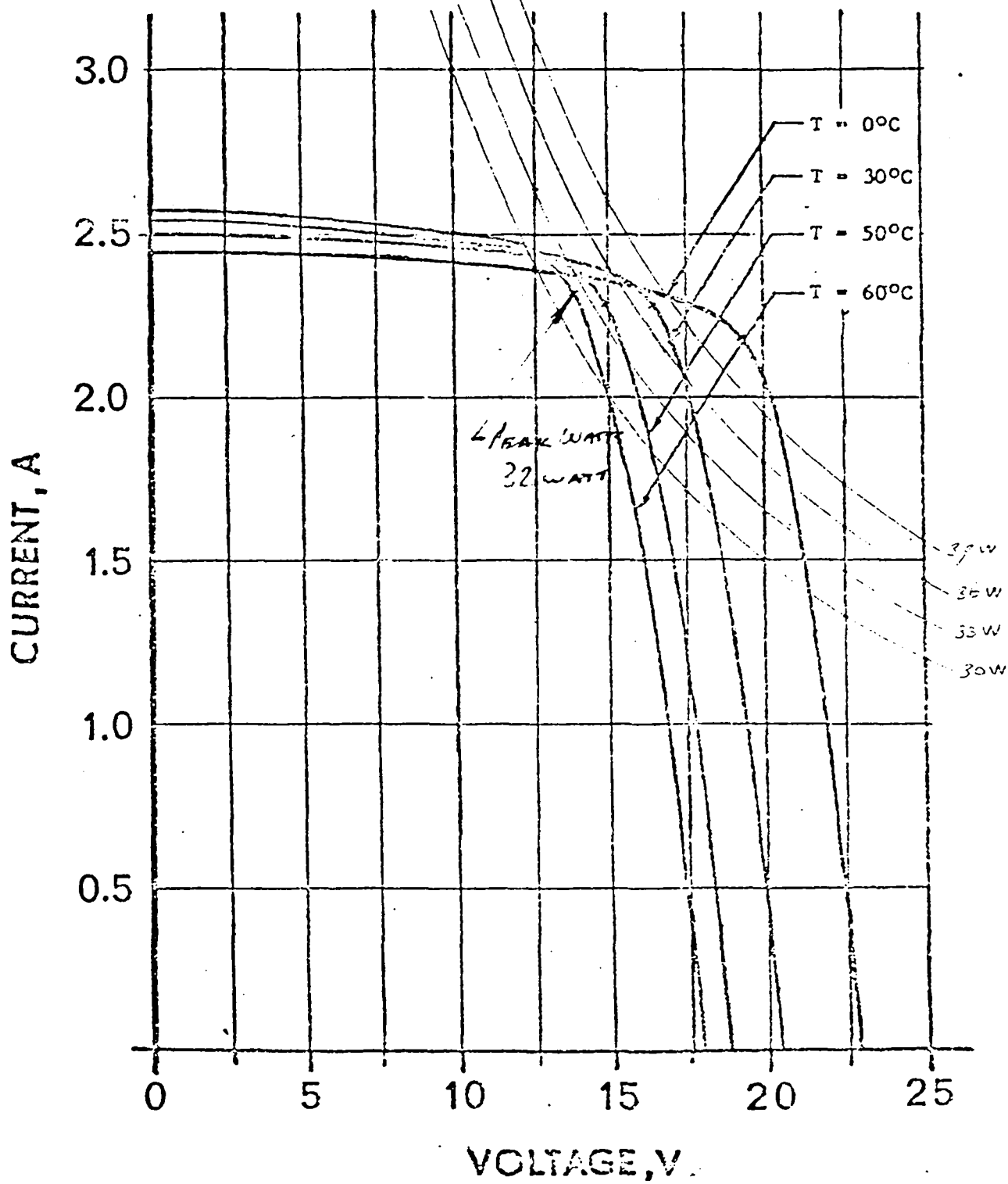

SOLAREX PTY. LIMITED
6 BELLONA AVE REGENTS PARK 2143-AUSTRALIA P.O. BOX 204 CHESTER HILL 2162
TELEPHONE (02) 644 5055 TELEX AA21975

Electrical Characteristics (Typical) ±10%

	X100GT
Peak power (Pp)	37w
Voltage at peak power (Vpp)	16.2v
Current at peak power (Ipp)	2.3A
Short-circuit current (Isc)	2.5A
Open-circuit voltage (Voc)	20.0v
Nominal current 14v (25°C)	2.4A
Nominal current 14v (50°C)	2.3A

NOTES:

1. Panels are measured under full sun illumination (1kW/m²) at 25°C ±3°C cell temperature. Minimum performance is 2 watts less than peak. The ruling specification is peak watts. For a more detailed explanation, see our *Electrical Performance Measurements* bulletin.

2. Electrical characteristics vary with temperature.

Voltage (Voc)	V_{oc}	increases by decreases by	2.4mV/°C/cell	below above	25°C
Current (Isc)	I_{sc}	increases by decreases by	25uA/°C/cm²	above below	25°C
Power (peak)	P_m	increases by decreases by	0.4%/°C	below above	25°C

X100GT
Performance at Various Light Intensities, T = 25°C

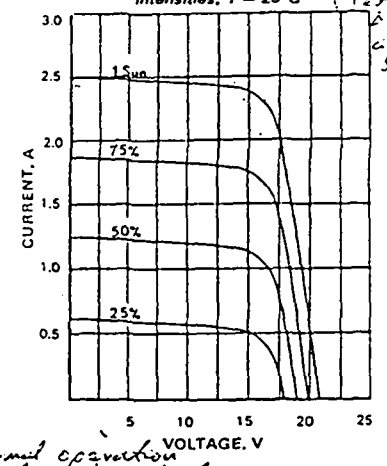

X100GT
Performance at Various Temperatures at AM1 (1kW/m²)

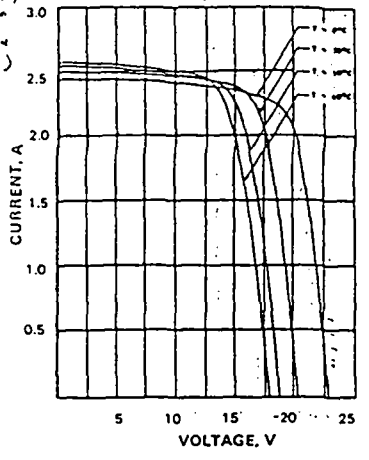

NOTE: These curves are representative of the performance of typical panels at the terminals, without any additional equipment such as diodes, cabling, etc. These curves are intended for reference only.

Regulators

Regulators for 12 volt and 24 volt D.C. systems are supplied in various current carrying capacities to suit the maximum charge current. They are recommended to ensure batteries are not overcharged.

Mechanical Specifications

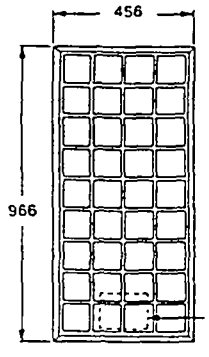

Weight:
8kg

Dimensions:
966mm x 456m x 25mm

CONSTRUCTION

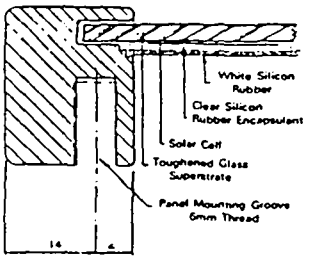

Mounting Frames

Frames can be supplied to accommodate single or multiple panel solar arrays.

Reliability and Environmental Specifications

These panels are subjected to intensive quality control during manufacture and testing before shipment to ensure optimum performance. They are designed to meet or exceed the following tests with no performance degradation:–

- Draft Australian standard solar module performance requirements and test methods
- Meet or exceed J.P.L. Environmental Requirements No. 5-342-1 Rev. B.
- Prolonged humidity cycling at elevated temperatures.
- Thermal cycling from −40°C to +90°C.
- All Solarex Unipanels are guaranteed for 5 years.

TERMINAL BOX

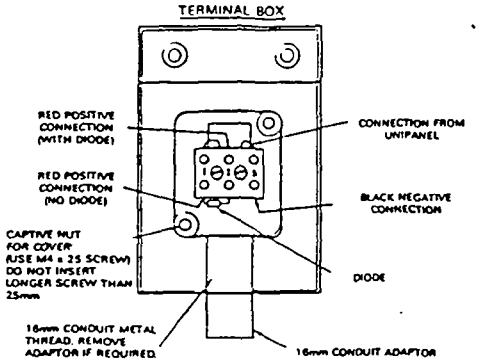

Applications

Providing reliable power systems for:–

- Microwave Repeaters.
- T.V. Translators.
- Cathodic Protection.
- Marine Beacons and Radio Navigation.
- Water Pumping and Irrigation.
- Railway Signalling.
- Battery Charging for caravans and boats.
- Homesteads and Villages in remote outback areas of Australia.

Specifications are subject to change without notice.

APPENDIX I.

SAMPLE PRINTOUT OF RECORDED DATA FOR 14th OCTOBER 1985

TIME	DATE	RADIATION INCL	RADIATION HOR	TEMP AMB	WINDSPEED AVG	WINDSPEED DIRN	VOLTS	AMPS	TEMP CELL	PRESS	FLOW
0 0	14 10 85	0	0	15.0	5.3	125	0.00	0.00	11.8	0.0	0.0
0 30	14 10 85	0	0	13.6	4.5	149	0.00	0.00	10.8	0.0	0.0
1 0	14 10 85	0	0	12.8	4.2	179	0.00	0.00	8.0	0.0	0.0
1 30	14 10 85	0	0	13.3	3.1	184	0.00	0.00	6.9	0.0	0.0
2 0	14 10 85	0	0	13.3	3.2	190	0.00	0.00	6.3	0.0	0.0
2 30	14 10 85	0	0	13.3	3.5	194	0.00	0.00	5.8	0.0	0.0
3 0	14 10 85	0	0	12.8	2.5	190	0.00	0.00	6.3	0.0	0.0
3 30	14 10 85	0	0	12.8	2.8	179	0.00	0.00	6.9	0.0	0.0
4 0	14 10 85	0	0	12.5	2.7	164	0.00	0.00	7.4	0.0	0.0
4 30	14 10 85	0	0	12.2	2.9	152	0.53	0.00	8.0	0.0	0.0
5 0	14 10 85	0	0	11.7	3.1	146	9.52	0.00	8.0	0.0	0.0
5 30	14 10 85	51	0	11.4	3.1	147	29.08	0.00	8.6	0.0	0.0
6 0	14 10 85	146	82	12.0	3.1	153	38.07	0.00	11.3	0.0	0.0
6 30	14 10 85	248	206	12.8	2.8	158	40.54	0.00	17.3	0.0	0.0
7 0	14 10 85	344	312	14.2	3.5	174	40.89	0.00	44.5	0.0	0.0
7 30	14 10 85	431	406	15.5	2.8	200	36.30	0.00	24.5	0.0	0.0
8 0	14 10 85	542	500	16.6	3.2	214	32.23	4.93	30.5	20.2	0.4
8 30	14 10 85	643	582	17.7	2.8	214	31.76	6.39	35.5	27.2	2.1
9 0	14 10 85	734	659	18.5	4.2	195	31.76	7.29	37.7	29.4	2.8
9 30	14 10 85	808	729	19.6	3.1	171	31.92	7.63	40.4	31.0	3.2
10 0	14 10 85	863	765	19.9	4.0	157	31.92	8.30	40.4	32.4	3.5
10 30	14 10 85	909	829	20.8	4.5	159	31.92	8.64	40.4	32.8	3.6
11 0	14 10 85	927	847	21.3	5.0	162	31.92	8.75	41.5	34.2	3.8
11 30	14 10 85	946	859	21.8	5.6	156	31.92	9.08	40.4	35.2	4.0
12 0	14 10 85	927	859	22.7	5.2	160	31.92	8.75	41.5	34.6	3.9
12 30	14 10 85	909	847	23.2	5.3	157	31.92	8.41	42.0	33.2	3.6
13 0	14 10 85	854	788	23.8	4.3	168	31.76	7.74	42.6	31.0	3.3
13 30	14 10 85	496	376	23.5	4.6	158	31.45	3.81	37.7	13.0	1.3
14 0	14 10 85	395	359	23.8	4.0	150	31.45	3.25	31.1	8.8	0.8
14 30	14 10 85	532	553	24.9	4.2	178	31.45	4.71	36.5	16.0	1.6
15 0	14 10 85	340	324	24.6	4.3	174	31.29	2.24	34.9	5.6	0.5
15 30	14 10 85	330	329	24.6	5.2	158	31.29	2.36	30.0	6.6	0.4
16 0	14 10 85	285	312	24.6	6.4	166	30.51	1.79	28.9	3.4	0.0
16 30	14 10 85	220	206	24.6	6.1	168	30.51	0.79	27.2	0.0	0.0
17 0	14 10 85	92	47	24.0	5.2	176	26.13	0.00	23.9	0.0	0.0
17 30	14 10 85	83	53	23.8	5.6	179	22.22	0.00	22.3	0.0	0.0
18 0	14 10 85	37	0	22.9	5.2	177	11.27	0.00	20.6	0.0	0.0
18 30	14 10 85	0	0	22.1	4.9	177	1.56	0.00	18.4	0.0	0.0
19 0	14 10 85	0	0	21.6	4.3	182	0.00	0.00	16.8	0.0	0.0
19 30	14 10 85	0	0	21.6	3.5	195	0.00	0.00	14.6	0.0	0.0
20 0	14 10 85	0	0	21.0	3.3	194	0.00	0.00	14.0	0.0	0.0
20 30	14 10 85	0	0	20.8	4.2	189	0.00	0.00	13.5	0.0	0.0
21 0	14 10 85	0	0	19.6	4.6	171	0.00	0.00	14.0	0.0	0.0
21 30	14 10 85	0	0	19.4	4.3	182	0.00	0.00	12.9	0.0	0.0
22 0	14 10 85	0	0	19.1	4.3	183	0.00	0.00	12.4	0.0	0.0
22 30	14 10 85	0	0	19.1	6.3	190	0.00	0.00	12.9	0.0	0.0
23 0	14 10 85	0	0	19.4	7.9	202	0.00	0.00	15.7	0.0	0.0
23 30	14 10 85	0	0	19.1	7.9	204	0.00	0.00	15.7	0.0	0.0

TYPE 35 (CON'T)

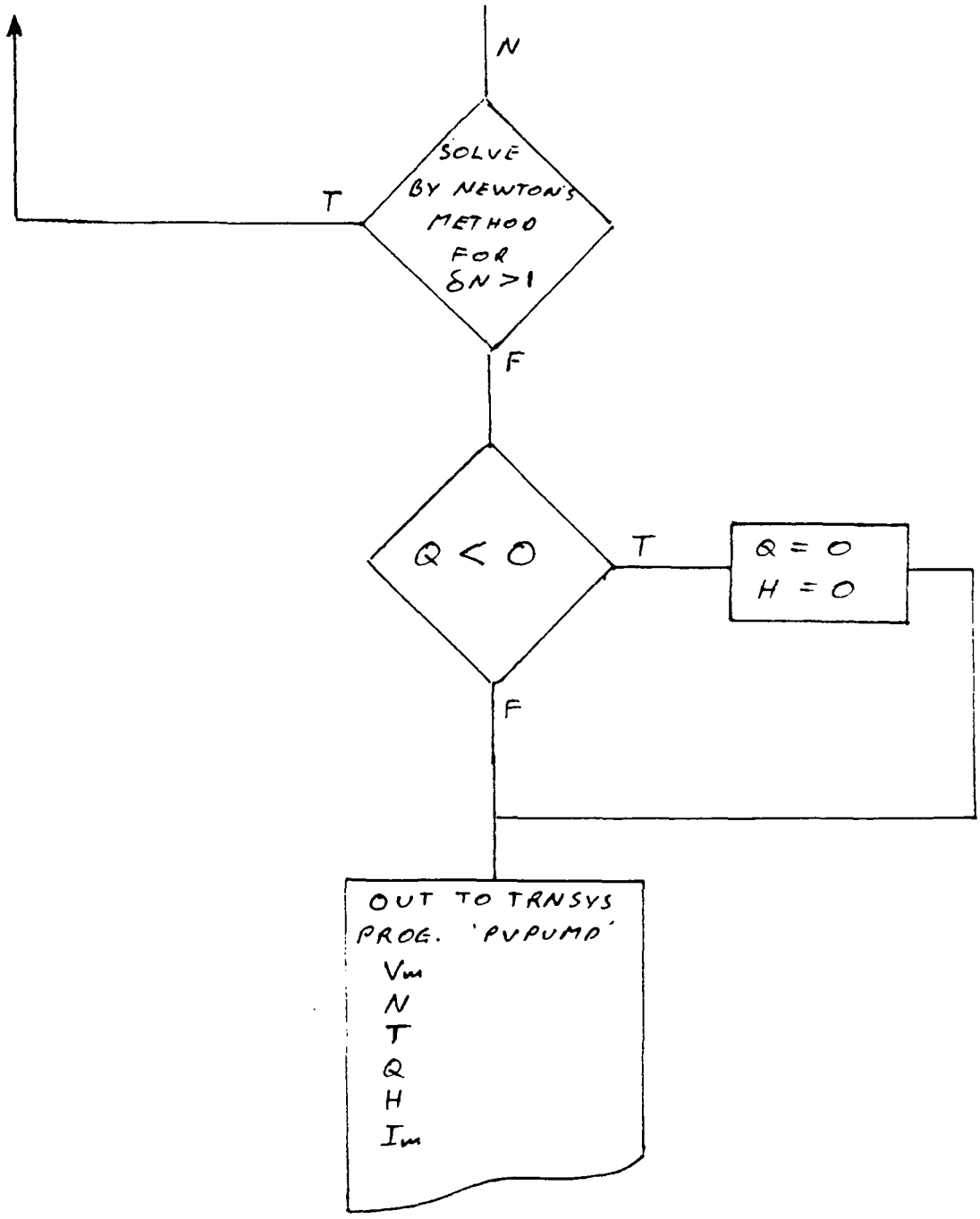
N
SOLVE BY NEWTON'S METHOD FOR δN > 1
T
F
Q < 0
T
Q = 0
H = 0
F
OUT TO TRNSYS PROG. 'PVPUMP'
Vm
N
T
Q
H
Im

SIMPLIFIED FLOW CHART FOR PROGRAM TYPE 351

PUMP - MOTOR - PIPELINE WITH MPPT

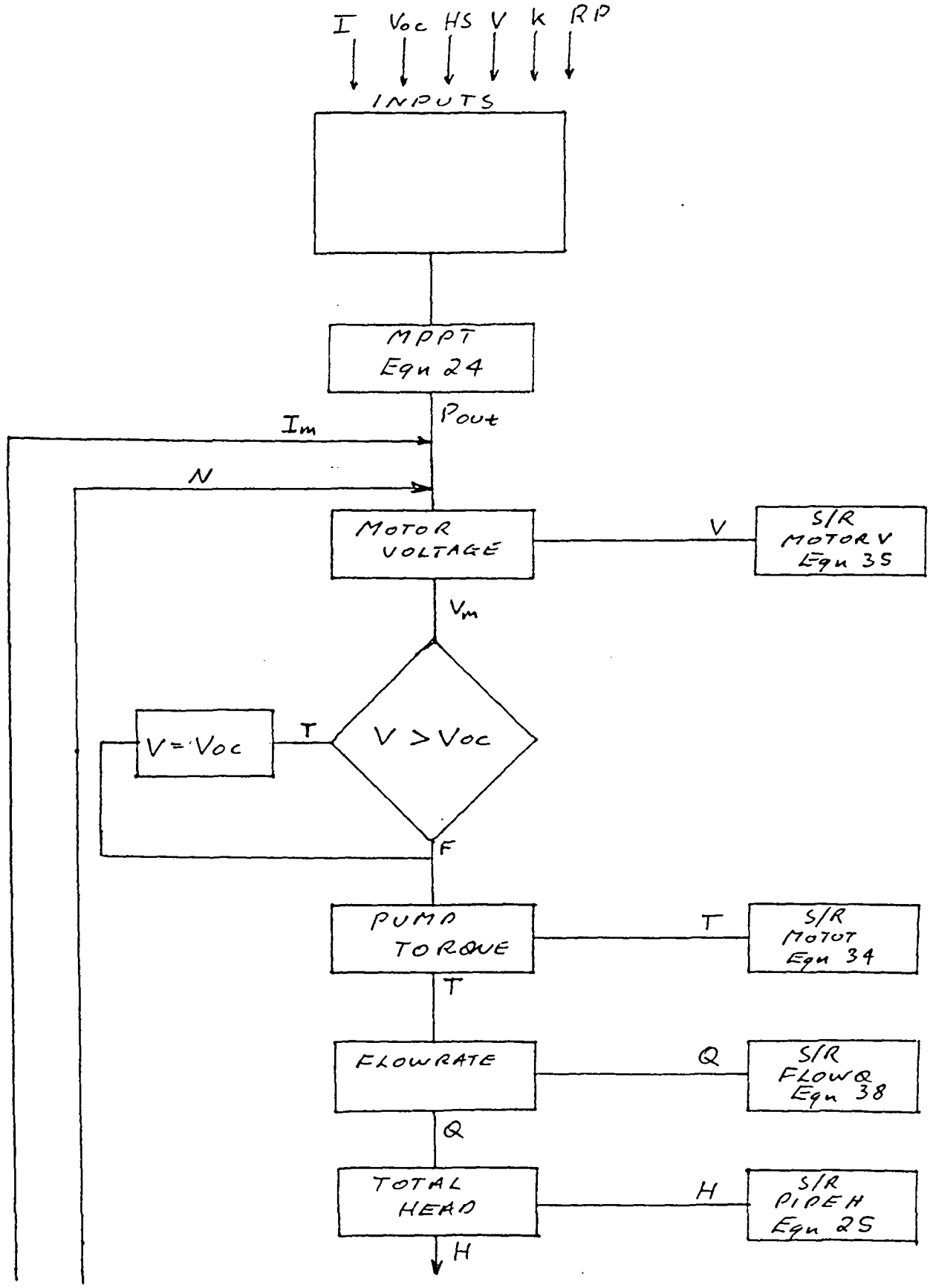

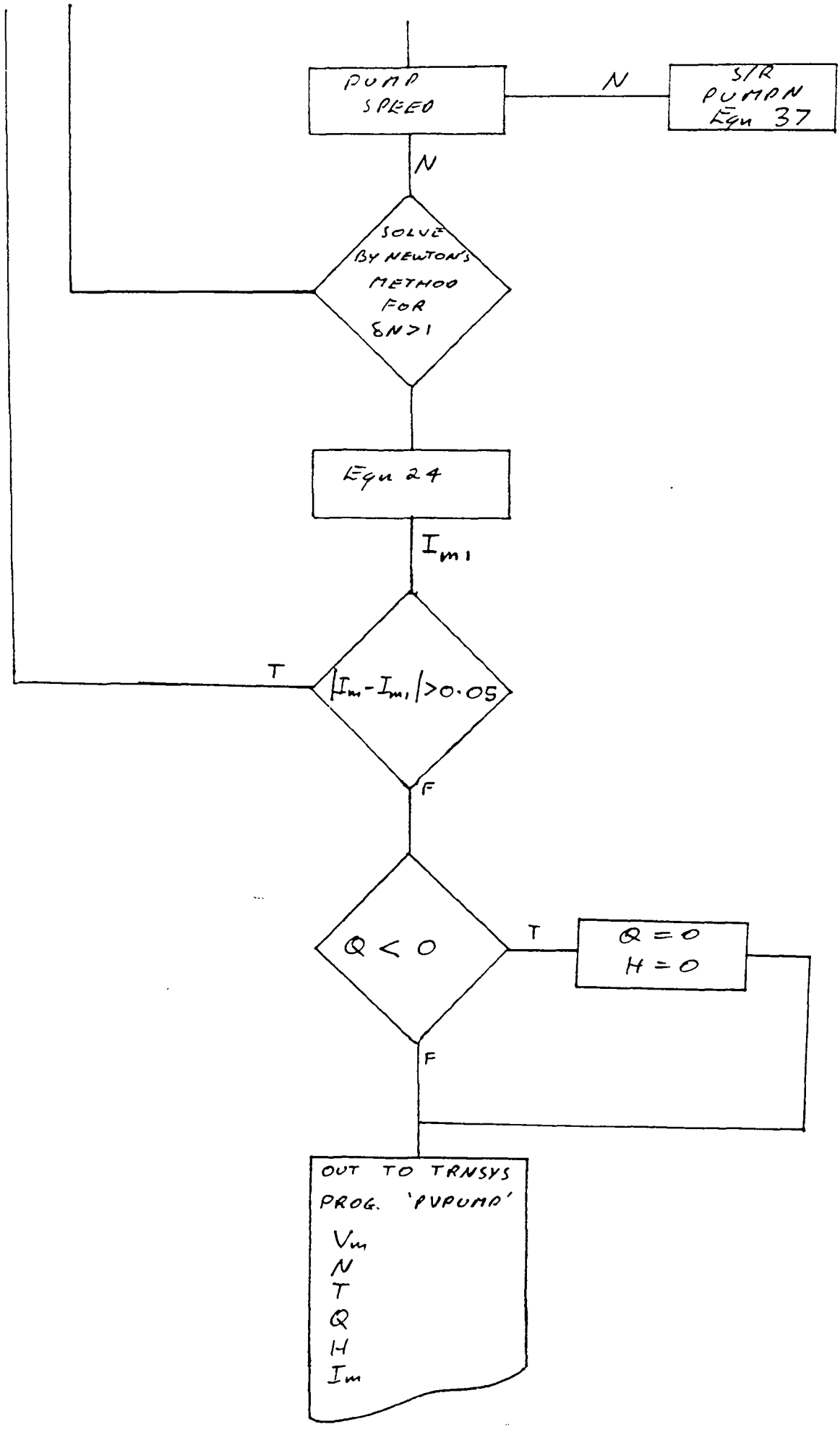
PUMP SPEED
N
S/R PUMPN Eqn 37
N
SOLVE BY NEWTON'S METHOD FOR δN>1
Eqn 24
I_{m1}
T
$|I_m - I_{m1}| > 0.05$
F
$Q < 0$
T
Q = 0
H = 0
F
OUT TO TRNSYS PROG. 'PVPUMP'
V_m
N
T
Q
H
I_m